

# 11

## Photochemistry of Azides: The Azide/Nitrene Interface

*Nina Gritsan<sup>1</sup> and Matthew Platz<sup>2</sup>*

*<sup>1</sup>Institute of Chemical Kinetics and Combustion of Siberian Branch of Russian Academy of Sciences, Novosibirsk, Russia; <sup>2</sup>Chemistry Department, the Ohio State University, Columbus, Ohio, USA*

### 11.1 Introduction

Organic azides are widely used in synthetic organic chemistry.<sup>1-4</sup> An important application of the photochemistry of organic azides is the photoaffinity labeling of biopolymers. This technique was invented by Singh *et al.*,<sup>5</sup> and adapted for use with azides by Bayley and Knowles.<sup>6</sup> For example, aryl azide based photoaffinity labeling has been employed to obtain information on the higher order structure of RNA and RNA-protein complexes.<sup>7</sup> For many years azide photochemistry was used by industrial scientists in the field of lithography.<sup>8</sup> Materials chemists use azide photochemistry in the formation of electrically conducting polymers<sup>9</sup> and for surface modification and functionalization.<sup>10</sup>

It is commonly believed<sup>1-3,11-15</sup> that photolysis and thermolysis of the organic azides leads mainly to the dissociation of N–N bond with formation of molecular nitrogen and nitrenes, as first proposed by Tiemann in 1891.<sup>16</sup> Nitrenes, species containing neutral, monovalent nitrogen atoms, are typically very reactive and short-lived intermediates. Azides form bonds to many elements,<sup>1-3,11-15</sup> and, consequently, many types of nitrenes are known or can be imagined. Nitrenes and other reactive intermediates can be involved in many types of reactions which results in complex mixture of possible products. Physical organic chemists seek to understand the role of nitrenes and other intermediates in azide photochemistry and how the structures of intermediates control their reactivity.<sup>1,2,11-15,17-20</sup>

Thus, the diverse applications of organic azides and the complicated nature of their photochemistry attract significant interest of the scientific community. There has been recent, dramatic progress in mechanistic understanding of the photochemistry of organic azides as a result of the application of modern spectroscopic techniques and high level *ab initio* molecular orbital (MO) calculations.<sup>14,15,17–20</sup> The goal of this chapter is to present a modern view of the mechanism of organic azide photochemistry. The most attention will be paid to the direct observations of the reactive intermediates and to the study of their reactions.

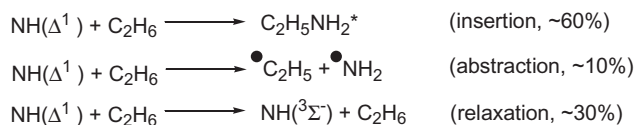
## 11.2 Photochemistry of Hydrazoic Acid (HN<sub>3</sub>)

Photodecomposition of the simplest azide, hydrazoic acid (HN<sub>3</sub>), yields the parent nitrene, imidogen (NH).<sup>21–26</sup> This nitrene can also be produced by thermolysis<sup>27</sup> and multiphoton dissociation<sup>28,29</sup> of HN<sub>3</sub>. Photolysis of HN<sub>3</sub> in the gas phase with 248, 266, 283 and 308 nm light generates NH almost exclusively in the lowest singlet state (<sup>1</sup>Δ).<sup>22–26</sup> The N<sub>3</sub> fragment and H atom were also observed as primary products of HN<sub>3</sub> photodissociation at 266, 248 and 193 nm<sup>30</sup> with quantum yields 0.04, 0.14 and 0.2, respectively.<sup>30c</sup> Formation of NH in different excited states was observed upon photolysis of HN<sub>3</sub> with light of wavelength shorter than 240 nm.<sup>21,22,25</sup> For instance, NH in the X <sup>3</sup>Σ<sup>-</sup>, a<sup>1</sup>Δ, b<sup>1</sup>Σ<sup>+</sup>, A<sup>3</sup>Π, and c<sup>1</sup>Π states were formed by UV photolysis of HN<sub>3</sub> at 193 nm, at 300 K with quantum yields ≤0.0019, 0.4, 0.017, 0.00015 and 0.00061, respectively.<sup>25</sup>

NH in its lowest singlet state (a<sup>1</sup>Δ) inserts readily into paraffin CH-bonds, abstracts hydrogen atoms from hydrocarbons and undergoes relaxation to the ground triplet state.<sup>31</sup> For example, the ratio of these channels is 0.6 : 0.1 : 0.3 in the case of reaction of <sup>1</sup>NH with ethane (Scheme 11.1).<sup>31b</sup>

Reactions of the ground state, <sup>3</sup>NH (X <sup>3</sup>Σ<sup>-</sup>), play an important role in combustion processes.<sup>32</sup> Triplet NH reacts with molecular hydrogen, water and CO<sub>2</sub>.<sup>33</sup> Modern theoretical study<sup>34</sup> demonstrates that reactions with H<sub>2</sub> and H<sub>2</sub>O proceed via hydrogen atom abstraction. The <sup>3</sup>NH abstracts hydrogen atoms from starting material, hydrazoic acid,<sup>35</sup> and from hydrocarbons to form aminyl (NH<sub>2</sub>·) and alkyl radicals<sup>36,37</sup> in spite of the fact that some reactions are endothermic, depending on the alkane.<sup>37</sup> Absolute rate constants for many of these reactions have been measured in the gas phase.<sup>36,37</sup> Triplet NH also reacts with alkenes via formation of an intermediate triplet diradical which then decomposes into several reaction channels.<sup>38</sup>

The major products of the gas phase reaction of <sup>3</sup>NH with molecular oxygen are NO· and OH· radicals.<sup>39,40</sup> It was proposed on the basis of quantum chemical calculations,<sup>40,41</sup> that the primary product is iminoperoxide (HNOO) which undergoes 1,3-hydrogen shift



**Scheme 11.1** Reactions of NH in the lowest singlet state (a<sup>1</sup>Δ) with ethane<sup>31b</sup>



**Scheme 11.2** Mechanism of the gas phase reaction of  ${}^3\text{NH}$  with molecular oxygen<sup>39–41</sup>

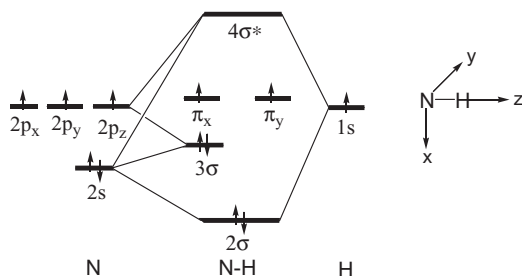


**Figure 11.1** Molecular orbitals of nitrene NH, the  $1\sigma$  orbital, which is not shown, is the  $1s$  AO on nitrogen

yielding hydroperoxinitrene (HOON). The latter undergoes fast dissociation to the  $\text{NO}^\bullet$  and  $\text{OH}^\bullet$  radicals (Scheme 11.2).

The photochemistry of  $\text{HN}_3$  in the argon and nitrogen matrices was studied for the first time by J. Pimentel *et al.* and the IR spectra of triplet nitrene NH and radical  $\text{NH}_2$  were recorded.<sup>42</sup> A series of studies of matrix isolated NH (in ground triplet  ${}^3\Sigma$  and excited singlet  ${}^1\Delta$  states) and its deuterio-substitute analogue (ND) were later performed using UV and luminescence spectroscopy.<sup>43–47</sup> The spectroscopy and relaxation of the lowest excited singlet state of NH / ND ( ${}^1\Delta$ ) were studied in detail in Ne, Ar, Kr and Xe matrices.<sup>46,47</sup>

The heavy atom host accelerates intersystem crossing in either the excited state of  $\text{HN}_3$  or  ${}^1\text{NH}$ , which led to good yields of  ${}^3\text{NH}$  in Xe.<sup>48</sup> Matrix isolated  ${}^3\text{NH}$  reacts with CO to form  $\text{NHCO}$ <sup>49</sup> and with molecular oxygen, an excellent triplet nitrene trap, to form *trans*-HNOO which was characterized by IR spectroscopy.<sup>48</sup> The EPR spectrum of triplet imidogen immobilized in a cryogenic matrix has not yet been observed. One negative attempt was reported in Ar, Kr and Xe matrices in 1967.<sup>50</sup> The zero-field splitting parameter for triplet NH ( $|D/hc| = 1.863 \text{ cm}^{-1}$ )<sup>51</sup> was obtained in the gas phase using laser magnetic-resonance spectroscopy.

Systematic mechanistic studies of the photochemistry of  $\text{HN}_3$  in solution and the chemistry of NH with hydrocarbons, particularly *cis*- and *trans*- alkenes have not been performed.

In the context of this chapter, the electronic structure and spectroscopy of the simplest nitrene, NH, are very important because they will be useful in the analysis of more complicated nitrenes. The electronic structure of NH can be understood on the basis of elementary molecular orbital considerations (Figure 11.1).

In NH, two valence molecular orbitals, corresponding to the N–H bond ( $2\sigma$ ) and the lone pair on nitrogen ( $3\sigma$ ), are occupied by electron pairs. Two more valence electrons must be distributed between two, degenerate, non-bonding molecular orbitals (NBMOs),  $\pi_x$ , and  $\pi_y$ , which consist of the  $2p_x$  and  $2p_y$  AOs on nitrogen (Figure 11.1). The three

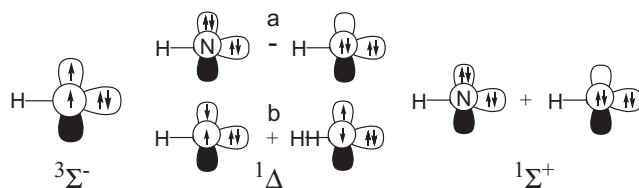


**Figure 11.2** Schematic depictions of one spin component of the lowest triplet state ( ${}^3\Sigma^-$ ), of the (a) ‘closed-shell’ and (b) ‘open-shell’ components of the lowest singlet state ( ${}^1\Delta$ ) and of the second singlet excited state ( ${}^1\Sigma^+$ ) of NH

lowest electronic states of NH –  ${}^3\Sigma^-$ ,  ${}^1\Delta$ , and  ${}^1\Sigma^+$  (Figure 11.2) – all arise from the electronic configurations in which the two electrons are distributed between these two NBMOs. The Pauli exclusion principle prevents electrons with the same spin from simultaneously appearing in the same region of space. Thus, the triplet has the lowest Coulombic repulsion energy of all of the low-lying states; hence, it is the ground state of NH ( ${}^3\Sigma^-$ , Figure 11.2).

The ‘closed-shell’ component of  ${}^1\Delta$  is a linear combination (with a minus sign) of two configurations in which the two non-bonding electrons occupy the same 2p orbital; whereas, in the ‘open-shell’ component one electron occupies each of the 2p AOs. The two components of a  ${}^1\Delta$  state (Figure 2) may look different, but symmetry considerations reveal shows that they are degenerate.

The third electronic state of NH,  ${}^1\Sigma^+$ , is a linear combination of the same configurations as in the  ${}^1\Delta$  state, but with a positive sign (Figure 11.2). The motions of the non-bonding electrons are ‘anti-correlated’ in the  ${}^1\Sigma^+$  state, so they have a higher Coulombic repulsion energy than in  ${}^1\Delta$ . This is the reason why  ${}^1\Sigma^+$  is a higher energy electronic state than  ${}^1\Delta$ .

The experimental absorption spectra of NH in the lowest triplet ( $X\ {}^3\Sigma^-$ ) and singlet ( $a\ {}^1\Delta$ ) states have similar bands in the near UV region with maxima at 336 and 324 nm, respectively.<sup>21,52,53</sup> Both transitions are associated with the electron promotion from a  $3\sigma$  (lone pair) orbital to singly occupied  $\pi$ -orbitals (Figure 11.1).<sup>14</sup> The singlet and triplet absorptions of imidogen are very similar because the same orbitals are involved in the excitation of each spin state. As the transitions are localized on the nitrogen atom, these bands are characteristic of nitrenes in general and will appear in the same spectral region in alkyl and aryl nitrenes.

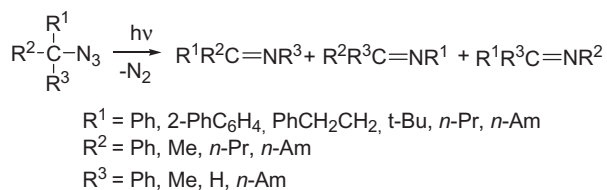
The singlet-triplet splitting of NH was determined experimentally by spectroscopy of neutral NH<sup>53,54</sup> and by negative ion photoelectron spectroscopy (PES) of the NH anion.<sup>55</sup> In the latter experiment, the anion NH is prepared in the gas phase and exposed to monochromatic UV-laser light. This leads to ejection of photoelectrons whose kinetic energies are analyzed. The imidogen anion (NH) can ionize to form either the singlet or triplet nitrene, thus, the difference in the kinetic energies of the photoelectrons leading to  ${}^1\text{NH}$  and  ${}^3\text{NH}$  is simply the singlet-triplet splitting of NH. A value of 1.561 eV (36 kcal/mol) for the singlet-triplet splitting ( $\Delta E_{\text{ST}}$ ) in NH was obtained very accurately from the spectroscopic data.<sup>53–55</sup>

### 11.3 Photochemistry of Alkyl Azides

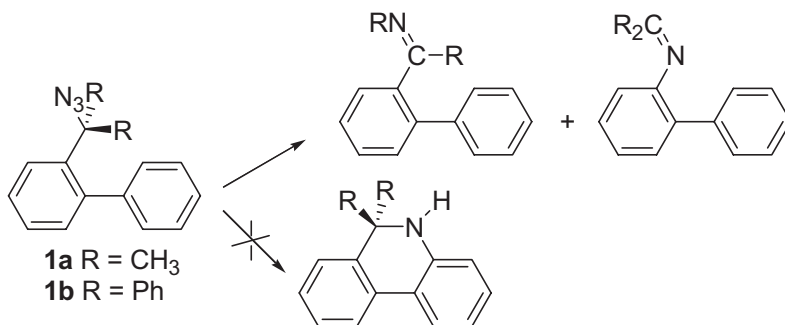
The photolysis of alkyl azides at room temperature cleanly forms imines as products.<sup>56-60</sup> In general, light and heat induced decomposition of alkyl azide does not produce alkyl nitrenes, which can be intercepted in respectable yields with a bimolecular trap.<sup>56,57</sup> For example, Moriarty and Reardon studied photolysis of *n*-butyl, *n*-amyl, 4-heptyl, 2-phenylethyl, 3-phenylpropyl, 4-phenylbutyl, phenylmethyl, 1-phenylbutyl, 1,1-diphenylethyl, and cyclohexyl azides.<sup>58</sup> The primary products of reaction were found to be nitrogen and imines derived from hydrogen, alkyl or aryl migration to nitrogen. Hydrogen atom was found to migrate up to five times faster than an *n*-alkyl group. For cyclohexyl azide only  $\alpha$ -hydrogen migration occurs.<sup>58</sup> In the case of phenylmethyl azide, the phenyl/hydrogen migration aptitudes is equal to unity.<sup>58</sup> The ethyl/methyl migration aptitudes were determined to be in the range 1.0–1.4 for photolysis of a series of 2-substituted 2-butyl azides, where the 2-substituent was an aryl, *n*-propyl or Ph(CH<sub>2</sub>)<sub>n</sub> (*n* = 1–3) groups.<sup>59</sup>

Later,<sup>60</sup> Kyba and Abramovitch studied the photolysis of nine *sec*- and *tert*-alkyl azides (Scheme 11.3) in detail and measured the migratory ratios.

It was found that the range of migratory aptitude does not deviate greatly from unity and photolysis of alkyl azides bearing pendant aryl groups (**1a,b**) does not lead to intramolecular trapping of a nitrene (Scheme 11.4). On the basis of these data, it was proposed that singlet excited alkyl azides eliminate nitrogen with concomitant rearrangement to form imine products, without the intervention of a nitrene intermediate.<sup>60</sup>

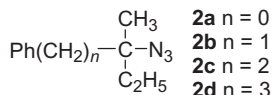


**Scheme 11.3** Photo-rearrangement of tert-alkyl azides



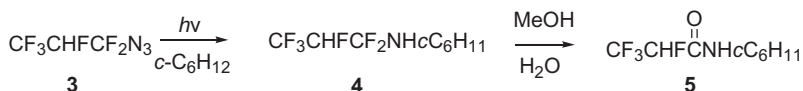
**Scheme 11.4** Photo-rearrangement of di-methyl and di-phenyl derivatives of 2-biphenyl-methyl azide<sup>60</sup>

The quantum yields of photolysis of a series of tertiary alkyl azides (**2a-d**) were measured and found to be in the range of 0.27–0.53.<sup>59</sup>



**Scheme 11.4a**

There are only few examples of photolysis of alkyl azides, which result in any process other than rearrangement to an imine.<sup>56,61,62</sup> Photolysis of highly fluorinated azide **3** in cyclohexane gave amide **5** in 18% yield after a hydrolytic workup, implicating a nitrene C–H insertion product **4**.<sup>61</sup>

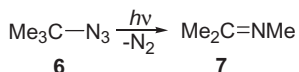


**Scheme 11.5** Phototransformation of fluorosubstituted *n*-propyl azide<sup>61</sup>

An intramolecular cyclization via a formal C–H insertion as a minor process was observed upon photolysis of a steroidal azide.<sup>62</sup> Unique features of the photochemistry of  $\alpha$ -azidoacetophenones and  $\beta$ -azidopropiophenones will be discussed later in this section.

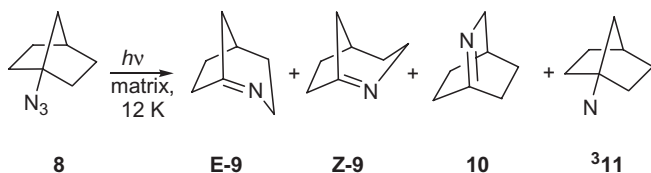
Since there is no evidence of nitrene intermediates in the solution photochemistry of alkyl azides, attempts were made to detect triplet alkylnitrenes in matrix photochemical experiments. Photolysis of  $\text{CH}_3\text{N}_3$  or  $\text{CD}_3\text{N}_3$  at cryogenic temperatures in Ar,  $\text{N}_2$  and  $\text{CO}_2$  matrices fails to produce an IR spectrum attributable to triplet methylnitrene.<sup>63,64</sup> The IR spectrum of imine  $\text{CH}_2=\text{NH}$  (or  $\text{CD}_2=\text{ND}$ ) is observed instead.

In subsequent studies, emphasis was given to studies of the matrix photochemistry of tertiary alkyl azides. Dunkin and Thomson studied the photochemistry of *tert*-butyl azide (**6**) in an  $\text{N}_2$  matrix at 12 K.<sup>65</sup> Using IR spectroscopy they detected the formation of only one product – imine **7**.

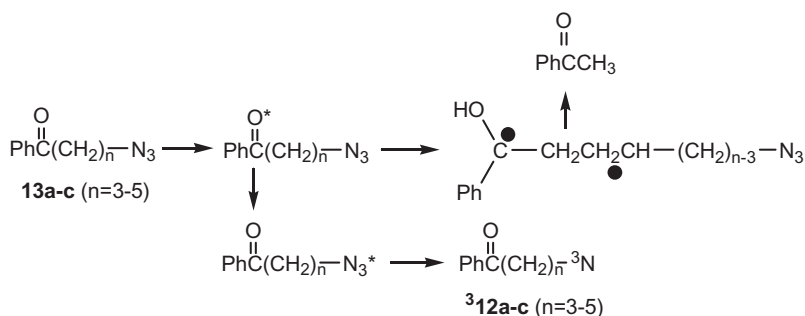


**Scheme 11.6** Matrix photochemistry of *tert*-butyl azide<sup>65</sup>

The formation of strained bridgehead imines was observed upon photolysis of a series of matrix-isolated bridgehead azides, namely, adamantyl, bicyclo[2.2.2]octyl, bicyclo[3.2.1]heptyl and norbornyl azides.<sup>66–70</sup> For example, the photochemistry of matrix-isolated 1-azidonorbornane (**8**) was studied using monochromatic irradiation, IR, UV and ESR spectroscopy, and trapping with methanol and  $\text{CO}$ .<sup>70</sup> Three types of imines (*E*- and *Z*-isomers of **9** and **10**) and traces of triplet nitrene **11** were detected (Scheme 11.7). Imines **9** and **10** are light-sensitive, undergo interconversion and decompose to form unidentified products.



**Scheme 11.7** Matrix photochemistry of 1-azidonorbornane (**8**)<sup>70</sup>



**Scheme 11.8** The primary processes in the photochemistry of  $\alpha$ -benzoyl- $\omega$ -azidoalkanes<sup>73</sup>

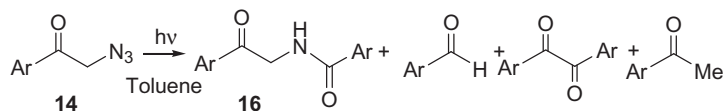
Triplet nitrene **11** was identified based on the ESR signal observed at 8124 G ( $E = 0$ ,  $|D/hc| = 1.65 \text{ cm}^{-1}$ ), the narrow band in the electronic absorption spectrum at 298 nm, and photochemical trapping with CO in Ar at 36 K.<sup>70</sup>

The first experimental evidence for the existence of alkylnitrenes was provided by ESR spectroscopy in glassy matrixes.<sup>71</sup> Very weak ESR signals were detected upon direct irradiation.<sup>71</sup> Sensitized photolysis of alkyl azides was found to be the most appropriate procedure to generate triplet alkylnitrenes in glassy matrixes.<sup>71,72</sup>

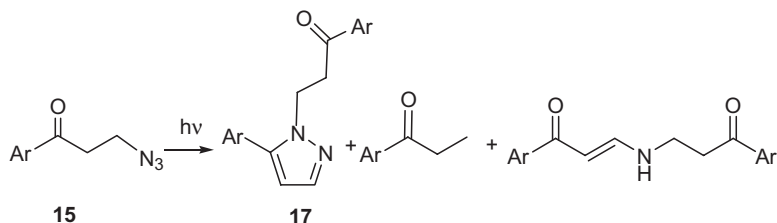
Later,<sup>73</sup> triplet alkylnitrenes **12a-c** were generated by intramolecular sensitization in solution. The photochemistry of three  $\alpha$ -benzoyl- $\omega$ -azidoalkanes ( $\text{PhCO}(\text{CH}_2)_n\text{N}_3$  (**13a-c**,  $n = 3-5$ )) was studied and two competitive processes were found to proceed from the triplet ketone (Scheme 11.8): energy transfer to azide to yield triplet alkyl nitrene and  $\gamma$ -hydrogen abstraction to yield Norrish type II products. Photolysis of azides with a longer methylene chain (**13b,c**) yields mainly acetophenone, a product of Norrish type II reaction. The major products of the azide **13a** photolysis were substituted pyrrole and pyrroline derived from triplet nitrene **12a**.<sup>73</sup>

Recently, the Gudmundsdottir group performed a detailed study of the intramolecular sensitization of a number of  $\alpha$ -azidoacetophenones (**14**) and  $\beta$ -azidopropiophenones (**15**) in solution (using product analysis and laser flash photolysis techniques)<sup>74,75</sup> and in argon matrixes.<sup>75</sup> Compounds **16** and **17** are the major products in solution and their yields are in the range of 50 up to >99% depending on the substituent in the aryl group (Schemes 11.9 and 11.10). Donating substituents ( $R = p\text{-OMe}$ ,  $p\text{-SMe}$ ) lead to the growth of this yield. The mechanisms of product formation were proposed but not sufficiently substantiated.<sup>74,75</sup>

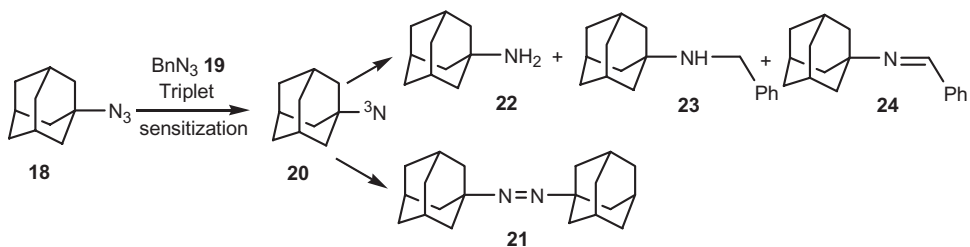
Transient absorption bands with maxima at  $\sim 320 \text{ nm}$  were detected in the laser flash photolysis of **14** and **15** in solution and assigned to triplet alkylnitrenes, which were found



**Scheme 11.9** Products of the  $\alpha$ -azidoacetophenones (**14**) photolysis<sup>74</sup>



**Scheme 11.10** Products of the  $\beta$ -azidopropiophenones (**15**) photolysis<sup>75b</sup>

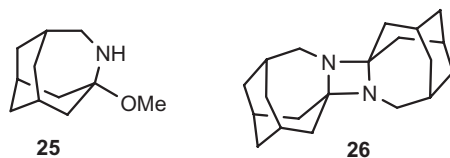


**Scheme 11.11** Triplet-sensitized photolysis of 1-azidoadamantane<sup>77</sup>

to be long-lived with a lifetime of tens of milliseconds. The rate constant of their reaction with oxygen was estimated<sup>74b,75b</sup> to be  $3\text{--}5 \times 10^4 \text{ M}^{-1} \text{ s}^{-1}$ . Corresponding nitro-compounds were isolated after photolysis of **14** and **15** in solutions saturated with oxygen.

Lewis and Saunders studied intermolecular sensitization of a series of alkyl azides.<sup>76</sup> It was found that the triplet energies of alkyl azides are 75–80 kcal/mol and the quantum yields for azide disappearance with appropriate triplet sensitizers approach unity. Recently,<sup>77</sup> the Gudmundsdottir group performed product analysis upon triplet sensitization of 1-azidoadamantane (**18**) and benzyl azide (**19**). It was found that triplet nitrene **20** undergoes dimerization yielding aza-adamantane **21** and hydrogen abstraction from the solvent yielding the following products (**22–24**, Scheme 11.11). Product distribution depends on the sensitizer and solvent nature. Formation of products typical<sup>78</sup> of direct irradiation of **18** (**25** and **26**) in a low yield have also been observed<sup>77</sup> (Scheme 11.12). The triplet benzyl nitrenes participate mainly in the reaction of hydrogen abstraction from the solvent (toluene).<sup>77</sup>

It was mentioned previously (Scheme 11.5), that photolysis of highly fluorinated azide **3** yields an intermolecular nitrene C–H insertion product. This implies a relatively long lifetime of fluorinated singlet nitrenes and the possibility of their relaxation to a ground triplet state. Indeed,<sup>79</sup> formation of triplet  $\text{CF}_3\text{N}$  was observed upon photolysis of  $\text{CF}_3\text{N}_3$



**Scheme 11.12** Products of direct irradiation of 1-azidoadamantane<sup>78</sup>

in an Ar matrix and in polycrystalline pentane at cryogenic temperatures. A persistent ESR spectrum of triplet  $\text{CF}_3\text{N}$  in pentane at 6–10 K ( $ID/h\nu = 1.736\text{ cm}^{-1}$ ) is very similar to that of triplet NH ( $ID/h\nu = 1.863\text{ cm}^{-1}$ )<sup>51</sup> and  $\text{CH}_3\text{-N}$  ( $ID/h\nu = 1.720\text{ cm}^{-1}$ ).<sup>80</sup> The electronic absorption spectrum of  $^3\text{CF}_3\text{N}$  was also detected in an Argon matrix at 14 K.

Note, that the absorption<sup>81–84</sup> and emission<sup>83–89</sup> spectra of triplet methylnitrene  $^3\text{MeN}$  are well known. The 0–0 transition in the absorption spectrum of  $^3\text{MeN}$  was found to be at 316.9 nm in an  $\text{N}_2$  matrix<sup>82</sup> and at 314.3 nm in the gas phase,<sup>83</sup> similar to the spectrum of the parent NH (336 nm).<sup>21,52</sup> The singlet methylnitrene  $^1\text{MeN}$  has never been produced as a trappable species and its detection by femtosecond spectroscopy has failed.<sup>90</sup> Nevertheless, negative ion photoelectron spectroscopy of MeN anion demonstrates that  $^3\text{MeN}$  is lower in energy than the singlet by  $1.352 \pm 0.011\text{ eV}$  ( $31.2 \pm 0.3\text{ kcal/mol}$ ).<sup>91</sup> The features assigned to singlet nitrene in the photoelectron spectrum of  $\text{MeN}^-$  were interpreted as belonging to a resonance, rather than to a true minimum on the singlet MeN potential energy surface.<sup>91</sup>

Therefore, no experimental data is available which indicates formation of singlet alkyl-nitrenes as discrete intermediates upon photolysis of alkyl azides with the exception of perfluorinated alkyl nitrenes. There is also doubt that  $^1\text{MeN}$  is a true intermediate, namely, a species which is characterized by a minimum on the potential energy surface (PES). To investigate this issue a series of quantum chemical calculations were performed.<sup>92–95</sup>

According to the early calculations,<sup>92</sup> there is no minimum on the PES that corresponds to singlet MeN. As these calculations were performed at low level of theory, they were repeated in the 1990s.<sup>93,95</sup> The most recent studies, performed using the CAS/MP2<sup>94</sup> and CASSCF/CASPT2<sup>95</sup> techniques, predict a very shallow minimum for singlet MeN in the  $^1\text{A}'$  state. The rearrangement of  $^1\text{MeN}$  to  $\text{CH}_2=\text{NH}$  was predicted to be very exothermic ( $\Delta H = -83\text{ kcal/mol}$ ) with a barrier 0.5–3.8 kcal/mol depending on the level of theory.<sup>94,95</sup> The thermal decomposition of  $\text{MeN}_3$  was also predicted to occur in two steps, via a singlet nitrene intermediate.<sup>94</sup>

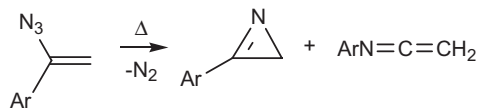
Thus, the predicted reaction mechanism is very dependant on the method employed in the calculations. The long wavelength transition of singlet  $\text{CH}_3\text{N}$  in the  $^1\text{A}'$  state was calculated<sup>14</sup> at 287 nm with oscillator strength  $f = 5 \times 10^{-3}$ . Therefore, spectroscopic detection with pico- or femtosecond time-resolution should be performed to solve this problem.

## 11.4 Photochemistry of Vinyl Azides

The simplest vinyl azide,  $\text{H}_2\text{C}=\text{CH}-\text{N}_3$ , has been known for about 100 years. However, vinyl azides became an important and synthetically useful class of organic compounds

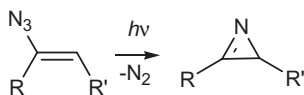
only in the late 1960s.<sup>96</sup> Until recently,<sup>97</sup> photolysis and thermolysis of vinyl azides have been the main methods for the synthesis of azirines – highly strained nitrogen-containing heterocycles.

Smolinsky and Pryde<sup>98</sup> first observed azirine formation, together with small amount of ketenimin, by gas-phase pyrolysis of  $\alpha$ -aryl substituted vinyl azides.



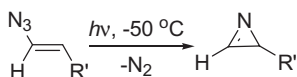
**Scheme 11.13** *Pyrolysis of  $\alpha$ -aryl substituted vinyl azides*<sup>98</sup>

Hassner and Fowler<sup>99</sup> first discovered that photolysis of  $\alpha$ -substituted vinyl azides produce 2-mono- or 2,3-disubstituted-1-azirines with a large chemical yield (80–90%).



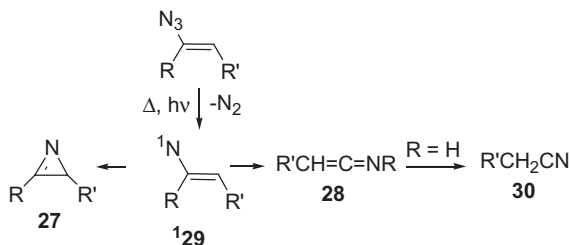
**Scheme 11.14** *Photolysis of  $\alpha$ -substituted vinyl azides*<sup>99</sup>

Isolable 1-azirines were formed upon photolysis of  $\alpha$ -unsubstituted ( $R=H$ ) vinyl azides only at low temperature and underwent further decomposition upon heating.<sup>100</sup>



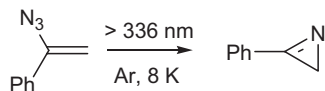
**Scheme 11.15** *Low temperature photolysis of  $\alpha$ -unsubstituted vinyl azides*<sup>100</sup>

The formation of 1-azirines (**27**) along with ketenimines (**28**) upon photolysis and thermolysis of vinyl azides was explained by the intermediacy of singlet vinylnitrenes (**<sup>1</sup>29**).<sup>101</sup> Ketenimins can serve as a precursor to nitriles (**30**) if  $R'=H$ .



**Scheme 11.16** *Step-wise mechanism of vinyl azide photolysis and thermolysis*<sup>101</sup>

However, singlet vinylnitrenes have never been observed by time resolved spectroscopy and triplet vinylnitrenes have not been observed by either time resolved or matrix spectroscopy. The formation of an azirine was observed upon photolysis of  $\alpha$ -azidostyrene in an argon matrix at cryogenic temperature (8 K), but even under these conditions nitrene



**Scheme 11.17** Photolysis of  $\alpha$ -azidostyrene in an argon matrix at 8 K<sup>102</sup>

species were not detected.<sup>102</sup> Therefore, the concerted formation of azirines (without intervention of a singlet nitrene) upon photolysis and thermolysis of vinyl azides was considered more reasonable.<sup>96,103</sup>

The situation with vinylnitrenes is analogous to methylnitrene and it is not clear if either of these singlet nitrenes are true reactive intermediates with finite lifetimes. Quantum chemical calculations can help to explain the properties of vinylnitrenes. All calculations reported in the literature have been concerned with only the simplest vinyl azide and vinylnitrene,  $\text{CH}_2=\text{CH}-\text{N}_3$  and  $\text{CH}_2=\text{CH}-\text{N}$  (**29a**), respectively.<sup>104–106</sup> Early theoretical studies on the vinyl azide to azirine transformation employed semi-empirical calculations,<sup>104a</sup> or *ab initio* calculations performed at relatively low levels of theory,<sup>104b,c</sup> and have focused only on the closed-shell singlet excited state ( $^1A'$ ) of vinylnitrene. We will discuss only the latest calculations.<sup>105,106</sup>

Cramer and Parasuk<sup>105</sup> have performed very accurate calculations of the electronic structure and energies of the lowest states of **29a**. Single-point calculations at the CASSCF(4,4) geometry were carried out at the MRCI and CASPT2 levels using cc-pVDZ and cc-pVTZ basis sets. Calculations predict **29a** to have a  $^3A''$  ground state and the lowest open-shell singlet ( $^1A''$ ) and closed-shell singlet ( $^1A'$ ) states lie 15 and 40 kcal/mol higher in energy, respectively. The C=C bond length (1.346 Å) in  $^1A'$  state is typical for the carbon-carbon double bond. It is lengthened to 1.391 Å in the  $^3A''$  state and to 1.461 Å in the  $^1A''$  state. The lowest singlet state of **29a** is open-shell and resembles a 1,3-biradical.

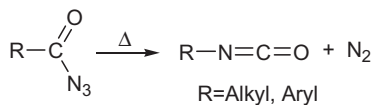
The  $\Delta E_{\text{ST}}$  is much lower in **29a** (15 kcal/mol)<sup>105</sup> than in NH (36 kcal/mol)<sup>53–55</sup> or  $\text{CH}_3\text{N}$  (31.2 kcal/mol)<sup>91</sup> because the C=C substituent allows the  $\pi$  electron in the  $^1A''$  state to become localized in a region of space that is disjoint from the region of space that is occupied by the  $\sigma$  electron. As will be discussed in Section 11.6 for the same reason, the lowest singlet state in phenylnitrene is also the open-shell  $^1A_2$  state of **29a**.

According to the (4,4) CASSCF/6-31G\* calculations, the nitrene  $^1\mathbf{29a}$  in the  $^1A''$  state can close to the azirine without any barrier and this state was found to be the transition state for interchange of the enantiotopic pair of hydrogens in 2*H*-azirine (**27a**).<sup>106</sup> Therefore, if a barrier does exist, it is probably very small. This conclusion, based on the results of calculations, is wholly consistent with the fact noted above, that the triplet and singlet vinyl nitrenes have escaped detection. However, further experimental studies, using very fast laser flash photolysis techniques, along with higher level *ab initio* calculations are certainly warranted.

## 11.5 Photochemistry of Carbonyl Azides and Azide Esters

The thermal rearrangement of carbonyl azides (Curtius rearrangement)<sup>107</sup> giving isocyanates in quantitative yields at 60–80 °C has been known over the years and has been

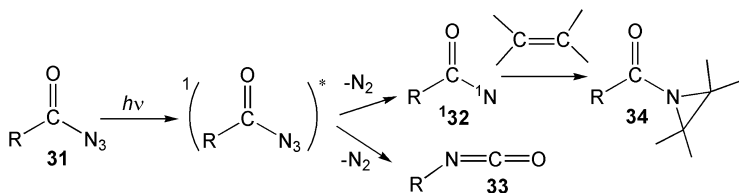
studied in detail.<sup>108–115</sup> It is now generally accepted<sup>14,108,113</sup> and supported by modern quantum chemical calculations<sup>114,115</sup> that loss of nitrogen and migration of R are concerted processes in the Curtius rearrangement of carbonyl azides.



**Scheme 11.18** Thermal decomposition of carbonyl azides<sup>108</sup>

In turn, photolysis of carbonyl azides gives rise to two types of reactions. The photo-Curtius rearrangement proceeds to form isocyanate. In addition, bimolecular trapping products, typical of the reactions of singlet carbonylnitrenes, are also observed.<sup>108–110,115–127</sup>

The mechanisms of photo-Curtius rearrangements have long been debated.<sup>108–110,119–133</sup> It has been shown that the yield of isocyanates, formed upon photolysis of a series of carbonyl azides (R–CO–N<sub>3</sub>, R = *t*-Butyl, Aryl), remains constant in the presence and in the absence of nitrene traps.<sup>111,112,117,118</sup> For example, the yield of isocyanate **33a** produced on photolysis of pivaloyl azide (R = *tr*-Butyl, **31a**) in methylene chloride (an inert solvent) is 40%. Photolysis of **31a** in cyclohexene leads to a 45% yield of aziridine adduct **34a** and a 41% yield of isocyanate **33a**. Trapping the nitrene does not depress the yield of isocyanate. Hence, isocyanate **33a** and adduct **34a** cannot be derived from the same reactive intermediate, but instead the isocyanate must be formed from the excited state of the azide or from the electronically or thermally excited nitrene.



**Scheme 11.19** Photolysis of carbonyl azides

The yields of the isocyanates produced upon photolysis of benzoyl azide (R=Ph, **31b**) and its *para*-methoxy, *para*-chloro and *meta*-fluoro derivatives were found to be in the range of 40–50% in both inert solvents and in solvents that intercept acylnitrenes.<sup>117,118</sup> Similar results were obtained for 2-naphthoyl azide (**35**).<sup>122</sup> Irradiation of **35** in cyclohexane at room temperature produces isocyanate (**36**, ~45%), *N*-cyclohexyl-2-naphthamide – the product of 2-naphthoylnitrene (**37**) insertion (~50%), and a trace (<1%) of 2-naphthamide (**38**).<sup>122</sup> Therefore, it was concluded that carbonylnitrenes (R–CO–N) do not rearrange to isocyanates (R–N=C=O) at a rate that is competitive with their capture by trapping agents.<sup>108,111,115,118,122</sup>

The Schuster group comprehensively studied the photochemistry of **35**<sup>122</sup> and substituted benzoyl azides<sup>123–125</sup> in order to determine the multiplicity of the ground state of aroylnitrenes. First, they demonstrated<sup>122</sup> that both direct and triplet-sensitized photolysis generates products characteristic of the reactions of **137**. Earlier,<sup>120,121</sup> similar results had

been obtained for benzoyl azide (R=Ph, **31b**). The direct and triplet sensitized photolysis of **31b** produced the same trapping products and these products were characteristic of a singlet nitrene **132b**.

Second, photolysis of **35** in cyclohexane solution containing either *cis*- or *trans*-4-methyl-2-pentene (0.2 M) forms aziridines (**40**) with complete (>98%) retention of olefin stereochemistry.<sup>122</sup> Based on the Skell-Woodworth hypothesis developed for carbenes,<sup>134</sup> they concluded, that aziridines are formed in the reaction of singlet 2-naphthoynitrenes (**137**).<sup>122</sup> Besides, extending the nitrene lifetime by diluting the concentration of the trapping agent (0.01 M) does not lead to relaxation of a putative excited singlet nitrene to its putative lower energy triplet state.<sup>122</sup>

Finally, ESR signals attributable to triplet nitrene **337** were not observed after irradiation of **35** in fluorolube at 77 K. A nitrene-like triplet ESR spectrum was not detected either after photolysis of benzoyl azide **31b** in glassy matrices.<sup>71,72b</sup>

Therefore, the experimental data are most consistent with a singlet ground state of carbonyl nitrenes. Triplet carbonylnitrenes were not detected in either chemical trapping or spectroscopic experiments. The explanation of these results was available only recently.<sup>135-137</sup>

To understand the reason for the singlet multiplicity of the ground state of carbonyl azides, the singlet-triplet splitting for benzoyl- (**32b**) and 2-naphthoynitrenes (**37**) were calculated at the B3LYP/6-31G\* level of theory.<sup>135</sup> The triplet states were still computed to be lower in energy by about 5.0 and 4.5 kcal/mol for **32b** and **37**, respectively. However, these values are much lower than the well known  $\Delta E_{ST}$  values for NH (36 kcal/mol)<sup>53-55</sup> and CH<sub>3</sub>N (31.2 ± 0.3 kcal/mol).<sup>91</sup> The significant stabilization of the singlet state relative to the triplet state in aroyl nitrenes is attributed to the bonding interaction between the nitrogen and oxygen atoms.<sup>135-137</sup> Due to this bonding, the structure of the singlet species resembles that of a cyclic oxazirine,<sup>135</sup> although the calculated N–O distance (~1.76 Å) is much longer than a normal N–O single bond (about 1.5 Å in strained rings).<sup>138</sup>

Later,<sup>115,136,137</sup> it was demonstrated by calculation of  $\Delta E_{ST}$  for formyl- and acetylnitrenes at very high levels of theory (CCSD(T) or CBS-QB3), that simple DFT calculations overestimate  $\Delta E_{ST}$  by about 9 kcal/mol. Therefore, aroylnitrenes are indeed species predicted to have a singlet ground state.

Having understood the nature of the singlet species, Pritchina and colleagues<sup>136,137</sup> studied the photolysis of benzoyl azide **31b** in argon matrix at cryogenic temperature in order to detect this species directly by spectroscopic methods. It was shown that photolysis (254 nm) of matrix isolated **31b** affords at least two products. One of these products has an IR spectrum characteristic of isocyanate **33b**. Another product ( $\lambda_{\max} = \sim 300$  nm) is transformed to **33b** upon further irradiation at 313 nm. The electronic absorption spectrum of the latter product as well as its IR spectrum coincide well with the calculated spectra of singlet species **132b** with a structure resembling that of cyclic oxazirine (Figures 11.3 and 11.4).<sup>136,137</sup>

Results of our investigations<sup>136,137</sup> were reproduced and the formation of a small amount of cyanate **41** was also detected.<sup>139</sup> Thus, the photolysis of **31b** could be described by Scheme 11.20.

Kinetics of the reactions of singlet species **132b** in solution at room temperature were studied using time-resolved IR spectroscopy (TRIR)<sup>136,140</sup> and nanosecond laser flash photolysis.<sup>115,141</sup> The absolute rate constants of bimolecular reactions of **132b** with

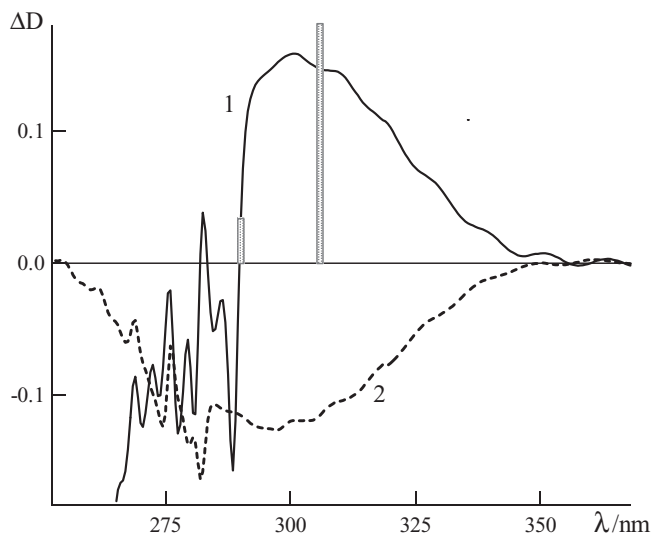


**Figure 11.3** Difference electronic absorption spectra recorded upon irradiation of **31b** at 254 nm for 2 min in argon matrix at 12 K (1) and the sample after further irradiation at 313 nm for 8 min (2).<sup>136</sup> The positions and relative intensities of the absorption bands calculated for species **132b** at the CASSCF/CASPT2 level are indicated by vertical bars

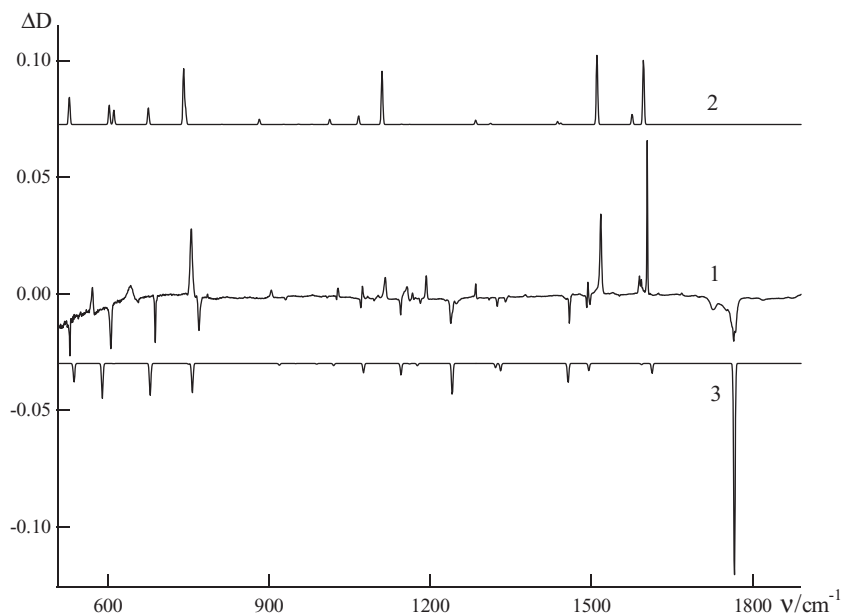
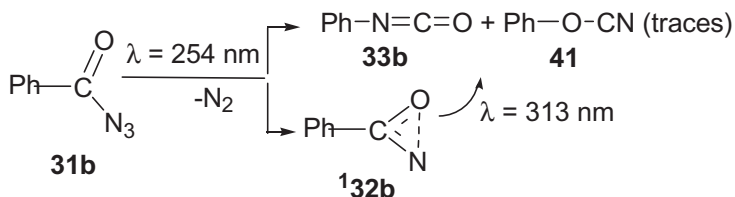


**Figure 11.4** Changes in the IR spectrum (1) recorded after additional irradiation at 313 nm (8 min) of the sample of **31b** irradiated at 254 nm (2 min).<sup>137</sup> Calculated IR spectra of isocyanate **33b** (2) and singlet species **132b** (3)



**Scheme 11.20** Photochemistry of benzoyl azide in argon matrix at 12 K<sup>136,137,139</sup>

acetonitrile, methanol, water, cyclohexene, a series of alkenes and some nucleophilic anions were measured.<sup>115,141</sup> A very small negative activation energy was determined for reaction of **132b** with 1-hexene. This result is in good agreement with theoretical predictions.<sup>115</sup>

### 11.5.1 Photochemistry of Azide Esters

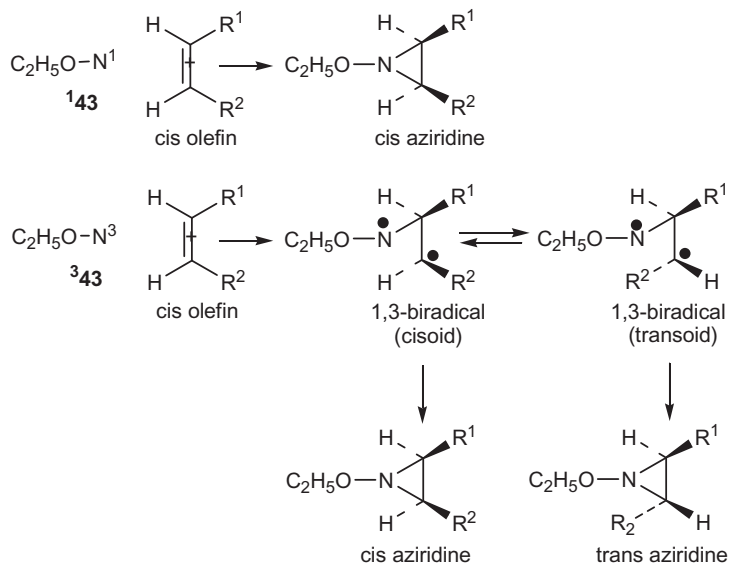
In contrast to carbonyl azides, photolysis and thermolysis of azidoformates (RO-CO-N<sub>3</sub>, R=Alkyl, Aryl) yield mainly products derived from capture of the nitrenes (RO-CO-N).<sup>108,142-146</sup> Carboethoxy azide **42** has been studied most extensively. Formation of products characteristic of reactions of carbethoxynitrene **143** have been observed by thermolysis and photolysis of azide **42**<sup>143,146</sup> and by  $\alpha$ -elimination of arylsulfonate ion from *N*-(*p*-nitrobenzenesulfonyloxy) urethane.<sup>143,145</sup> The reaction of **143** with *cis* and *trans*-4-methyl-2-pentene was studied as a function of alkene concentration. At large alkene concentrations, aziridination is stereospecific, but upon dilution of the alkene, the stereospecificity is lost.<sup>143</sup> The triplet nitrene **343** also reacts with the olefins, but non-stereospecifically, presumably through intermediate biradical formation (Scheme 11.21).<sup>107,143</sup> These results are completely analogous to studies of carbenes in which a stereospecific singlet intermediate is produced initially, and subsequently relaxes to a less selective, lower energy triplet intermediate.<sup>147</sup>

Insertion of **143** into the CH bond of alkanes and the OH bond of alcohols, addition of **143** to acetylenes, and its reaction with benzene, followed by azepine formation, are all well documented.<sup>108</sup>

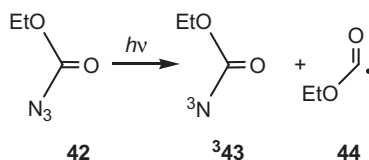
Similar results (formation of nitrene derived products and the absence of isocyanate and products of its transformations) were obtained upon photolysis of (4-acetylphenoxy) carbonyl azide.<sup>122,123</sup>

The triplet ground state of nitrene **43** was proven by ESR spectroscopy ( $|D| = 1.603 \text{ cm}^{-1}$ ,  $|E| = 0.0215 \text{ cm}^{-1}$ ).<sup>72b</sup> A similar ESR spectrum ( $|D| = 1.65 \text{ cm}^{-1}$ ,  $|E| = 0.024 \text{ cm}^{-1}$ ) was recorded for the triplet (4-acetylphenoxy)carbonylnitrene.<sup>122,123</sup>

Recently, the photochemistry of azide **42** was studied by laser flash photolysis ( $\lambda_{\text{ex}} = 266 \text{ nm}$ ) techniques in Freon-113 (CF<sub>2</sub>ClCFCl<sub>2</sub>) at room temperature.<sup>148</sup> The formation of at least two intermediates, viz., triplet nitrene **343** ( $\lambda_{\text{max}} = 400 \text{ nm}$ , lifetime 1.5  $\mu\text{s}$ ) and ethoxycarbonyl radical **44** ( $\lambda_{\text{max}} = 333 \text{ nm}$ , lifetime 0.4  $\mu\text{s}$ ), was observed (Scheme 11.22). The singlet nitrene **143** was deduced to have a lifetime between 2 and 10 ns in Freon-113 at ambient temperature. The kinetics of reactions of **343** with tetramethylethylene and triethylsilane were also measured.<sup>148</sup>

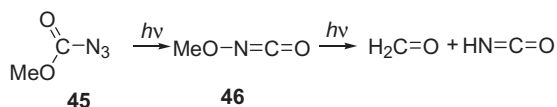


**Scheme 11.21** The stereospecific and non-stereospecific addition of carbethoxynitrenes **43** to alkenes<sup>143</sup>



**Scheme 11.22** Laser flash photolysis of carbethoxy azide **42** in Freon-113 at ambient temperature<sup>148</sup>

The photochemistry of carbomethoxy azide (**45**) and its deuterated derivative was studied in inert gas matrices at 4 and 10 K.<sup>149,150</sup> The IR spectrum of the reaction products shows characteristic lines assigned to methoxyisocyanate (**46**) and the products of its further phototransformations, viz., formaldehyde and isocyanic acid.<sup>149</sup> Triplet carbomethoxynitrene was not detected,<sup>149,150</sup> apparently due to the photochemical transformation of the latter to **46**.



**Scheme 11.23** Photolysis of carbomethoxy azide in neon matrix at 4 K<sup>149</sup>

To understand the difference in the properties of carbonylnitrenes ( $\text{R}-\text{CO}-\text{N}$ ) and nitrenoformates ( $\text{RO}-\text{CO}-\text{N}$ ), the structures and  $\Delta E_{\text{ST}}$  for simplest nitrenes ( $\text{R}=\text{H}$  and  $\text{Me}$ )

were analyzed at the CCSD(T) and CBS-QB3 levels of theory.<sup>115,137</sup> According to the calculations both nitrenoformates ( $\text{CH}_3\text{O}-\text{CO}-\text{N}$  and  $\text{HO}-\text{CO}-\text{N}$ ) have triplet ground states, whereas carbonylnitrenes ( $\text{CH}_3-\text{CO}-\text{N}$  and  $\text{H}-\text{CO}-\text{N}$ ) are singlet ground state species. At this level of theory, the singlet excited states of nitrenoformates have the same nature as the ground singlet states of carbonylnitrenes, viz., they have a structure resembling that of a cyclic oxazirine. The difference in the  $\Delta E_{ST}$  between carbonylnitrenes and nitrenoformates was attributed to the smaller bonding interaction between the nitrogen and oxygen atoms in the latter case.<sup>115,137</sup>

## 11.6 Photochemistry of Phenyl Azide and Its Simple Derivatives

The photochemistry of phenyl azide and its simple derivatives have received the most attention in the literature. The results of early studies were summarized in a number of reviews.<sup>1,2,11-13,151-153</sup> Over the last decade, modern time-resolved spectroscopic techniques and high level *ab initio* calculations have been successfully applied and reveal the detailed description of aryl azide photochemistry. This progress was analyzed in recent reviews.<sup>14,15,17-20</sup> Femtosecond time resolved methods have been recently employed to study the primary photophysical and photochemical processes upon excitation of aryl azides.<sup>154-161</sup> The precise details by which aryl azide excited states decompose to produce singlet aryl nitrenes and how rapidly the seminal nitrenes lose heat to solvent and undergo unimolecular transformations were detailed. As a result of the application of modern experimental and theoretical techniques, phenylnitrene (PhN) – the primary intermediate of phenyl azide photolysis, is now one of the best characterized of all known organic nitrenes.<sup>14,15,17-20,157-159</sup>

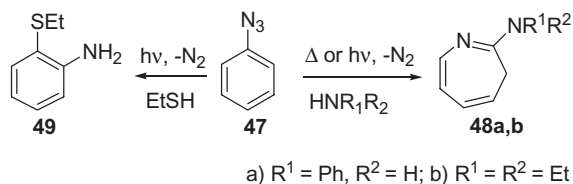
In this section we will briefly consider the most important early results which created the basis for the interpretation of the more recent studies. The largest part of this section will be devoted to the experimental and theoretical discoveries of the last decade.

### 11.6.1 Photochemistry of Phenyl Azide

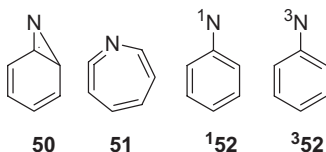
Photolysis and pyrolysis of phenyl azide (**47**) and most of its derivatives in hydrocarbons leads to polymeric tars instead of diagnostic insertion products and aziridines.<sup>162</sup> A fortunate exception is the formation of azepines in the presence of primary and secondary amines. The Huisgen group<sup>163</sup> was the first to observe that thermolysis of **47** in the presence of aniline leads to extrusion of molecular nitrogen and formation of azepine **48a** (Scheme 11.24). Eight years later, Doering and Odum<sup>164</sup> demonstrated that azepine **48b** is formed with a high yield ( $\geq 70\%$ ) upon photolysis of **47** in diethylamine (Scheme 11.24). Aside from azepines, the formation of *ortho*-substituted aniline **49** (in a yield of 39%) was discovered upon photolysis of **47** in ethanethiol (Scheme 11.24).<sup>165</sup>

The azirine **50** and/or ketenimine (1,2-didehydroazepine) **51** were proposed as the trappable reactive intermediates produced upon photolysis of **47** in solution (Scheme 11.25).<sup>162-165</sup>

The high dilution of solutions of phenyl azide suppresses polymer formation and azobenzene forms instead.<sup>166,167</sup> This indicates that singlet intermediates (**50** and/or **51**) serve as a reservoir for triplet phenylnitrenes (**52**), which either undergo dimerization or react



**Scheme 11.24** Adduct formation upon photolysis and pyrolysis of phenyl azide<sup>163–165</sup>



**Scheme 11.25** Structure of intermediates of phenyl azide photolysis

with azide **47** to give azobenzene. These reactions have never been directly monitored for <sup>3</sup>**52** by time-resolved techniques. However, dimerization of substituted triplet phenylnitrenes (*para*-nitro<sup>167</sup> and 2,4,6-tribromo<sup>168</sup>), as well as polycyclic 1-naphthyl-,<sup>169,170</sup> 1-anthranlyl-<sup>169</sup> and 1-pyrenylnitrenes,<sup>170,171</sup> were studied by laser flash photolysis techniques. The decay of triplet arylnitrenes and/or formation of corresponding azo-compounds were found to obey second-order kinetics with rate constants in the range of  $0.55\text{--}2.1 \times 10^9 \text{ M}^{-1} \text{ s}^{-1}$  in benzene at room temperature.<sup>168–171</sup>

Later, it was demonstrated that photolysis of the dilute hydrocarbon solutions ( $<10^{-4} \text{ M}$ ) of simple derivatives of **47** in the presence of oxygen gives the corresponding nitro- and nitrosobenzenes with a yield of  $\sim 80\%$ .<sup>13,172,173</sup> The latter are also the products of triplet arylnitrenes reactions.<sup>13,172–175</sup>

Formation of triplet phenylnitrene (<sup>3</sup>**52**) was detected by EPR spectroscopy after photolysis of **47** in glassy matrices at 77 K.<sup>176</sup> The temperature dependence of the EPR signal demonstrated that the triplet state is the ground state of phenylnitrene.<sup>176</sup> Shortly thereafter, Reiser's group<sup>177</sup> recorded the UV-Vis spectrum of <sup>3</sup>**52** in a glassy matrix. Later it was found that <sup>3</sup>**52** is extremely light sensitive and that upon photoexcitation at 77 K, it rapidly isomerizes to the isomeric ketenimine **51**.<sup>168</sup> Figure 11.5 shows the spectrum of <sup>3</sup>**52** recorded in EPA at 77 K.

In 1978, Chapman and LeRoux detected the formation of ketenimine **51** using matrix isolation IR spectroscopy.<sup>102</sup> Irradiation of **47** in an argon matrix at 8 K with light of  $\lambda > 360 \text{ nm}$  (or  $\lambda > 216 \text{ nm}$ ) led to the formation of a product giving an intense IR band at  $1895 \text{ cm}^{-1}$  characteristic of a heterocumulene structure ( $-\text{N}=\text{C}=\text{C}-$ ). The ketenimine **51** was unstable upon further irradiation ( $\lambda > 360 \text{ nm}$ ); however, the formation of azirine **50** was not observed.<sup>102</sup> The later spectroscopic studies in matrices<sup>178–180</sup> demonstrated the formation of both **51** and <sup>3</sup>**52** with a characteristic triplet EPR spectrum ( $lD/hcI = 1.027 \text{ cm}^{-1}$ ,  $lE/hcI = 0 \text{ cm}^{-1}$ ).<sup>179</sup> The ratio of <sup>3</sup>**52** and **51** in the initial steps of irradiation was found to be  $\sim 4:1$  at 334 nm excitation.<sup>179</sup> Irradiation of **47** in argon matrix at 280 nm preferentially gave **51**.<sup>180</sup> The shorter wavelength excitation (254 nm) of **47** in an argon matrix yields <sup>3</sup>**52** and **51** in the ratio of  $\sim 1:2$ .<sup>181</sup>

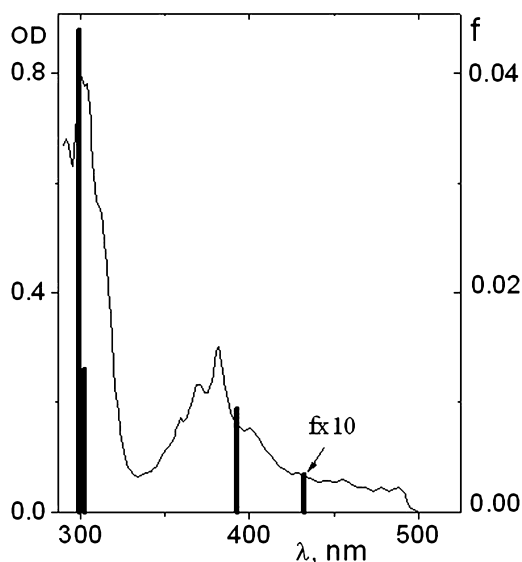
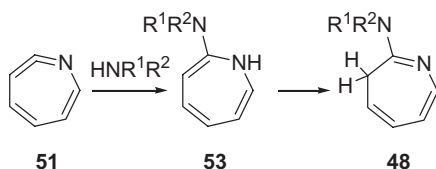


**Figure 11.5** The difference absorption spectrum of  $^352$  in EPA glass at 77K.<sup>168</sup> The computed positions and oscillator strengths ( $f$ , right-hand axis) of the absorption bands of  $^352$  are depicted as solid vertical lines.<sup>197</sup> Reprinted with permission from ref.<sup>197</sup> Copyright 1999 ACS Publications



**Scheme 11.26** Reaction of ketenimine with primary and secondary amines

The solution phase photochemistry of phenyl azide **47** is temperature dependent.<sup>168</sup> Photolysis of **47** in the presence of diethylamine at ambient temperature yields azepine **48b**. Lowering the temperature suppresses the yield of **48b** and below 160 K, azobenzene, the product of triplet nitrene dimerization, is produced. Thus, high temperature favors reactions of singlet state intermediates whilst low temperatures favor reactions associated with triplet phenylnitrene.

The formation of **51** in solution was recorded by laser flash photolysis techniques (broad band at  $\sim 350$  nm),<sup>168,171</sup> and this assignment was unambiguously proved by time-resolved IR spectroscopy (TRIR).<sup>182,183</sup> It was also established that ketenimine **51** is the species trapped by nucleophiles in solution.<sup>183</sup> The tautomerization of the primary trapping product, 1H-azepine (**53**), to the final 3H-azepine (**48**) was also studied in detail in the 1970's (Scheme 11.26).<sup>184</sup>

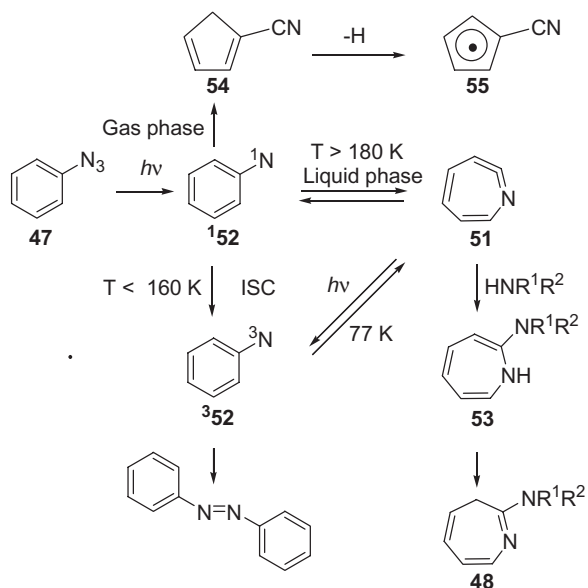
Recently,<sup>185</sup> the low temperature  $^{13}\text{C}$  NMR and IR spectra of **51** incorporated into a hemicarcerand were reported. The lifetime of **51** in the inner phase of a hemicarcerand

was found to be 32 min at 194 K. Encapsulation also dramatically increased the lifetime of the triplet nitrene  $^3\mathbf{52}$  ( $\tau \approx 75$  days at 194 K).<sup>185b</sup>

The photochemistry of  $\mathbf{47}$  was also studied in the gas phase.<sup>186,187</sup> Some groups reported that gas-phase photolysis of  $\mathbf{47}$  produced the absorption and emission spectra of  $^3\mathbf{52}$ .<sup>186</sup> Cullin and co-workers<sup>187</sup> demonstrated that the spectra observed were actually that of the cyanocyclopentadienyl radical. UV-photolysis of  $\mathbf{47}$  produces singlet phenylnitrene ( $^1\mathbf{52}$ ) with excess vibrational energy, which in the gas phase can not be shed by collisions with solvent molecules. Thus, hot  $^1\mathbf{52}$  explores the  $\text{C}_6\text{H}_5\text{N}$  surface and eventually finds the global minimum, cyanocyclopentadiene ( $\mathbf{54}$ ), which can shed its excess energy by losing a hydrogen atom to form the cyanocyclopentadienyl radical ( $\mathbf{55}$ ). These results are in excellent agreement with Wentrup's gas-phase pyrolysis studies.<sup>188</sup> To date, phenylnitrene has not been detected in the gas-phase.

Thus, in the late 1980s a series of intermediates produced by the photolysis of phenyl azide had been directly observed ( $^3\mathbf{52}$  in matrices and low temperature glasses,  $\mathbf{51}$  in matrices and liquids, and  $\mathbf{55}$  in the gas-phase). However, the results obtained in solution and inert gas matrices differ substantially from those obtained in low temperature glasses. In glasses, triplet nitrene  $^3\mathbf{52}$  is the major product, whereas ketenimine  $\mathbf{51}$  is the major product in solution at ambient temperature and often in the inert gas matrices at  $\sim 10$  K. Formation of  $\mathbf{51}$  in inert gas matrices was explained by the slow vibrational relaxation of the hot singlet nitrene  $^1\mathbf{52}$  in these matrices, which competes with fast isomerization to  $\mathbf{51}$ .<sup>168,180</sup>

At that time, the primary intermediate, singlet phenylnitrene  $^1\mathbf{52}$ , had still escaped direct detection. The benzazirine  $\mathbf{50}$  had not been detected either, although the formation of  $\mathbf{49}$  in ethanthiol (Scheme 11.24) was an indication of its intermediacy in the phototransformation of  $\mathbf{47}$ . A series of reviews were published in 1992,<sup>12,13,153</sup> which economically explained much of the photochemistry of phenyl azide (Scheme 11.27).



**Scheme 11.27** Mechanism of photolysis of phenyl azide proposed in 1992

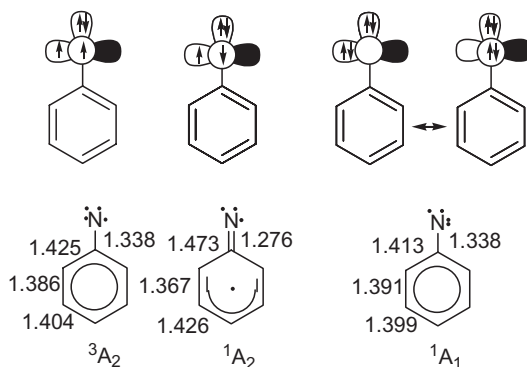


**Figure 11.6** Orbital occupancies for nonbonding electrons and CASSCF(8,8)/6-31G(d) optimized geometries of the lowest triplet and singlet states of phenylnitrene **52**. Reprinted with permission from ref.<sup>20</sup> Copyright 2006 ACS Publications

At the same year, two computational studies clarifying the electronic structure of nitrene **52** were published.<sup>189,190</sup> In phenylnitrene **52**, a lone pair of electrons occupies a hybrid orbital, rich in 2s character and the two non-bonding electrons both occupy pure 2p orbitals. One of these is a p- $\pi$  orbital, and the other a p orbital on nitrogen that lies in the plane of the benzene ring. The near-degeneracy of the two 2p orbitals gives rise to four low-lying spin states – a triplet ( $^3A_2$ ), an open-shell singlet ( $^1A_2$ ), and two closed-shell singlets ( $^1A_1$ ). The orbital occupancies and CASSCF(8,8)/6-31G\* geometries of the three lowest spin states are shown in Figure 11.6.

In the  $^3A_2$  and  $^1A_2$  states, the 2p- $\pi$  orbital and the in-plane 2p orbital on N are both singly occupied. The two  $^1A_1$  states of **52** are a mixture of two dominant configurations – one in which the in-plane p orbital on N is doubly occupied and the 2p- $\pi$  orbital is empty. The latter is slightly lower in energy than the configuration in which these orbital occupancies are reversed.<sup>106,189,190</sup> The two  $^1A_1$  states differ only by the sign of this linear combination. In both the  $^3A_2$  and  $^1A_1$  states the C–N bond is relatively long, and the phenyl ring shows little bond-length alternation (Figure 11.6). In the  $^1A_2$  state, however, strong delocalization of the electron in the nitrogen p- $\pi$  orbital into the aromatic ring leads to a very short C–N bond (1.276 Å).<sup>106,189,190</sup> This delocalization confines the electron in the  $\pi$ -orbital and the electron of opposite-spin in the in-plane 2p AO on nitrogen to different regions of space, thus minimizing their mutual Coulombic repulsion energy.<sup>106</sup> This is the reason for the strong stabilization of the  $^1A_2$  state relative to the  $^1A_1$  state of **52**.

High levels of theory predict that the lowest singlet state ( $^1A_2$ ) of **52** lies about 18 kcal/mol higher in energy than the triplet ground state ( $^3A_2$ ),<sup>106,189–192</sup> in excellent agreement with the experimental results obtained by photoelectron ( $18 \pm 2$  kcal/mol)<sup>193</sup> and electron detachment ( $18.3 \pm 0.7$  kcal/mol)<sup>194</sup> spectroscopy. The second singlet state of **52**,  $^1A_1$ , lies about 30 kcal/mol above the ground triplet state.<sup>106,189–193</sup>

In 1997 the primary intermediate – singlet phenylnitrene **52**, was finally directly detected by LFP techniques. Gritsan, Yuzawa and Platz<sup>195</sup> and the Wirz group<sup>196</sup> simultaneously reported the observation of singlet phenylnitrene (**52**) with  $\lambda_{\max}$  at about 350 nm and a lifetime of  $\approx 1$  ns at ambient temperature. More accurate measurements<sup>197</sup>

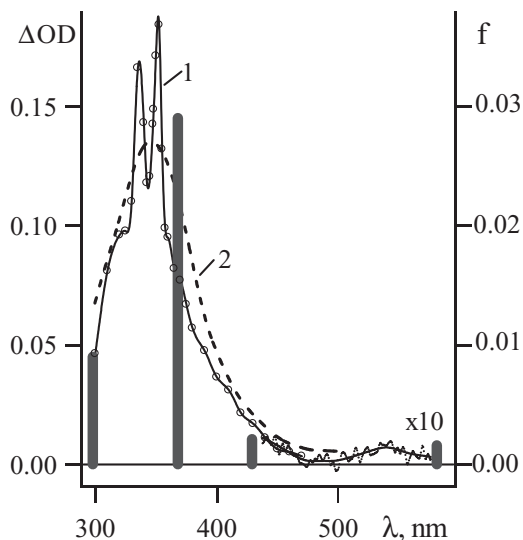


**Figure 11.7** Transient absorption spectra recorded after laser excitation (266 nm, 35 ps) of phenyl azide **47** in pentane: after 2 ns at 233 K (1) and after 10 ns at 295 K (2). The computed positions and oscillator strengths ( $f$ , right-hand axis) of the absorption bands of  $^1\mathbf{52}$  are depicted as solid vertical lines

revealed the structure of this band (336 and 352 nm) and also a very low intensity band at 540 nm (Figure 11.7). Figure 11.7 also demonstrates the electronic absorption spectrum of ketenimine **51** (spectrum 2), recorded on a nanosecond time scale at ambient temperature.<sup>195</sup>

The assignment of the transient absorption in Figure 11.7 to the  $^1\mathbf{52}$  was supported by the calculation of its electronic absorption spectrum. Indeed, the spectrum of  $^1\mathbf{52}$  ( $^1A^2$ ) calculated at the CASPT2 level is in good agreement with the transient spectrum of Figure 11.7. The only intense absorption band in the spectrum of  $^1\mathbf{52}$  is localized around 350 nm (Figure 11.7). According to the calculations the main configuration involved in this transition consists of excitation of an electron from the lone pair orbital ( $n_z$ ) on nitrogen to the singly occupied nitrogen 2p orbital that lies in the molecular plane ( $p_y$ ). A similar type of transition contributes to the intense absorption band of  $^3\mathbf{52}$  at  $\sim 300$  nm<sup>197</sup> (Figure 11.5). The spectra of the simplest nitrenes  $^3\text{NH}$  ( $\lambda_{\text{max}} = 336$  nm)<sup>21,52</sup> and  $^3\text{NCH}_3$  ( $\lambda_{\text{max}} = 316.9$  nm)<sup>82</sup> are also associated with these types of analogous transitions.

The calculations also demonstrate that the electronic absorption spectra of  $^1\mathbf{52}$  and  $^3\mathbf{52}$  are very similar, but that all of the calculated and experimentally detected bands of  $^1\mathbf{52}$  (Figure 11.7) exhibit a red-shift compared to those of  $^3\mathbf{52}$  (Figure 11.5).<sup>197</sup> This is reasonable because both of these species have very similar open-shell electronic configurations ( $^3A_2$  and  $^1A_2$ ).

The decay of  $^1\mathbf{52}$  in pentane was monitored at 350 nm over a wide temperature range of 150–270 K. This allowed direct measurement of the rate constants for intersystem crossing ( $k_{\text{ISC}}$ ) and for rearrangement ( $k_{\text{R}}$ ), and the Arrhenius parameters for the latter.<sup>197</sup>

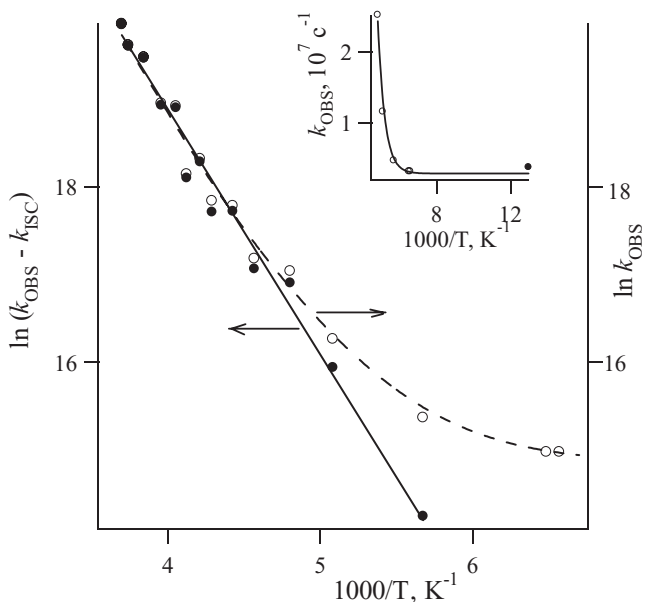


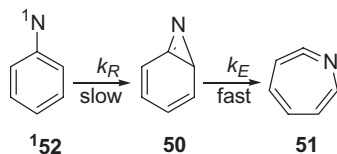
**Figure 11.8** Arrhenius treatment of the  $k_{\text{OBS}}$  data (open circles) and  $k_{\text{R}} = k_{\text{OBS}} - k_{\text{ISC}}$  (filled circles) for singlet phenylnitrene **152** deduced upon assuming that  $k_{\text{ISC}}$  is independent of temperature. Insert: temperature dependence of  $k_{\text{OBS}}$  data. Reprinted with permission from ref.<sup>197</sup> Copyright 1999 ACS Publications

The decay of **152** and the growth of the products (**51** and or **352**) are first order and can be analyzed to yield an observed rate constant,  $k_{\text{OBS}}$ . The magnitude of  $k_{\text{OBS}}$  decreases with decreasing temperature until about 170 K, whereupon it reaches a limiting value.<sup>197</sup> Analysis of this temperature dependence (Figure 11.8) gave the rate constant of intersystem crossing ( $k_{\text{ISC}} = 3.2 \pm 0.3 \times 10^6 \text{ s}^{-1}$ ) and the Arrhenius parameters for the rearrangement of **152** ( $E_{\text{a}} = 5.6 \pm 0.3 \text{ kcal/mol}$ ,  $A = 10^{13.1 \pm 0.3} \text{ s}^{-1}$ ).<sup>197</sup>

Recently,<sup>198</sup> the LFP of **47** was studied at 77 K where singlet nitrene **152** cleanly relaxes to the triplet state **352**. The rate constant of intersystem crossing at 77 K was found to be  $3.8 \pm 0.3 \times 10^6 \text{ s}^{-1}$ . Thus  $k_{\text{ISC}}$  for **152** is indeed temperature independent. The spectrum of **152** at 77 K is similar to that detected in solution (Figure 11.7, spectrum 1).<sup>197,198</sup>

Scheme 11.27 describes the rearrangement of **152** to **51** as one-step reaction. However, the computational work of Karney and Borden<sup>106</sup> demonstrates this to be a two-step process involving benzazirine **50**, the species trapped by ethanethiol (Scheme 11.24). The first step, cyclization of **152** to the azirine **50**, is predicted to be the rate-determining step (Scheme 11.28). The CASPT2 energetics of rearrangement is depicted in Figure 11.9.

The CASPT2 calculated barrier to cyclization of  $9.2 \text{ kcal/mol}$ <sup>106</sup> is somewhat higher than the experimental barrier of  $5.6 \pm 0.3 \text{ kcal/mol}$ .<sup>197</sup> The discrepancy between the calculated and experimental barrier heights is due to the general tendency of the CASPT2 method to overstabilize open-shell species (in this case,  $^1\text{A}_2\text{-3}$ ) relative to closed-shell species (in this case, all the other stationary points on the reaction path).<sup>199</sup> For an



**Scheme 11.28** Two-step rearrangement of singlet phenylnitrene to azepine

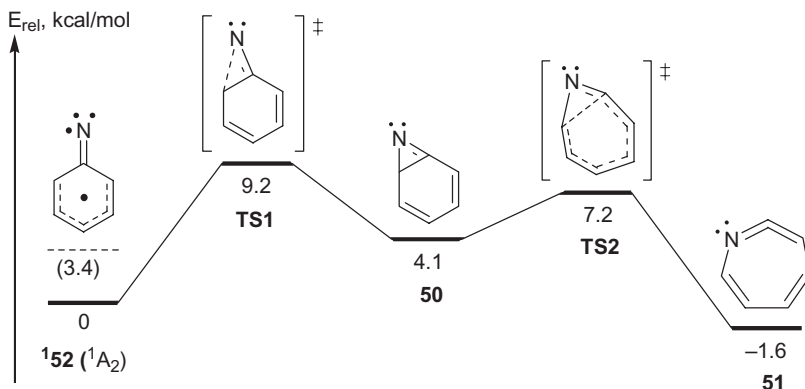


**Figure 11.9** Energetics of the ring expansion of singlet phenylnitrene **152** ( $^1A_2$ ), calculated at the CASPT2/6-311G(2d,p)//CASSCF(8,8)/6-31G(d) level. Reprinted with permission from ref.<sup>20</sup> Copyright 2006 ACS Publications

analogous system, the error was 3.4 kcal/mol.<sup>106</sup> Taking into account this error, the theoretical barrier for the cyclization of **152** is predicted to be 5.8 kcal/mol, which is in excellent agreement with the experimental activation energy ( $5.6 \pm 0.3$  kcal/mol).<sup>197</sup>

The CASPT2 barrier for the process **50**  $\rightarrow$  **51** is only ca. 3 kcal/mol, and this reaction is calculated to be exothermic by about 6 kcal/mol (Figure 11.9). These computational results are consistent with the failure to detect **50**.<sup>182,183</sup> Nevertheless, although **50** has not been observed spectroscopically, it can be intercepted by ethanethiol (Scheme 11.24).

On this basis, in recent reviews<sup>14,15,17,19,20</sup> the mechanism of phenyl azide photolysis described by Scheme 11.27 was accepted and supplemented by the two-step mechanism of the singlet phenylnitrene rearrangement to azepine **51** (Scheme 11.28).

However, the formation of azepine **51**, upon photolysis of **47**, in inert gas matrices was not fully understood.<sup>102,178–181</sup> Nevertheless, it was reasonably explained by the formation of **51** in the reaction of the hot singlet nitrene, **152**<sup>#</sup>.<sup>168,180</sup> This hypothesis is consistent with the results of recent studies of the photolysis of **47** and a series of its simple derivatives in solution at room temperature by femtosecond transient absorption spectroscopy<sup>154–157</sup> and femtosecond IR spectroscopy.<sup>158</sup>

It was found that the N–N bond cleavage in aryl azides proceeds on a femtosecond time scale (ca. 100–500 fs).<sup>154–157</sup> For example, the times of formation of singlet nitrenes in acetonitrile produced upon excitation at 266 nm are  $\sim 100$  fs for biphenyl-4-yl nitrene and  $280 \pm 150$  fs for biphenyl-2-yl nitrene<sup>155,156</sup> and the singlet aryl nitrenes are formed

with an excess of vibrational energy. Moreover, the shorter excitation wavelength results in a greater excess of vibrational energy. Vibrational cooling proceeds on a picosecond time scale (10 ps for singlet biphenyl-4-yl nitrene in acetonitrile<sup>155,156</sup> and 11 ps for 3,5-dichlorobiphenyl-2-yl nitrene<sup>154</sup> in cyclohexane).

The singlet phenyl nitrene **152**, which is formed upon photodissociation of **47**, has a considerable excess of vibrational energy and can easily overcome the potential energy barrier for isomerization. Indeed, studies utilizing femtosecond time-resolved IR spectroscopy<sup>158</sup> have demonstrated that a portion of the total yield of ketenimine **51** is formed on a picosecond time scale. The ketenimine **51** was also formed in the vibrationally hot state. The formation of ketenimine **51** and its vibrational cooling proceed within 10–50 ps. Unfortunately, attempts to separate these two processes and determine the characteristic time of the ketenimine formation failed.<sup>158</sup>

The vibrational cooling of the singlet nitrene **152** competes with its transformation to ketenimine **51** on a picosecond time scale.<sup>158</sup> The singlet nitrene **152** in its ground vibrational state also undergoes two-step transformation to the same product **51** with a time constant ~1 ns in pentane at ambient temperature.<sup>195–197</sup>

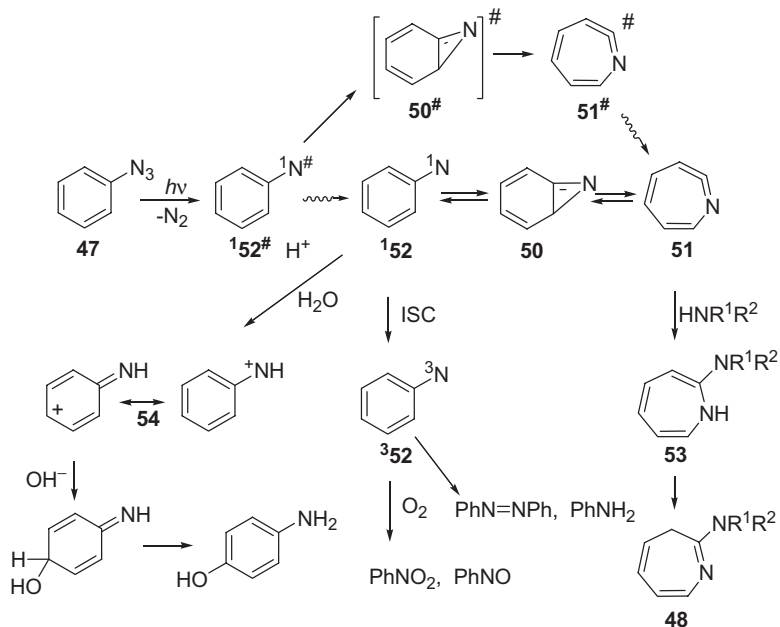
Due to its short lifetime, the singlet phenyl nitrene **152** has never been trapped chemically, the only exception being protonation with the formation of phenyl nitrenium ion **54**.<sup>200–202</sup> It was predicted theoretically, that **54** has a singlet ground state which is favored by 21.2 kcal/mol over the lowest triplet state.<sup>203</sup> Protonation of **152** competes with its isomerization to **51** only at low pH ≤ 1.<sup>200</sup> McClelland and co-workers performed product analysis and LFP studies of the photolysis of phenyl azide in water at pH = 0–2 and proposed a mechanism of reactions of nitrenium ion **54** (Scheme 11.29).<sup>200,201</sup> The nitrenium ion **54** reacts with water or other nucleophiles yielding substituted anilines.<sup>200,201</sup> Note, that lifetime of **152** in water (25–50 ps) was estimated to be much shorter than in hydrocarbons (~1 ns).

Recently, the nitrenium ion **54** was directly detected by transient absorption spectroscopy in pure formic acid.<sup>202</sup> The decay of nitrene **152** ( $\tau = 12$  ps) produces **54** with a broad absorption band centered at 500 nm. The lifetime of **54** is 110 ps in pure formic acid.<sup>202</sup>

Taking into account very recent results the mechanism of phenyl azide photolysis in condensed phase could be described as shown in Scheme 11.29.

Recently, the theoretical analysis of the PES along the reaction coordinate corresponding to the elimination of molecular nitrogen has been performed for phenyl azide and a number of its derivatives.<sup>156</sup> These PES sections were calculated for the ground ( $S_0$ ) and two excited ( $S_1$  and  $S_2$ ) states. It was predicted,<sup>156</sup> that the first excited singlet state of aryl azides apparently is dissociative. The second excited state ( $S_2$ ) is a bound state, and its geometry is similar to that of the ground  $S_0$  state. Moreover, the oscillator strength of the  $S_0 \rightarrow S_1$  transition is much lower than that of  $S_0 \rightarrow S_2$ . Thus, the absorption of the UV light leads to the population of the  $S_2$  state. The characteristic time of the formation of the vibrationally hot singlet nitrene (100–500 fs) most probably corresponds to the internal conversion from the  $S_2$  to the dissociative  $S_1$  state.

It was also found,<sup>156</sup> that the PES of the  $S_0$  and  $S_1$  states intersect. This means that the  $S_0$  state of phenyl azide correlates with ground state of the molecular nitrogen and the upper state of singlet nitrene (the closed-shell  $^1A_1$  state). In turn, the phenyl azide  $S_1$  state correlates with ground state molecular nitrogen and the lowest state of singlet nitrene (the open-shell  $^1A_2$  state). Consequently, the  $S_1$  state of phenyl azide and some of its



**Scheme 11.29** Full scheme of the condensed phase photochemistry of phenyl azide **47**<sup>14,15,17,19,20,158,200–202</sup>

derivatives can undergo very fast relaxation to the ground state through the conical intersection. This explains why, in spite of the very short time of singlet nitrene formation, the quantum yield of the phenyl azide photodissociation is much less than unity. It was measured to be about 0.5 at ambient temperature and in glasses at 77 K.<sup>204–206</sup>

Therefore, the mechanism of phenyl azide photolysis is now understood in detail. Most of the intermediates have been directly detected and their spectroscopy and reactivity have been studied experimentally and analyzed theoretically. It should be noted that great progress has been achieved only in the last decade.

### 11.6.2 Photochemistry of Simple Derivatives of Phenyl Azide

The photochemistry of simple derivatives of **47** has also been studied in solution using product analysis and time-resolved techniques and in matrices at cryogenic temperatures using spectroscopic methods.<sup>11–13,162</sup> In the last decade, a comprehensive study of the substituent effect on the reactivity of phenylnitrenes have been performed.<sup>154,207–214</sup> The influence of substituents on the spectroscopy and dynamics of singlet phenylnitrene has been reviewed recently.<sup>19,20</sup>

Photolysis of most substituted phenyl azides in hydrocarbons, as in the case of parent **47**, leads to modest yields of identifiable products (azo-benzenes, nitro- and nitroso-benzenes, anilines etc.) along with polymeric tars or resins.<sup>162</sup> Formation of azepines in the presence of primary and secondary amines is also typical of photolysis of the most substituted phenyl azides.<sup>162,183</sup> In some cases, the products of formal bond insertion or

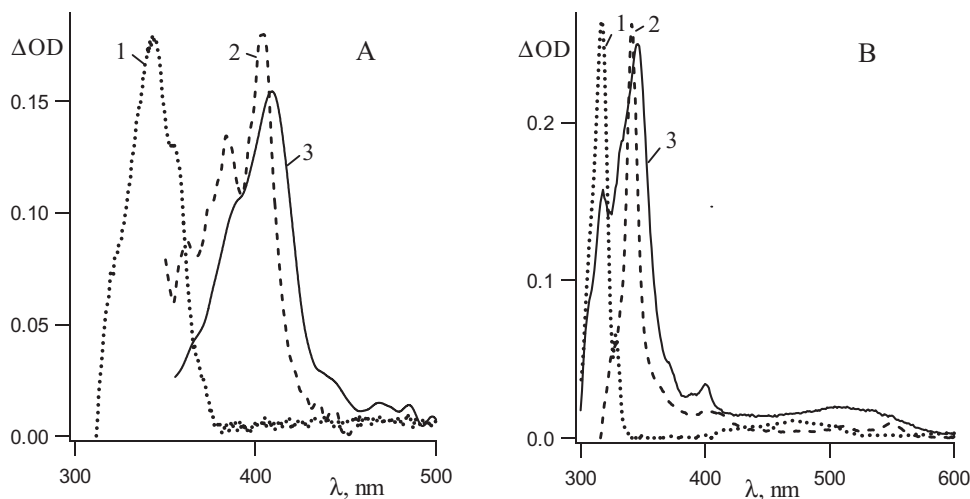


**Figure 11.10** A: Transient absorption spectra recorded after laser excitation (266 nm, 35 ps) of *para*-phenyl (1), *ortho*-dicyano (2) and *ortho*-phenyl (3) substituted phenyl azides in pentane. B: The difference absorption spectra of triplet *para*-phenyl (1), *ortho*-dicyano (2) and *ortho*-phenyl (3) substituted phenylnitrenes in glassy methylcyclohexane at 77 K

addition to the double bonds were also identified.<sup>12,13,19,162</sup> A number of *ortho*-substituted phenyl azides give clean reactions with high yields of identifiable products of cyclization involving the *ortho*-substituent.<sup>162</sup> The variety of products formed upon the aryl azide photolysis is a result of different reactions of the reactive intermediates – arylnitrenes, azirines and azepines. Therefore, the influence of the substituents on the reactivity of these intermediates will be discussed in this section.

The transient absorption spectra of a series of substituted singlet phenylnitrenes are characterized by an intense absorption band in the near-UV or visible region with maxima at 320–440 nm (Figure 11.10A). Analysis of the data available verifies that the *ortho*-substituents influence the absorption spectra of singlet phenylnitrenes more significantly than do *para*-substituents.<sup>19</sup> Moreover, the shift of the near-UV absorption band of singlet arylnitrenes correlates with the shift of the intense near-UV absorption bands of triplet nitrenes (Figure 11.10A,B).

The values of  $k_{\text{OBS}}$  in the substituted singlet phenylnitrenes were also measured over a wide temperature range.<sup>154,207–214</sup> As in the case of **52** (Figure 11.8), the magnitude of  $k_{\text{OBS}}$  decreases as the temperature decreases, until a limiting value is reached (Figure 11.11). The temperature-independent rate constant, observed at low temperature, was associated with intersystem rate constant –  $k_{\text{ISC}}$ .

In addition, the  $k_{\text{ISC}}$  of **52** and a series of its *ortho*-dialkyl derivatives,<sup>198</sup> as well as *para*- and *ortho*-biphenylnitrenes<sup>154,214</sup> were measured recently in glassy matrices at 77 K. It was demonstrated that the  $k_{\text{ISC}}$  measured at 77 K and estimated from liquid phase measurements are in very good agreement (Table 11.1). Thus, the value of  $k_{\text{ISC}}$  is indeed temperature independent and could be estimated from the analysis of the temperature dependence of  $k_{\text{OBS}}$  (Figure 11.11).

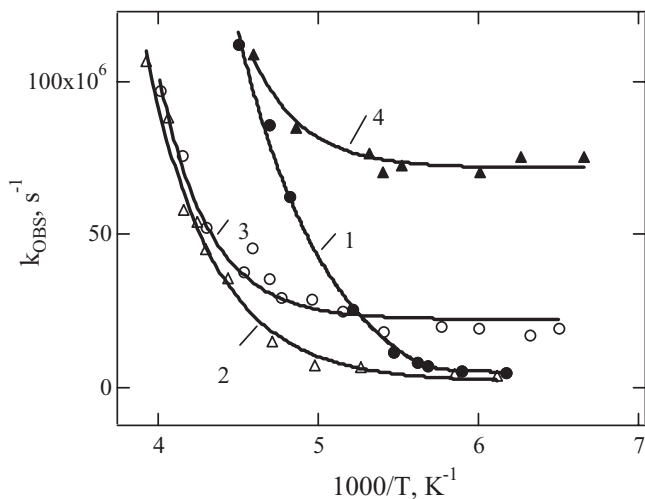


**Figure 11.11** Temperature dependence of the  $k_{\text{OBS}}$  values of para-fluoro (1), para-chloro (2), para-bromo (3), and para-iodo (4) singlet phenylnitrene in pentane. Reprinted with permission from ref.<sup>208</sup> Copyright 1999 ACS Publications

**Table 11.1** Kinetic parameters of para substituted singlet aryl nitrenes ( $X\text{-C}_6\text{H}_4\text{-N}$ ) in pentane

Para-X	$\tau_{295\text{K}}$ ns	$k_{\text{ISC}}$ ( $\times 10^6 \text{ s}^{-1}$ )	$E_a$ (kcal/mol)	Log A ( $\text{s}^{-1}$ )	Ref.
H	~1	$3.2 \pm 0.3$ ~3.8 <sup>a</sup>	$5.6 \pm 0.3$	$13.1 \pm 0.3$	197 198
CH <sub>3</sub>	~1	$5.0 \pm 0.4$	$5.8 \pm 0.4$	$13.5 \pm 0.2$	208
CF <sub>3</sub>	1.5	$4.6 \pm 0.8$	$5.6 \pm 0.5$	$12.9 \pm 0.5$	208
C(O)CH <sub>3</sub>	5.0	$8 \pm 3$	$5.3 \pm 0.3$	$12.5 \pm 0.3$	208
F	~0.3	$3.5 \pm 1.4$	$5.3 \pm 0.3$	$13.2 \pm 0.3$	208
Cl	~1	$3.9 \pm 1.5$	$6.1 \pm 0.3$	$13.3 \pm 0.3$	208
Br	~3	$17 \pm 4$	$4.0 \pm 0.2$	$11.4 \pm 0.2$	208
I	b	$72 \pm 10$	b	b	208
OCH <sub>3</sub>	<1	>500	b	b	208
CN	$8 \pm 4$	$6 \pm 2$	$7.2 \pm 0.8$	$13.5 \pm 0.6$	212
Ph	$15 \pm 2$	$12 \pm 1$ $9.3 \pm 0.4^a$	$6.8 \pm 0.3$	$12.7 \pm 0.3$	214 214
N(CH <sub>3</sub> ) <sub>2</sub> <sup>c</sup>	0.12	$8300 \pm 200$	b	b	216
NO <sub>2</sub> <sup>d</sup>	<20	>50	b	b	217

<sup>a</sup> Measured at 77 K in 3-methylpentane glassy matrix,

<sup>b</sup> not measured,

<sup>c</sup> in toluene,

<sup>d</sup> in benzene.

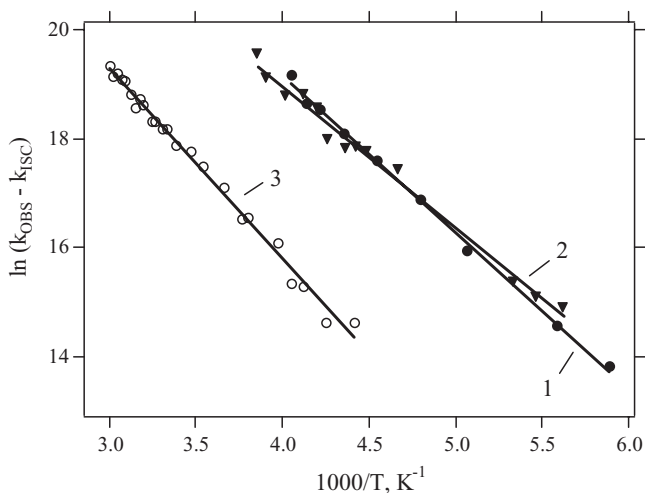


**Figure 11.12** Arrhenius treatment of the  $k_R (=k_{OBS} - k_{ISC})$  data for singlet *para*-methyl (1), *ortho*-methyl (2) and *ortho,ortho*-dimethyl- (3) phenylnitrene in pentane. Reprinted with permission from ref.<sup>209</sup> Copyright 1999 ACS Publications

After taking into account that  $k_{ISC}$  is temperature independent, plots of  $\ln(k_{OBS} - k_{ISC})$  were used to deduce the Arrhenius parameters for cyclization of the substituted singlet arylnitrenes (Figure 11.12, Tables 11.1 and 11.2).

Table 11.1 demonstrates that there is a noticeable heavy atom (Br, I) effect on  $k_{ISC}$ . However, the influence of the  $\pi$  donating substituents ( $OCH_3$ ,  $N(CH_3)_2$ ) is more pronounced. This is consistent with the solution phase photochemistry of *para*-methoxy and *para*-dimethylaminophenyl azides, which largely yield azobenzenes on photolysis.<sup>183</sup> It is interesting to note, that both electron donating and withdrawing substituents accelerate ISC. Noticeable acceleration of ISC (by a factor of 5) was also revealed for *ortho*-alkyl and *ortho,ortho*-dialkyl substituents (Table 11.2).<sup>198,209</sup> Thus, all simple derivatives of phenylnitrene have a  $k_{ISC}$  value similar or higher than that of parent **152**.

Unfortunately, there is no straightforward explanation for the substituent effect on the ISC rate for arylnitrenes. It was only concluded that the vibrationally-averaged SOC matrix elements are required for a quantitative description of the ISC in arylnitrenes.<sup>215</sup>

Table 11.1 shows also that *para*-substituents have little influence on the rate constant of singlet phenylnitrene rearrangement,  $k_R$ . This is not very surprising given that theory predicts that singlet phenylnitrene has an open-shell electronic structure.<sup>106,189–192</sup> Therefore, cyclization of singlet arylnitrenes requires only that the nitrogen bend out of the molecular plane, so that the singly occupied  $\sigma$  non-bonding molecular orbital (NBMO) can interact with the singly occupied  $\pi$  NBMO.<sup>106</sup> Azirine formation is simply the cyclization of a quinoidal 1,3-biradical, which originally has two orthogonal, anti-parallel spins. Thus, large substituent effects are not anticipated.

Note, that similar to the case of **47**, photolysis of a series of *para*- and *meta*-substituted phenyl azides in nitrogen and argon matrices at 12 K yield corresponding ketenimines as major products.<sup>218</sup>

**Table 11.2** Kinetic parameters of *ortho*-substituted phenylnitrenes in Hydrocarbons

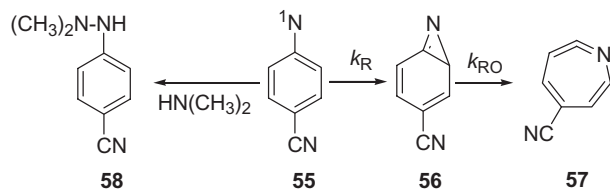
Substituent	$\tau_{295K}$ , ns	$k_{ISC}$ ( $\times 10^6 s^{-1}$ )	Log A ( $s^{-1}$ )	$E_a$ (kcal/mol)	Ref
2-methyl ( <b>59a</b> )	$\sim 1$	$10 \pm 1$	$12.8 \pm 0.3$	$5.3 \pm 0.4$	209
2,6-dimethyl ( <b>59b</b> )	$12 \pm 1$	$15 \pm 3$	$13.0 \pm 0.3$	$7.0 \pm 0.3$	209
2,4,6-trimethyl ( <b>59c</b> )	$8 \pm 1$	$29 \pm 3$	$13.4 \pm 0.4$	$7.3 \pm 0.4$	209
2,6-diethyl ( <b>59d</b> )	$\sim 9$	$10 \pm 2^a$	$12.1 \pm 0.5$	$5.2 \pm 0.5$	198
2,4,6-tri- <i>tert</i> -Bu ( <b>59f</b> )		6.8	–	–	198
2-fluoro ( <b>62a</b> )	$8 \pm 1$	$3.3 \pm 0.5$	$13.0 \pm 0.3$	$6.7 \pm 0.3$	213
2,6-difluoro ( <b>62d</b> )	240	$2.4 \pm 0.3$	$11.5 \pm 0.5$	$7.3 \pm 0.7$	213
2,3,4,5,6,-penta- fluoro ( <b>62e</b> )	$56 \pm 4$	$3.3 \pm 1.5$	$12.8 \pm 0.6$	$7.8 \pm 0.6$	213
2-cyano	$\sim 2$	$2.8 \pm 0.3$	$12.8 \pm 0.3$	$5.5 \pm 0.3$	212
2,6-dicyano	$\sim 2.3$	$6.2 \pm 0.8$	$13.5 \pm 0.2$	$6.5 \pm 0.4$	212
2-pyrimidyl	$\sim 13^b$	$80 \pm 20$	–	–	210
2-phenyl	$0.016^c$	$17 \pm 1^a$	–	–	214
2-phenyl-4,6-dichloro	0.26	$14 \pm 1^a$	$11.6 \pm 0.2^d$	$2.7 \pm 0.2^d$	154

<sup>a</sup> Measured at 77 K in 3-methylpentane glassy matrix;

<sup>b</sup> 295 K,  $CH_2Cl_2$ ;

<sup>c</sup> 295 K,  $CH_3CN$ ;

<sup>d</sup> the effective Arrhenius parameters.

**Scheme 11.30** Reactions of singlet *para*-cyanophenylnitrene<sup>212,219</sup>

Two *para* substituents, phenyl and cyano, depress  $k_R$  and retard the rate of cyclization significantly (Table 11.1). Phenyl and cyano are both radical stabilizing substituents. When attached to the carbon atom *para* to the nitrene nitrogen, these substituents concentrate spin density at this carbon and reduce the spin density at the carbons *ortho* to the nitrene nitrogen. The reduced spin density at carbons *ortho* to the nitrogen atom lowers the rate at which the 1,3-biradical cyclizes. The lifetimes of these singlet nitrenes at ambient temperature are 15 ns (phenyl) and 8 ns (cyano) and the activation barriers to cyclization are 6.8<sup>214</sup> and 7.2 kcal/mol,<sup>212</sup> respectively, compared to 5.6 kcal/mol for parent **52**. These results are in quantitative agreement with the CASPT2/6-31G\* calculations.<sup>212,214</sup> The longer lifetime of singlet *para*-cyanophenylnitrene (**55**) explains the high yield (>70%) of hydrazine (**58**) observed upon photolysis of *para*-cyanophenyl azide in dimethylamine (Scheme 11.30).<sup>219</sup>

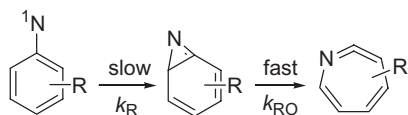
No traces of the 3*H*-azepines were reported among the products of *para*-nitro- and *para*-dimethylaminophenyl azide photolysis in the presence of diethylamine<sup>183</sup> or even in neat dimethylamine.<sup>219a</sup> This agrees with the results of calculations of Cramer and co-

authors.<sup>215</sup> In the case of the highly electron-withdrawing NO<sub>2</sub> substituent, the barrier to cyclization was calculated to be 1 kcal/mol higher than that for parent <sup>1</sup>52. For the highly electron-donating NHMe substituent, this barrier is about 4 kcal/mol higher than that of <sup>1</sup>52.<sup>215</sup> The predicted reduction of the reactivity, along with much faster ISC (Table 11.1), accounts for the absence of 3H-azepines for these *para*-substituted phenyl azides. Photolysis of *para*-azidoaniline in an argon matrix also yields mainly triplet nitrene.<sup>175</sup> Secondary photolysis of the triplet *para*-aminophenylnitrene gives not only ketenimine, but the corresponding azirine as well.<sup>175</sup>

The influence of *ortho*-substituents on the singlet aryl nitrene rearrangement is more pronounced. Thus photolysis of *ortho*-alkyl substituted aryl azides (e.g. *o*-methyl, *o*-ethyl and *o*-isopropyl) in diethylamine affords nucleophilic trapping products that are consistent with initial cyclization of singlet nitrene to the unsubstituted *ortho* carbon only.<sup>220</sup> Murata and Tomioka have observed the tetracyanoethylene trapping of singlet 2,4,6-tri-methylphenylnitrene, as well as of its ring-expansion product.<sup>221</sup> The cyclization of singlet nitrene to the unsubstituted *ortho* carbon only was observed also in the case of *ortho*-fluorophenylnitrene.<sup>222</sup> These results<sup>220–222</sup> demonstrate that steric effects play a role in determining the barrier to ring expansion.

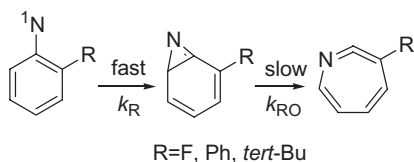
On the other hand, singlet *ortho*-cyano<sup>211,223</sup> and *ortho*-acetylphenylnitrenes<sup>224</sup> undergo cyclization not only away from the substituent, but also toward the cyano or acetyl group. Both steric and electronic effects play important roles in these cases and nearly cancel each other.<sup>212</sup>

For most *ortho*-substituted phenylnitrenes, as well as for *para*-substituted ones,<sup>198,207–214</sup> the cyclization to benzazirine is the rate-determining step of the process of nitrene isomerization to ketenimine (Scheme 11.31), similar to the case of the parent <sup>1</sup>52. The lifetimes of these singlet nitrenes and Arrhenius parameters for their rearrangement are summarized in Table 11.2.



**Scheme 11.31** The rearrangement of substituted phenylnitrenes

However for a few *ortho*-substituted phenylnitrenes (namely, *ortho*-fluorophenyl-, *ortho*-biphenyl- and 2,4,6-tri-*tert*-butylphenylnitrene), the ring-opening reaction was found to be the rate-limiting step (Scheme 11.31).<sup>154,198,213,214</sup> In the case of these nitrenes, the Arrhenius parameters for the ring-opening reaction ( $k_{RO}$ ,  $A_{RO}$ ,  $E_{RO}$ ) could be obtained (Table 11.3).

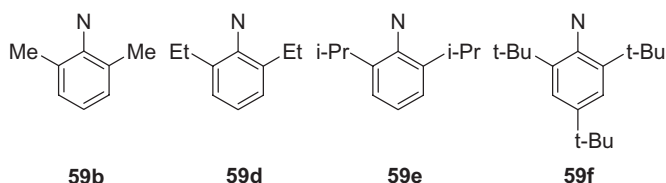


**Scheme 11.32** The rearrangement of some *ortho*-substituted phenylnitrenes

**Table 11.3** Lifetime of benzazirines, kinetic parameters for their ring-opening reaction in pentane and calculated barriers of this reaction ( $\Delta H^\ddagger$ )

Substituent	$\tau_{298}$ (ns)	$\log A_{RO}$ ( $s^{-1}$ )	$E_{RO}$ (kcal/mol)	$\Delta H^\ddagger$ (kcal/mol)	Ref
2,4,6-tri- <i>tert</i> -butyl	$62 \pm 2$	$12.6 \pm 0.2$	$7.4 \pm 0.2$	6.3	198
2-fluoro	$100 \pm 10$	$13.5 \pm 0.4$	$9.0 \pm 0.5$	7.0	213
2-phenyl	$13 \pm 1$	$12.1 \pm 0.1$	$5.7 \pm 0.2$	4.7	214
2-phenyl ( <i>d</i> <sub>9</sub> -analogue)	$11 \pm 1$	$12.6 \pm 0.1$	$6.3 \pm 0.1$	–	214

A detailed kinetic study<sup>209</sup> demonstrated that a single *ortho*-methyl substituent has no influence on the rate of cyclization of the singlet tolylnitrene (**59a**, Table 11.2). In contrast to the case of **59a**, cyclization of di-*ortho*-methyl substituted nitrenes **59b,c** necessarily proceeds towards a carbon bearing a substituent. In the case of **59b,c** the resulting steric effect extends the lifetimes of **59b,c** at ambient temperature to about 10 ns and raises the barrier to cyclization by about 1.5 kcal/mol,<sup>209</sup> in quantitative agreement with the results of CASPT2 calculations of Karney and Borden.<sup>225</sup> Note, that photolysis of *ortho,ortho*-dimethylphenyl azide in a nitrogen matrix at 12 K gives only triplet nitrene.<sup>226</sup>

**Scheme 11.33** Structures of the *ortho*-alkyl substituted singlet phenylnitrenes

Unexpected results were obtained for the rearrangement of singlet arylnitrenes with bulky *ortho*-alkyl substituents (**59d-f**).<sup>198</sup> The lifetimes of the nitrenes **59d** and **59e** were found to be shorter than that of **59b** and singlet nitrene **59f** was not observed in liquid solution due to its very short lifetime. The benzazirine **60f** was detected instead ( $\lambda_{max} = 285$  nm, Figure 11.13, spectrum 1) and proven to be a precursor of ketenimine **61f** (350 nm, Figure 11.13, spectrum 2). Therefore it was possible to measure the barrier for its ring-opening reaction (Table 11.3).<sup>198</sup>

According to the calculations,<sup>198</sup> the origin of the dramatic drop of the barrier in the case of **59f** is due to the strain released between the nitrogen atom and the alkyl substituent when the nitrogen atom moves away from the substituent during the cyclization (Scheme 11.34).

Theory predicts that the bulky alkyl substituents will alter not only the energy barrier of the first cyclization step but the second ring-expansion step as well.<sup>198</sup> Therefore in the case of **59f**, the rate-determining step is the second ring-expansion reaction as was found experimentally. The calculated barrier (6.3 kcal/mol) is very close to the experimentally determined activation energy of this reaction ( $E_{RO} = 7.4 \pm 0.2$  kcal/mol, Table 11.3).<sup>198</sup>

Unlike most arylnitrenes, polyfluorinated arylnitrenes have bountiful bimolecular chemistry (Scheme 11.36).<sup>12,227,228</sup> Therefore, polyfluorinated aryl azides are useful

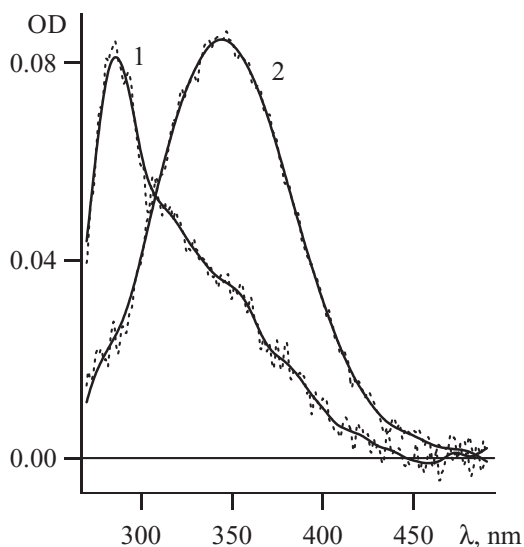
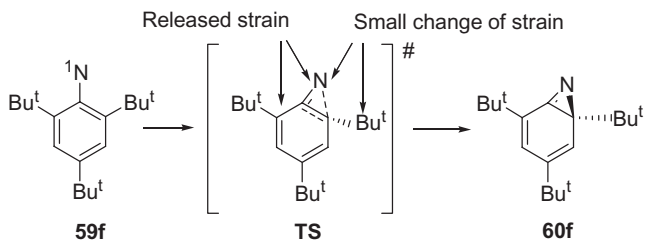
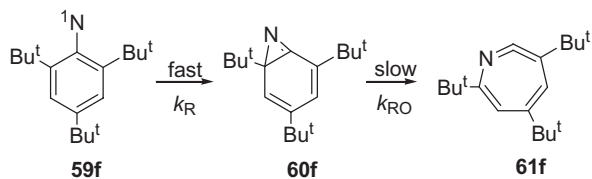


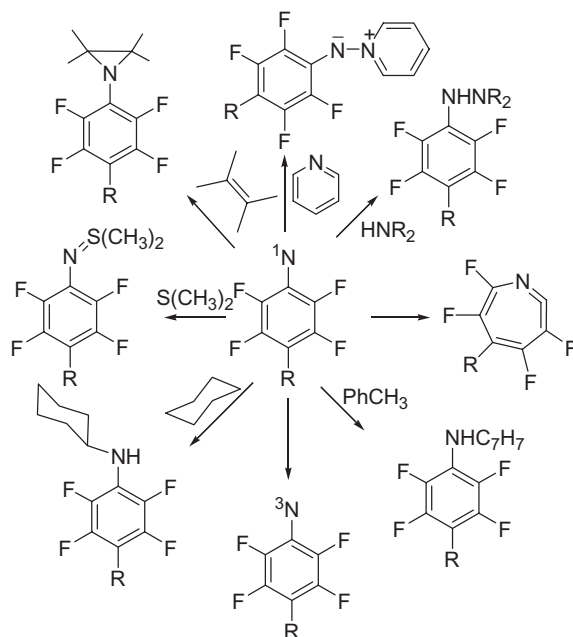
**Figure 11.13** Transient absorption spectra produced upon LFP (266 nm) of 2,4,6-tri-tert-butylphenyl nitrene in pentane at ambient temperature over a window of 10 ns just after the laser pulse (1) and 1  $\mu$ s after the laser pulse (2). Reprinted with permission from ref.<sup>20</sup> Copyright 2006 ACS Publications



**Scheme 11.34** Effect of the bulky ortho-tert-butyl substituent on the reaction of singlet nitrene cyclization



**Scheme 11.35** Two-step rearrangement of the singlet 2,4,6-tri-tert-butylphenyl nitrene **59f**<sup>198</sup>



**Scheme 11.36** Products of bimolecular reactions of singlet perfluorophenyl nitrenes

reagents in synthetic organic chemistry,<sup>229</sup> in photoaffinity labeling,<sup>7,230</sup> and for the covalent modification of polymer surfaces.<sup>9,10</sup>

The effects of the number and positions of fluorine substituents on the ring expansion of phenylnitrene have been extensively investigated by the Platz group.<sup>229,231</sup> They concluded that fluorine substitution at both *ortho* positions is required to inhibit the ring expansion effectively.<sup>12</sup> Similar to the case of *ortho,ortho*-dimethylphenyl azide,<sup>226</sup> photolysis of perfluoro- and *ortho,ortho*-difluorophenyl azides in a nitrogen matrix at 12 K gives only triplet nitrenes.<sup>232–234</sup>

To understand the fluorine effect quantitatively, the kinetics of fluoro substituted phenylnitrenes (**62a–d**, Figure 11.14) was studied<sup>213</sup> and the data were interpreted with the aid of molecular orbital calculations.<sup>213,225</sup>

Although the singlet *ortho*-fluorophenylnitrene (**62a**) undergoes cyclization to the unsubstituted *ortho* carbon only,<sup>222</sup> the barrier to this process is larger by ~1 kcal/mol than that of the parent system (Tables 11.1, 11.2). Placement of fluorine substituents at both *ortho* positions (**62d**) raises the barrier to cyclization by about 3 kcal/mol, relative to the unsubstituted system. Both results are consistent with the calculations of Karney and Borden (Figure 1.14).<sup>225</sup>

According to the calculations,<sup>213</sup> the origin of the pronounced influence of *ortho*-fluoro substitution on prolonging the lifetime of singlet aryl nitrene **62d** and increasing the activation energy for cyclization is due to a combination of the steric effect and the extraordinary electronegativity of the fluorine atom which reinforce each other.

The nitrene **62a** was the first singlet aryl nitrene for which the ring-opening reaction was experimentally found to be the rate-determining step of rearrangement to azepine.<sup>213</sup>

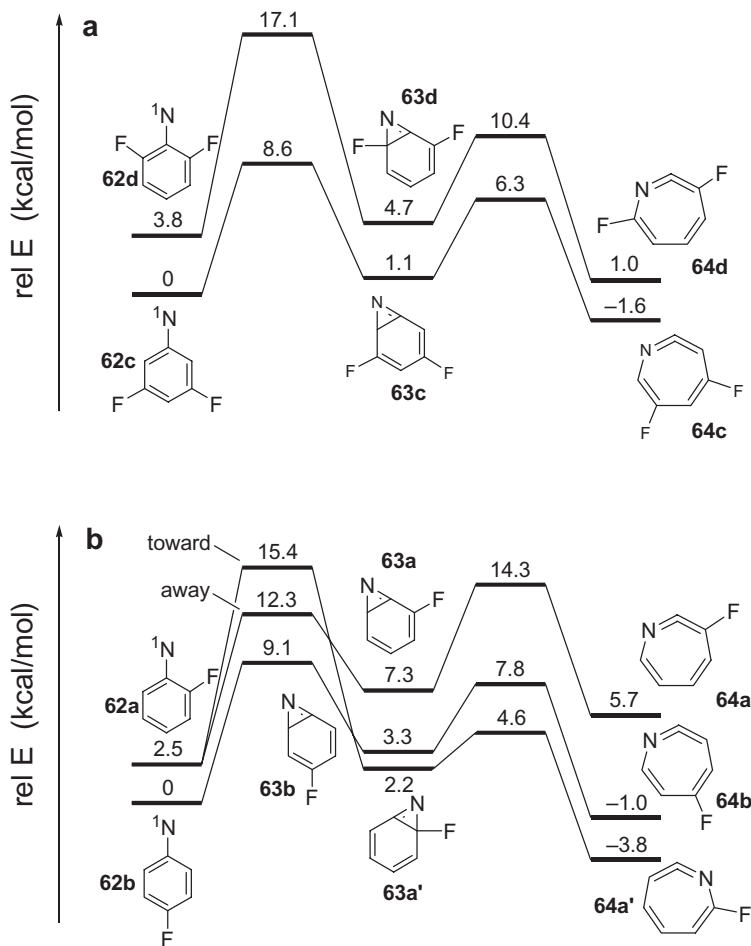


**Figure 11.14** Relative energies (in kcal/mol) of species involved in the ring expansions of singlet fluoro-substituted phenylnitrenes calculated at the CASPT2/cc-pVDZ//CASSCF(8,8)/6-31G\* level. (a) Difluorinated phenylnitrenes. (b) Monofluorinated phenylnitrenes. Reprinted with permission from ref.<sup>213</sup> Copyright 2001 ACS Publications

This is consistent with the results of CASSCF/CASPT2 calculations (Figure 11.14).<sup>213</sup> As shown in Figure 11.14, in all cases except the ‘away’ ring expansion of **62a**, the transition state for the second step of the ring expansion (**63** → **64**) is computed to be lower in energy than that for the first step (**62** → **63**) at the CASPT2 level of theory. The rate constant,  $k_{RO}$ , for the ring-opening reaction of **63a** was measured and the Arrhenius parameters were found to be  $A_{RO} = 10^{13.5 \pm 0.4} \text{ M}^{-1} \text{ s}^{-1}$  and  $E_{RO} = 9000 \pm 500 \text{ cal/mol}$  (Table 11.3).

The addition of the second fluorine substituent (benzazirine **63d**) decreases the barrier to conversion of azirine **63d** to ketenimine **64d** slightly (Figure 11.14), although the

**Table 11.4** Rate constants of reaction of substituted ketenimines (1,2-didehydroazepines) with diethylamine (DEA) in cyclohexene<sup>182,183,212</sup>

XPhN <sub>3</sub> , X	k <sub>DEA</sub> , M <sup>-1</sup> s <sup>-1</sup>	XPhN <sub>3</sub> , X	k <sub>DEA</sub> , M <sup>-1</sup> s <sup>-1</sup>	XPhN <sub>3</sub> , X	k <sub>DEA</sub> , M <sup>-1</sup> s <sup>-1</sup>
H	6.5 × 10 <sup>6</sup>	<i>p</i> -CO <sub>2</sub> NMe <sub>2</sub>	4.4 × 10 <sup>7</sup>	<i>p</i> -CN	1.6 × 10 <sup>9</sup>
<i>p</i> -Ph	3.6 × 10 <sup>5</sup>	<i>p</i> -COMe	2.8 × 10 <sup>8</sup>	<i>o</i> -CN	3.5 × 10 <sup>9</sup>
<i>p</i> -SMe	1.6 × 10 <sup>5</sup>	<i>p</i> -Cl	1.3 × 10 <sup>8</sup>	<i>o,o</i> -diCN	8.3 × 10 <sup>9</sup>
<i>p</i> -OMe	2.5 × 10 <sup>4</sup>	<i>p</i> -Br	1.7 × 10 <sup>8</sup>		
<i>p</i> -CO <sub>2</sub> H	3.0 × 10 <sup>7</sup>	<i>p</i> -I	2.7 × 10 <sup>8</sup>		

barrier for **63d** → **64d** is still predicted to be ca. 2.5 kcal/mol higher than the barrier for **50** → **51** at the same level of theory.<sup>106</sup> Note, that formation of the corresponding azirines was observed upon irradiation of triplet perfluoro- and *ortho,ortho*-difluorophenylnitrenes in an argon matrix at 77 K.<sup>233,234</sup>

It was mentioned previously that protonation of phenyl azide **152** yields phenylnitrenium ion (Scheme 11.29).<sup>200–202</sup> However, the protonation of **152** competes with its isomerization to **51** only at low pH ≤ 1.<sup>200</sup> Surprisingly, the *para*-biphenylnitrene, 2-fluorenylnitrene and a series of their derivatives yield nitrenium ions without the added acids.<sup>200,235</sup> The water is the proton-donor in this case. The reactivity of these nitrenium ions has been studied in some detail,<sup>236,237</sup> since the nitrenium ions are proposed to be the DNA-binding intermediates responsible for carcinogenicity of aromatic amines.<sup>236,238</sup>

Along with the substituent effect on the reactivity of singlet phenylnitrenes, the influence of substituents on the reactions of ketenimines with nucleophiles was also studied in detail. As in the case of unsubstituted ketenimine **51**, its simple derivatives could be trapped by nucleophiles in solution.<sup>182–184</sup> The primary products, corresponding 1H-azepines, undergo subsequent isomerization to final products.<sup>162,184</sup> Reaction of ketenimines with primary and secondary amines is the most studied of the reactions with nucleophiles. Rate constants of this reaction with DEA (Table 11.4) were measured for a series of substituted ketenimines using TRIR spectroscopy,<sup>182,183</sup> as well as conventional LFP techniques.<sup>212</sup>

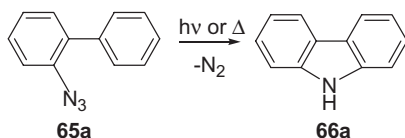
Table 11.4 demonstrates that substituents exert considerable influence on the rate constant of this reaction. The rate constant of reaction with DEA varies over more than 5 orders of magnitude depending on the nature and position of substituents and increases significantly with the electron-withdrawing power of the substituents.

Recently<sup>239</sup> the absolute rate constants of reactions of **51** and a number of its derivatives with typical amino acids, nucleosides and other simple reagents of biological interest were measured in water and HEPES buffer using LFP technique.

It is also known,<sup>183</sup> that ketenimines react with aryl azides, the rate constant of reaction between **51** and **47** is 7.5 × 10<sup>4</sup> M<sup>-1</sup> s<sup>-1</sup>. At very low concentration of aryl azides, the lifetimes of **51** and of its 5-iodo derivative was measured to be 4–5 ms<sup>183</sup> and 24 ms for the 5-methyl derivative<sup>173</sup> (i.e. *k*<sub>OBS</sub> ≈ 40–250 s<sup>-1</sup>). The latter values represent the rate of irreversible conversion of ketenimines to triplet arylnitrenes. In the absence of nucleophilic agents, photolysis of aryl azides yields typical products of triplet arylnitrene reactions – azo compounds and anilines in the absence of oxygen<sup>12,13,162,166,167,183</sup> and nitro and

**Table 11.5** Rate constant of reaction of triplet para-substituted phenylnitrenes ( $X-C_6H_4N_3$ ) with oxygen at ambient temperature<sup>172,173,241</sup>

X	H	CH <sub>3</sub>	NO <sub>2</sub>	NH <sub>2</sub>	NH <sub>2</sub>
$k, 10^6 M^{-1} s^{-1}$	2.4 ± 0.1	1.9 ± 0.2	0.8 ± 0.1	4.5 ± 1.2	8 ± 2
Solvent	CH <sub>3</sub> CN	CH <sub>3</sub> CN	C <sub>6</sub> H <sub>12</sub>	C <sub>6</sub> H <sub>12</sub>	PhCH <sub>3</sub>

**Scheme 11.37** Photolysis and thermolysis of ortho-biphenyl azide

nitroso compounds in the presence of oxygen.<sup>13,172–175</sup> The decrease of aryl azide concentration leads to the growth of detectable products.<sup>166,167,172,173</sup>

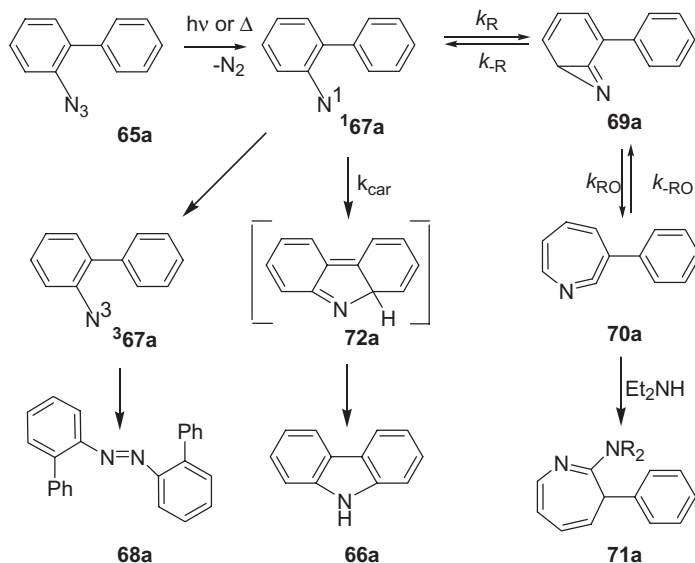
Reaction of triplet arylnitrenes with oxygen and subsequent reactions of primary intermediates – arylnitrosooxides, are reviewed earlier<sup>13,240</sup> and will not be discussed here. The rate constant of reaction of triplet arylnitrenes with molecular oxygen are presented in Table 11.5. It appeared that the rate constants are substantially lower than the diffusion limit and are in the range  $(0.8 - 8) \times 10^6 M^{-1} s^{-1}$ . For **352**, the temperature dependence for this reaction in acetonitrile was measured and the Arrhenius parameters were estimated ( $E_a = 4.3 \pm 0.5 \text{ kcal/mol}$ ,  $A = 10^{9.6 \pm 0.4} s^{-1}$ ).<sup>241</sup>

Alkyl, cyano, acetyl and fluoro substituents in the *ortho*-position do not change the mechanism of phenyl azide photochemistry influencing only the rate constants of elementary reactions ( $k_{ISC}$ ,  $k_R$ ,  $k_{RO}$ ,  $k_{NUC}$ ). At the same time, a number of photochemical and thermal cyclizations involving the *ortho*-substituents are known for *ortho*-substituted phenyl azides.<sup>162</sup> The most interesting, important and well understood reaction of this type is formation of carbazoles **66** on pyrolysis<sup>242</sup> and photolysis.<sup>154,184a,214,243,244</sup> of *ortho*-biphenyl azide **65a** and a series of its derivatives (Scheme 11.37).

Since the early 1970s, the reactive intermediates involved in the transformation of **65** to **66** were studied by trapping,<sup>184a,244</sup> matrix spectroscopy,<sup>169,177</sup> and flash photolysis.<sup>244b,245</sup> Swenton, Ikeler, and Williams<sup>243</sup> demonstrated that carbazole is derived from reaction of a singlet state species, presumably singlet nitrene **167a**, whereas triplet nitrene **367a** dimerizes to form azo compound **68**.

It was also demonstrated that, in the presence of DEA, photolysis of azide **65a** leads to the formation of 3H-azepine **71a** (Scheme 11.38), with a concomitant reduction in the yield of carbazole **66a**.<sup>183,244a</sup> The carbazole formation was measured at its absorption maximum (289.4 nm),<sup>244b,245</sup> and a rate constant was found to be  $2.2 \times 10^3 s^{-1}$  at 300 K in cyclohexane.<sup>243</sup> This value is about 5–6 orders of magnitude lower than the rate constants of singlet arylnitrenes rearrangement (Tables 11.1 and 11.2). Therefore, the following scheme (Scheme 11.38) could economically describe the early results.<sup>242–245</sup>

Recently the mechanism of carbazole formation upon photolysis of *ortho*-biphenyl azide (**65a**), its deuterio- (**65a-d**) and dichloro (**65b**) derivatives was studied in detail



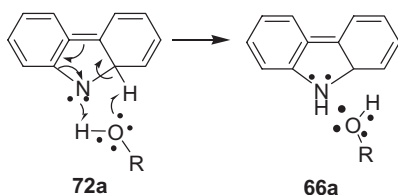
**Scheme 11.38** Mechanism of photolysis of ortho-biphenyl azide proposed based on the early studies<sup>243–245</sup>

using nanosecond laser flash photolysis,<sup>154,214</sup> time-resolved IR,<sup>158,214</sup> femtosecond transient absorption spectroscopy<sup>154–156</sup> and computational chemistry.<sup>154,156,214</sup>

LFP data obtained at room temperature<sup>214</sup> demonstrate that, in agreement with previous flash photolysis studies,<sup>244b,245</sup> carbazole **66a** is mainly formed on the millisecond time scale in pentane. Moreover, the characteristic ketenimine IR band was detected at  $1868\text{ cm}^{-1}$  in  $\text{CD}_3\text{CN}$ . This band appeared faster than the time resolution of the apparatus ( $\sim 100\text{ ns}$ ). The decay of this band was accompanied by the appearance of the carbazole band at  $1241\text{ cm}^{-1}$  with a rate constant of  $1.0 \pm 0.2 \times 10^4\text{ s}^{-1}$ , which is close to the value measured by Sundberg *et al.*<sup>244b</sup> The TRIR experiments thus demonstrate,<sup>214</sup> that ketenimine **70a** does indeed serve as a source of **66a** on the longer time scale, via the mechanism shown in Scheme 11.38.

In addition to the formation of **66a** on the millisecond time scale, discussed previously,<sup>244b,245</sup> some formation of **66a** was detected on the nanosecond time scale as well.<sup>214</sup> The ns growth of carbazole absorption at 290 nm was accompanied by the ns decay of a transient absorption in the visible region between 400 and 500 nm. The time constants for the growth and decay functions are equal to  $70 \pm 5\text{ ns}$  in pentane at ambient temperature. The precursor of **66a** was assigned to isocarbazole **72a** (Scheme 11.38).<sup>214</sup>

LFP of perdeuterated azide **65a-d<sub>6</sub>** at ambient temperature<sup>214</sup> demonstrated a pronounced kinetic isotope effect on the kinetics of carbazole formation on the ns time scale ( $k_{\text{H}}/k_{\text{D}} = 3.4 \pm 0.2$ ), which is consistent with the reaction being the isomerization of isocarbazole **72a** into carbazole **66a** by a 1,5-hydrogen shift. In addition methanol and water were found to accelerate the disappearance of the transient absorption of **72a** produced upon LFP of **65a** in pentane.<sup>214</sup> A reasonable mechanism for this catalysis is shown in Scheme 11.39.



**Scheme 11.39** Catalysis of isocarbazole isomerization by water<sup>214</sup>

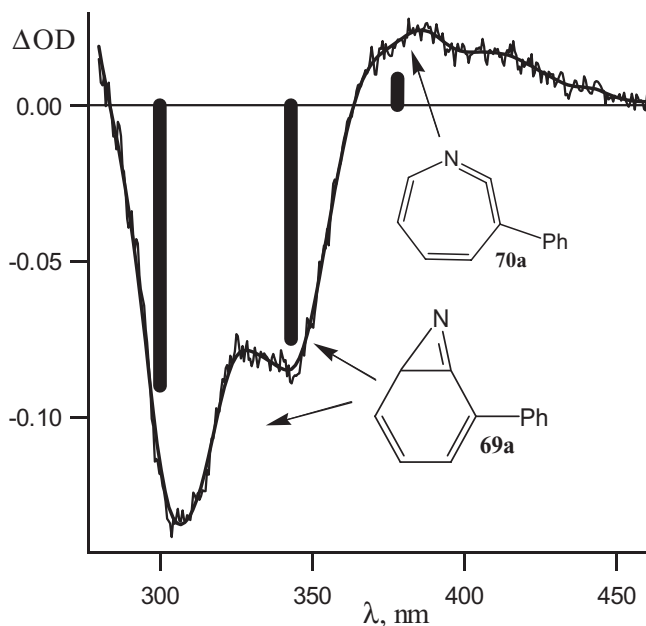
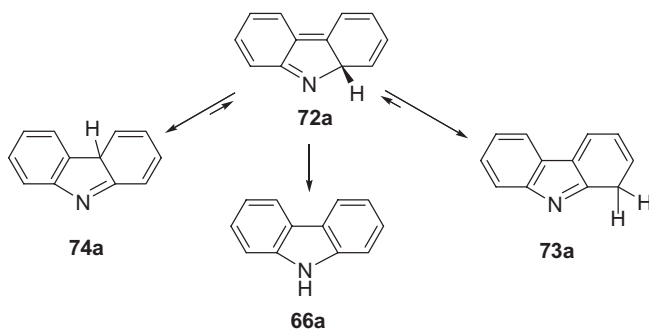


**Figure 11.15** The difference spectrum obtained by LFP of ortho-biphenyl azide **65a** in pentane at 161 K. The computed positions and relative oscillator strengths of the absorption bands of benzazirine **69a** and azepine **70a** are depicted as solid vertical lines (negative and positive, respectively)

Benzazirine **69a** has strong absorptions with maxima at ~305 and 340 nm and was observed upon the LFP of **65a** at low temperature (e.g. 160 K). Decay of **69a** was accompanied by azepine **70a** formation with absorption at 350–400 nm (Figure 11.15).<sup>214</sup>

In Freon-113 at ambient temperature, the lifetime of azirine **69a** is  $12 \pm 2$  ns, which is about 6 times shorter than that for isocarbazole **72a** disappearance and carbazole **66a** formation. The temperature dependence of the observed rate constants for the decay of azirines **69a** and **69a-d**, were studied and the activation parameters were found to be  $E_{\text{RO}} = 5.7 \pm 0.1$  kcal/mol and  $A_{\text{RO}} = 10^{12.1 \pm 0.1} \text{ s}^{-1}$  for **69a** and  $E_{\text{RO}} = 6.3 \pm 0.1$  kcal/mol and  $A_{\text{RO}} = 10^{12.6 \pm 0.1} \text{ s}^{-1}$  for **69a-d**, in satisfactory agreement with DFT calculations (Table 11.3).

At least one additional long lived intermediate absorbing in the range 350–450 nm was observed upon LFP of **65a**.<sup>214,244</sup> According to the DFT calculations,<sup>214</sup> isocarbazole **72a**



**Scheme 11.40** Mechanism of carbazole formation on a longer time scale

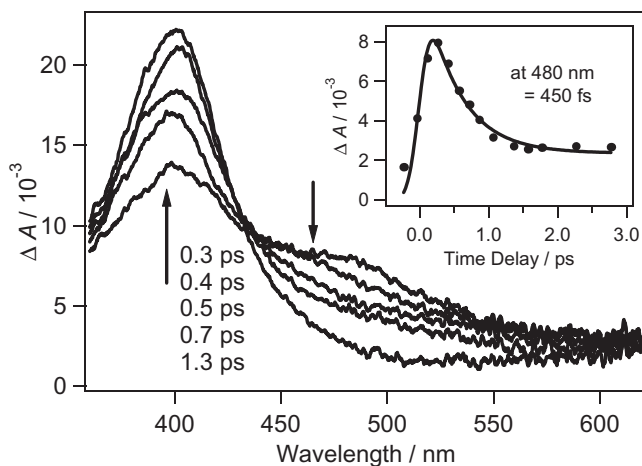


**Figure 11.16** Transient absorption spectra recorded between 0.3–1.3 ps after the laser pulse for *ortho*-biphenyl azide in acetonitrile. The time dependence of the signal measured at 480 nm is shown as inset. Reprinted with permission from ref.<sup>156</sup> Copyright 2006 ACS Publications

can undergo exothermic 1,5-hydrogen shifts to form not only carbazole **66a**, but isomeric isocarbazoles **73a** and **74a** (Scheme 11.40) as well. Both of these isocarbazoles were predicted to have intense absorption around 360 nm. Presumably, subsequent 1,5-shifts in **73a** and **74a**, reform **72a**, and eventually yield more carbazole **66a**, seconds to minutes after the laser pulse (Scheme 11.40).<sup>214</sup> Therefore the formation of carbazole is not only biphasic, but is most probably triphasic.

The spectrum ( $\lambda_{\max} = 410$  nm) and kinetics of singlet *ortho*-biphenylnitrene **167a** were recorded by LFP of **65a** in glassy 3-methylpentane at 77 K. The lifetimes of **167a** and **167-d**, at 77 K are equal to  $59 \pm 3$  ns and  $80 \pm 2$  ns, respectively.<sup>214</sup> A similar spectrum was detected recently at room temperature using femtosecond transient absorption spectroscopy (Figures 11.16 and 11.17).<sup>155,156</sup>

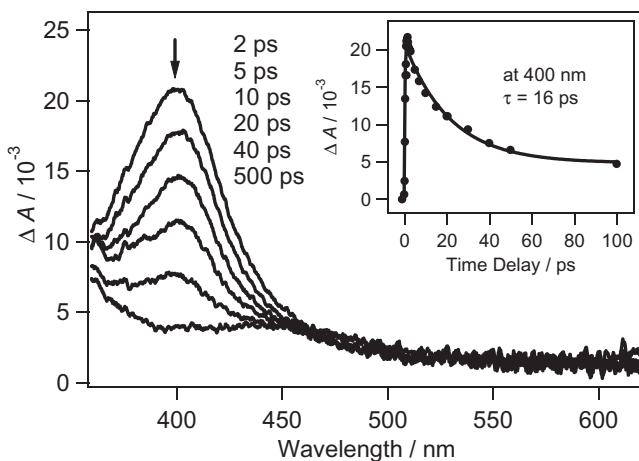


**Figure 11.17** Transient absorption spectra recorded between 2–500 ps for *ortho*-biphenyl azide in acetonitrile. The time dependences of the signal measured at 400 nm is shown as inset. Reprinted with permission from ref.<sup>156</sup> Copyright 2006 ACS Publications

It was found that the absorption of singlet nitrene **167a** grows with a time constant  $280 \pm 150$  fs and decays with time constant  $16 \pm 3$  ps. Note, that as in the case of phenyl azide **47**, the quantum yield of photolysis of **65a** is significantly less than unity (about 0.44 at ambient temperature and in glasses at 77 K).<sup>204</sup> Therefore, the  $S_1$  state of **65a**, similar to the case of parent system **47**, undergoes very fast relaxation to the ground state through the conical intersection.

The 16 ps time constant ( $k = 6.3 \times 10^{10} \text{ s}^{-1}$ ) represents the population decay time of singlet nitrene **167a** by isomerization to isocarbazole **72a** and benzazirine **69a** with the latter process being predominant. Assuming that the pre-exponential factor for cyclization of **167a** is  $\sim 10^{13} \text{ s}^{-1}$ , the activation energy could be estimated as  $\sim 3$  kcal/mol. This value is in excellent agreement with the (14/14) CASPT2/6-31G\*\*/(14,14)CASSCF/6-31G\* calculations (Figure 11.18),<sup>214</sup> if one takes into account the typical underestimation by  $\sim 3.4$  kcal/mol<sup>106</sup> of the energy of open-shell **167**. The *ortho*-phenyl group lowers the enthalpy of activation for cyclization, compared to parent phenylnitrene **152**, by destabilizing singlet nitrene **167a** sterically, as in the case of *ortho-tert*-butyl substituent (Scheme 11.34).<sup>198</sup> According to the calculations<sup>214</sup> both **69a** and **72a** should be formed from **167a**, however azirine **69a** should be the kinetically favored product around room temperature in accord with experiment.

It was mentioned above that formation of ketenimine **70a** from azirine **69a** proceeds on a nanosecond time scale ( $\tau \sim 12$  ns in Freon 113).<sup>214</sup> However, formation of vibrationally hot **70a** was also detected on a ps time scale in  $\text{CH}_3\text{CN}$  using time resolved IR spectroscopy.<sup>158</sup> Fits to the kinetic traces indicated that ketenimine **70a** is formed with a time constant of  $\sim 10$  ps and undergoes vibrational cooling with a time constant of  $\sim 29$  ps. These data demonstrate that as in the case of parent nitrene **152**, the singlet nitrene **167a** is born on a fs time scale with excess vibrational energy and isomerizes to vibrationally excited 1,2-dihydroazepine **70a** on a ps time scale.

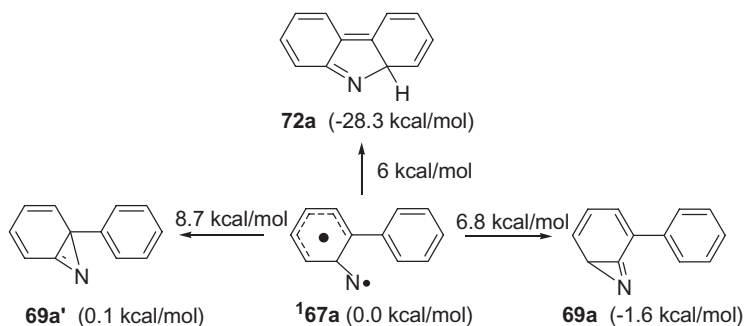
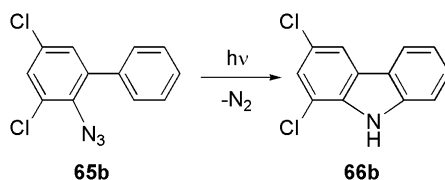


**Figure 11.18** Structures of the intermediates formed upon cyclization of singlet *ortho*-biphenylnitrene ( $^1\mathbf{67a}$ ), their electronic energies relative to the nitrene  $^1\mathbf{67a}$  (in parenthesis) and the energy differences between the transition states (TSs) and  $^1\mathbf{67a}$ . Reprinted with permission from ref.<sup>20</sup> Copyright 2006 ASC Publications



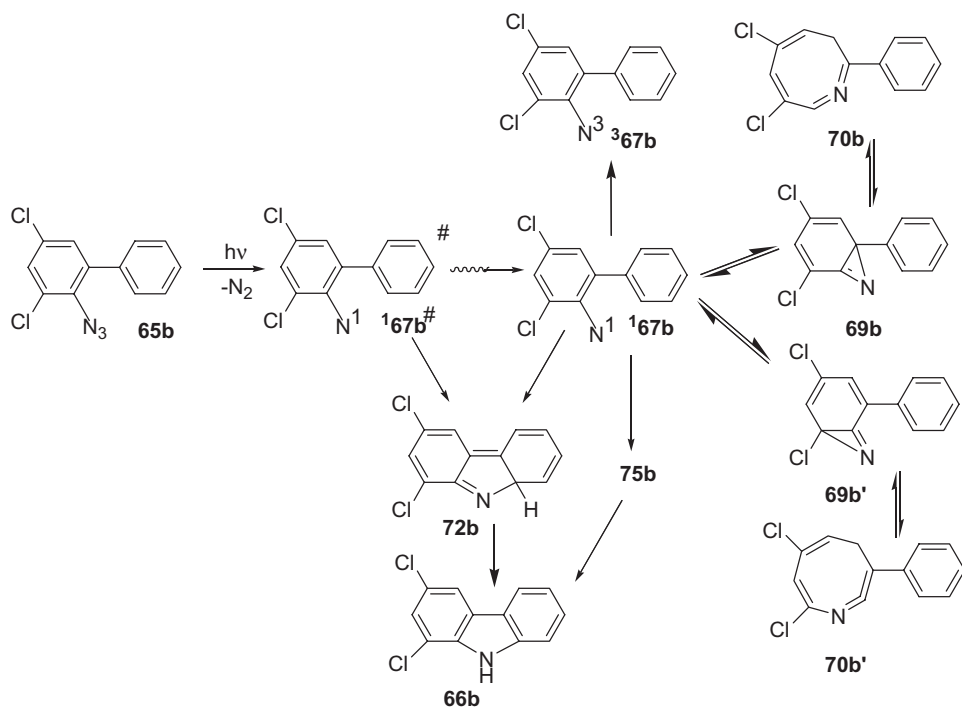
**Scheme 11.41** Photochemistry of 2-azido-3,5-dichlorobiphenyl ( $\mathbf{65b}$ )

Therefore, Scheme 11.38 represents the oversimplified mechanism of carbazole  $\mathbf{66a}$  formation upon photolysis of *ortho*-biphenyl azide  $\mathbf{65a}$  and should be supplemented with the processes described in Schemes 11.39 and 11.40, as well as by fast formation of  $\mathbf{70a}$  from a hot singlet nitrene  $^1\mathbf{67a}$ .

The chemistry of the unsubstituted *ortho*-biphenyl system is complicated by the fact that the key intermediate of this reaction,  $^1\mathbf{67a}$ , undergoes two cyclization processes at competitive rates, and that azepine formation is reversible. To simplify the chemistry of singlet nitrene and allow straightforward study of the isocarbazole formation, 2-azido-3,5-dichlorobiphenyl ( $\mathbf{65b}$ ) was synthesized (Scheme 11.41) and its photochemistry was studied using nano- and picosecond transient absorption spectroscopy.<sup>154</sup>

Indeed, the chlorinated carbazole  $\mathbf{66b}$  is produced predominantly on the nanosecond time scale and only to a minor extent from the corresponding didehydroazepines  $\mathbf{70b}$  and/or  $\mathbf{70b}'$  (Scheme 11.42).<sup>154</sup> The transient absorption in the visible region (Figure 11.19) was assigned to a mixture of two intermediates with maxima at 470 nm, 440 and 425 nm, respectively. One of the intermediates is isocarbazole  $\mathbf{72b}$  ( $\lambda_{\max} = 320$  and 470 nm). Its lifetime in pentane at room temperature is  $65 \pm 4$  ns and is  $263 \pm 4$  ns for perdeuterated analogue, similar to the case of  $\mathbf{72a}$ .<sup>154</sup> The second intermediate ( $\mathbf{75b}$ ,  $\lambda_{\max} = 360$ , 420 and 440 nm) unfortunately could not be identified.<sup>154</sup>

As in the case of  $\mathbf{65a}$ , the transient absorption spectrum of singlet nitrene  $^1\mathbf{67b}$  was detected at ambient temperature using a fs transient absorption spectroscopy and at 77 K



**Scheme 11.42** Mechanism of photolysis of 2-azido-3,5-dichlorobiphenyl (**65b**)

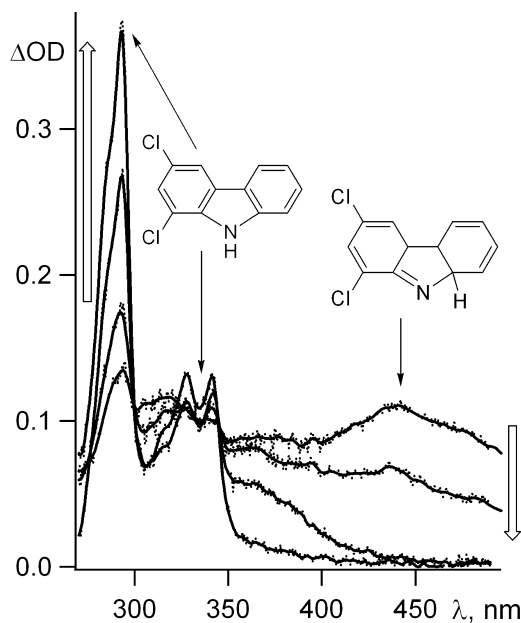


**Figure 11.19** Transient absorption spectra detected over a window of 10 ns following LFP of 2-azido-3,5-dichlorobiphenyl **65b** in pentane at ambient temperature 15 ns, 60 ns 1  $\mu s$  and 30 ms after the laser pulse

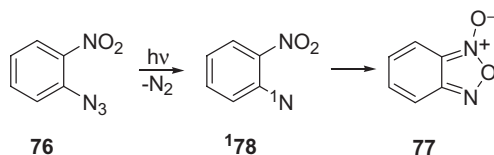
by conventional LFP.<sup>154</sup> The spectrum detected in cyclohexane 40 ps after the laser pulse was a mixture of spectra of at least two species – singlet nitrene **167b** and isocarbazole **72b**. It was proposed, that a part of isocarbazole **72b** is formed from vibrationally hot singlet nitrene **167b**. The time constant for vibrational relaxation of **167b** was estimated to be  $11 \pm 2$  ps.

The decay of vibrationally cooled **167b** was accompanied by the growth of isocarbazole **72b** with the rate constant  $k_{\text{OBS}} = 3.8 \pm 0.8 \times 10^9 \text{ s}^{-1}$  ( $\tau = 260 \pm 70$  ps).<sup>154</sup> A considerable acceleration of the singlet nitrene **167b** rearrangement was observed in methanol. The rate constant of its decay was found to be  $1.6 \pm 0.2 \times 10^{10} \text{ s}^{-1}$  ( $\tau = 62 \pm 10$  ps).<sup>154</sup> Nevertheless, this value is about 4 times lower than that for **167a** in  $\text{CH}_3\text{CN}$  ( $6.3 \times 10^{10} \text{ s}^{-1}$ ).<sup>155,156</sup> The main contribution to the latter process is the reaction of the azirine formation (**167a**  $\rightarrow$  **69a**). This process is significantly retarded by *ortho*-chlorine substitution and isocarbazole formation gives the main contribution to the decay of **167b**.

The decay of singlet nitrene **167b** in hydrocarbon solutions was measured in three different types of experiments and the Arrhenius parameters for the rate constant of **167b** rearrangement were estimated to be:  $E_a = 2.7 \pm 0.2 \text{ kcal/mol}$  and  $A = 10^{11.6} \pm 0.2 \text{ s}^{-1}$ .<sup>154</sup> The measured activation energy is in perfect agreement with the predicted barrier to isocarbazole formation ( $\sim 3 \text{ kcal/mol}$ ).<sup>154,214</sup>

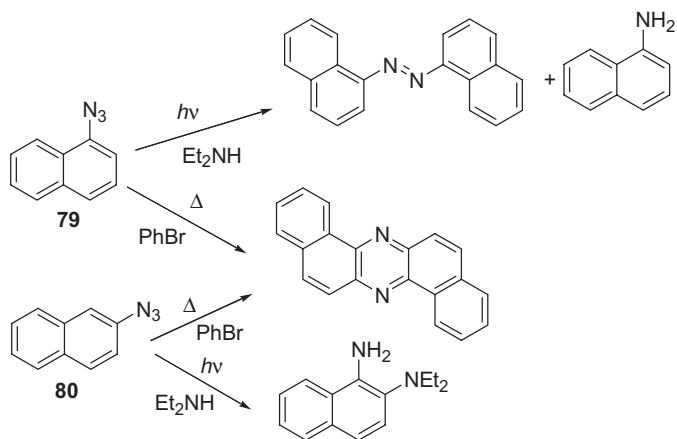
Unexpectedly, the yield of isocarbazole **72b** was found to depend on the energy of the photons used for the excitation of azide **65b**.<sup>154</sup> It drops significantly on going from excitation by a YAG (266 nm) to excimer (308 nm) laser radiation.<sup>154</sup> It is in line with the observation, that in part the isocarbazole **72b** is formed from vibrationally hot singlet nitrene **167b**.

Recently,<sup>157</sup> very fast intramolecular cyclization of singlet nitrene was observed upon photolysis of *ortho*-nitrophenyl azide (**76**). It is well known,<sup>246</sup> that pyrolysis and photolysis of **76** leads cleanly to benzofuroxan (**77**). According to the results of recent computational study<sup>247</sup> and early experiments,<sup>246a,b</sup> the pyrolysis of **76** produces **77** by a concerted one-step mechanism. However, photolysis of **76** produces **77** through a stepwise mechanism.<sup>157</sup> Formation of singlet nitrene **178** from excited **76** was detected to occur with a time constant  $\sim 500$  fs. The lifetime of nitrene **178** is very short – 8.3 ps, and corresponds to ring-closure reaction rate constant  $1.2 \times 10^{11} \text{ s}^{-1}$ .



**Scheme 11.43** Mechanism of photolysis of *ortho*-nitrophenyl azide

Therefore, the photochemical cyclizations of *ortho*-substituted aryl azides involving the *ortho*-substituents (such as formations of carbazoles upon photolysis of *ortho*-biphenyl azides and of benzofuroxan upon photolysis of *ortho*-nitrophenyl azide) are found to occur by stepwise mechanism with intermediacy of singlet nitrenes. The cyclizations of singlet nitrenes occur on a picosecond time scale.



**Scheme 11.44** Photolysis and pyrolysis of 1- and 2-azidonaphthalene

### 11.6.3 Photochemistry of Polynuclear Aromatic Azides

Fusion of a benzene ring to another aromatic ring or rings changes the electronic structure of the modified nitrenes and related intermediates sufficiently enough to alter their chemistry, kinetics and thermodynamics. Thus photolysis of polynuclear aromatic azides in the presence of primary and secondary amines leads not to 3H-azepines, but to corresponding diamino-products instead.<sup>162,170,248–250</sup> Nevertheless, in some cases photolysis and thermolysis of polynuclear aromatic azides yields the products (azo-compounds, nitro-compounds etc.) typical of photochemistry of phenyl azides.<sup>11,151,162,169–171,251</sup> For instance, photolysis of polycyclic aromatic azides in glassy matrixes at 77 K gives corresponding arylnitrenes in the ground triplet state, as was demonstrated by the EPR spectroscopy.<sup>170,171,251</sup> In solution, dimerization of triplet polynuclear aromatic nitrenes or their reaction with starting azides produces azo-compounds.<sup>169–171</sup> The photochemical and thermal reactions of polycyclic aromatic azides have been reviewed periodically.<sup>1,11,162,252</sup> Therefore, recent results will be mainly discussed in this chapter.

Much effort has been devoted to the study of the photochemistry of 1- and 2-naphthyl azides (**79** and **80**). The products obtained upon pyrolysis and photolysis of the naphthyl azides were reported in the 1970s and 1980s.<sup>165,248–250,253,254</sup> In 1974, the Suschitzky group<sup>248</sup> discovered that pyrolysis of **79** and **80** in bromobenzene yields a significant amount of dibenzo[a,h]phenazine (Scheme 11.44). The photolytic decomposition of **80** in DEA leads to a diamine product.<sup>248</sup> On the contrary, photolysis of **79** in DEA produces mostly azonaphthalene and aminonaphthalene in low yields<sup>248</sup> along with a very low yield of diamine adduct.<sup>250</sup>

Carroll *et al.* found that the yield of diamine product is sensitive to the photolysis time.<sup>254a</sup> A drastic reduction in the photolysis time leads to a much-improved yield of the diamines. It was also discovered that the yield of diamine products formed upon photolysis of the 1- and 2-naphthyl azides can also be significantly improved by the presence of (Me<sub>2</sub>NCH<sub>2</sub>)<sub>2</sub> (or TMEDA) as co-solvent.<sup>249</sup>

Leyva and Platz demonstrated<sup>250</sup> that reaction temperature plays an important role in the photochemistry of **79**, as with the case of parent phenyl azide **47**. Moderate yields of adducts were observed by simply lowering the temperature of the photolysis of **79** with DEA.

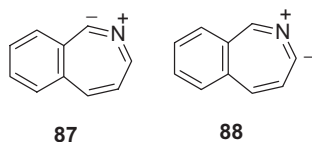
The photoproduct studies mentioned above suggest the intermediacy of azirines in the photochemistry of **79** and **80**. Additional evidence of these intermediates was provided by the observations of adducts in the photolysis of **80** with ethanethiol<sup>254b</sup> and with methanolic methoxide.<sup>253a</sup>

Direct evidence for azirines and didehydroazepines was obtained by Dunkin and Thomson upon UV-irradiation ( $\lambda > 330\text{ nm}$ ) of **79** and **80** in nitrogen or argon matrices at 12 K.<sup>255</sup> In the case of **79** the IR band at  $1730\text{ cm}^{-1}$  was formed upon initial photolysis and was assigned to tricyclic azirine. The IR bands at  $1926$  and  $1912\text{ cm}^{-1}$ , formed on secondary photolysis of the tricyclic azirine, were attributed to didehydroazepine intermediates. Similarly, photolysis of **80** produces IR bands at  $1708$ ,  $1723$  and  $1736\text{ cm}^{-1}$  assigned to corresponding azirines. The IR bands at  $1911$ ,  $1923\text{ cm}^{-1}$  were formed on secondary photolysis and assigned to azepines. However, a detailed assignment has not been performed.

Recently,<sup>256</sup> the photochemistry of azides **79** and **80** in an argon matrix was reinvestigated and new assignments of the experimental UV-vis and IR spectra of the species observed were presented on the basis of quantum chemical calculations. The primary products were found to be the corresponding triplet nitrenes <sup>3</sup>**81** and <sup>3</sup>**82**. According to the new assignment,<sup>256</sup> the peaks at  $1710$ – $1740\text{ cm}^{-1}$ , observed by Dunkin and Thompson,<sup>255</sup> belong to azirines **83** and **84** (Figures 11.20, 11.21). The peaks at  $1910$ – $1930\text{ cm}^{-1}$ , observed on prolonged irradiation, were assigned to azepines **85** and **86**. In addition, evidence was presented for the formation of novel ring expansion products, the cyclic ylides **87** and **88** (Scheme 11.45).

A comprehensive computational study of the potential energy surfaces on the rearrangements leading to ylides **87** and **88** was performed (Figures 11.20 and 11.21).<sup>256</sup> It was predicted that singlet 1-naphthyl nitrene (<sup>1</sup>**81**) cyclizes selectively at the beta carbon with the formation of azirine **83**. The azirine **90** derived from cyclization at carbon atom 9 is predicted to be very high in energy (Figure 11.20).

Argon matrix photolysis of 1- and 2-naphthyl azides **79** and **80** at  $313\text{ nm}$  initially produced the singlet naphthyl nitrenes, <sup>1</sup>**81** and <sup>1</sup>**82**. Relaxation to the corresponding lower energy, persistent triplet nitrenes <sup>3</sup>**81** and <sup>3</sup>**82** competes with cyclization to the azirines **83** and **84** which can also be formed photochemically from the triplet nitrenes (Figures 11.20 and 11.21). On prolonged irradiation, the triplet nitrenes <sup>3</sup>**81** and <sup>3</sup>**82** can be converted to the 7-membered cyclic ketenimines **85** and **86**, respectively, as described earlier by Dunkin and Thomson.<sup>255</sup>



**Scheme 11.45** Structures of cyclic ylides

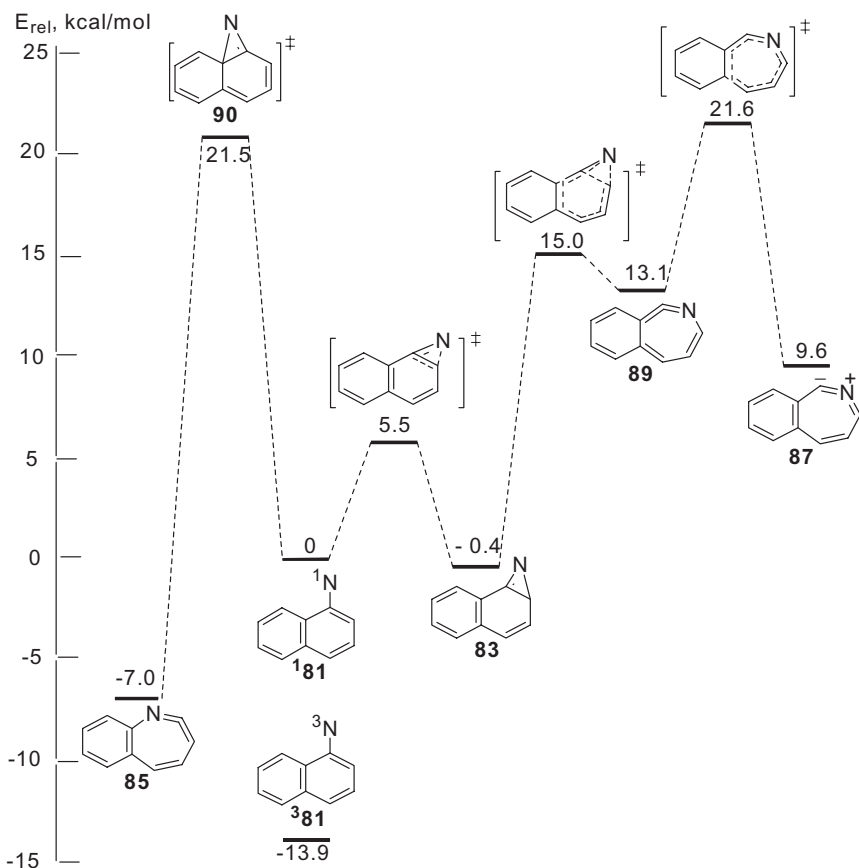


**Figure 11.20** The relative energies of valence isomers of 1-naphthyl nitrene **181** calculated at the CASPT2//CASSCF(12,12)/6-31G\* level.<sup>256</sup> All energies include zero-point energy corrections. Note, that **90** is a transition state by DFT, but a shallow minimum by CASSCF

However, instead of the *o*-quinoid ketenimines **89** and **91**, which are the expected primary ring-opening products of azirines **83** and **84**, respectively, the novel bond-shift isomers **87** and **88** were observed, which may be formally regarded as cyclic nitrile ylides. The existence of such ylidic heterocumulenes had been predicted previously.<sup>257</sup>

The photochemistry of naphthyl azides **79** and **80** in solution at ambient temperature has been studied using LFP<sup>170</sup> and TRIR<sup>258</sup> techniques and the femtosecond transient absorption spectroscopy.<sup>156,160,259</sup> LFP study of naphthyl azide photochemistry in glassy solvents at 77 K has also been performed.<sup>258</sup>

In an early ns time resolved study,<sup>170</sup> no transient absorption above 350 nm was observed immediately after pulsed laser excitation of **79**. However, the transient absorption spectrum of triplet nitrene (**<sup>3</sup>81**,  $\lambda_{max} = 370$  nm) was observed a few microseconds after the laser pulse. The intensity of the transient absorption of **<sup>3</sup>81** increased exponentially with a time constant of 2.8  $\mu$ s in benzene at ambient temperature. The **<sup>3</sup>81** decay monitored within 100  $\mu$ s of the laser pulse was accompanied by the concurrent formation of

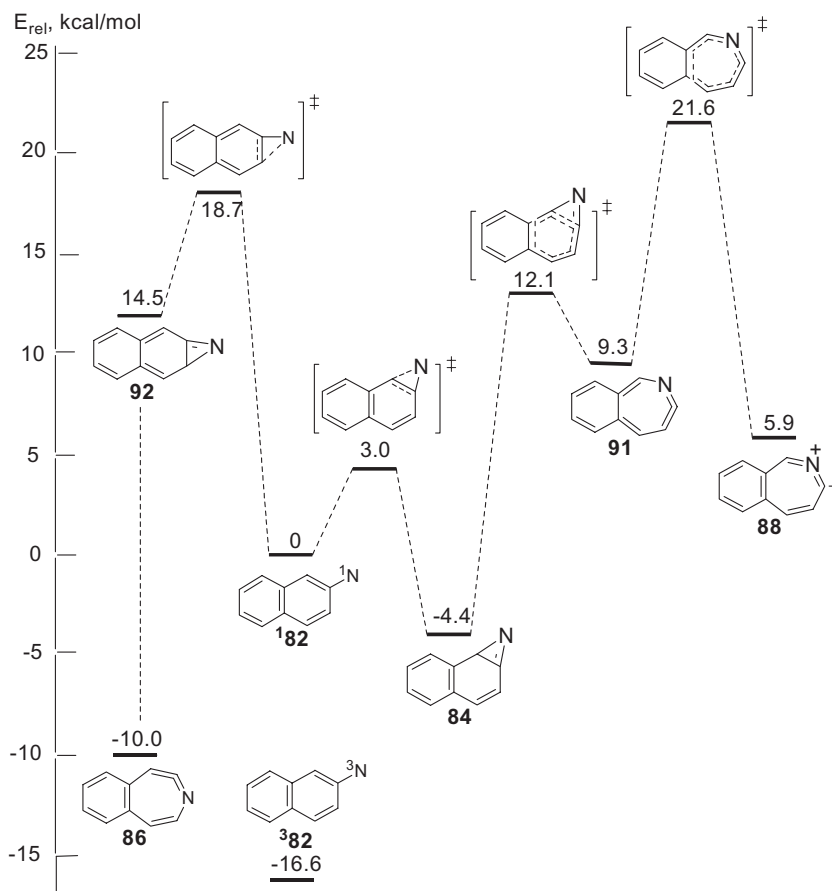
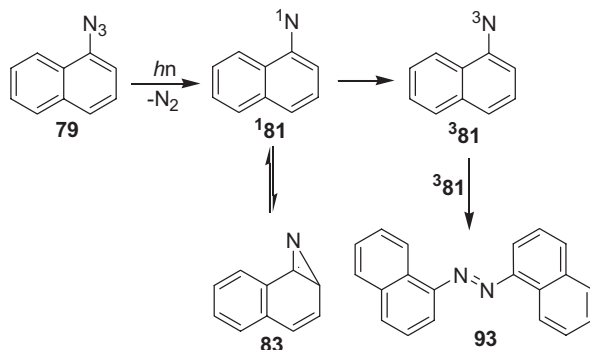


**Figure 11.21** Relative energies of valence isomers of singlet 2-naphthylnitrene **182** calculated at the CASPT2//CASSCF(12,12)/6-31G\* level.<sup>256</sup> All energies include zero-point energy corrections

1,1'-azonaphthalene (**93**,  $\lambda_{\text{max}} = 420$  nm), by the second-order reaction with a rate constant of  $1 \times 10^9 \text{ M}^{-1} \text{ s}^{-1}$ . The precursor to **381** was assigned to tricyclic azirine **83** (Scheme 11.46), a species which serves as a reservoir for singlet 1-naphthylnitrene **181**.<sup>170</sup>

The expected azirine **83** with lifetimes of  $3.2 \pm 0.6 \mu\text{s}$  was detected by TRIR spectroscopy.<sup>258</sup> The lifetime of **83** was also measured in solvent mixtures of 1:3 and 1:1 DEA/ acetonitrile. The absolute bimolecular rate constant of reaction of **83** with DEA was estimated to be  $\sim 1.4 \times 10^5 \text{ M}^{-1} \text{ s}^{-1}$ , a value much smaller than that of a diffusion-controlled process. The slow rate of reaction of **83** with DEA is consistent with the reported low yield of DEA photo-adduct observed upon photolysis of **79**.<sup>249</sup>

LFP of **79** in glassy 3-methylpentane at 77 K produces singlet nitrene **181**, which is characterized by a structured band in the near-UV region with maxima at 362, 383 and 397 nm in agreement with calculations.<sup>258</sup> At 77 K the singlet nitrene **181** cleanly relaxes to the lower energy triplet nitrene **381** with  $k_{\text{ISC}} = 1.1 \pm 0.1 \times 10^7 \text{ s}^{-1}$ .



**Scheme 11.46** Photochemistry of 1-naphthyl azide **79** in solution at ambient temperature

A similar transient absorption spectrum ( $\lambda_{\text{max}} = 385 \text{ nm}$ ) was detected at ambient temperature in acetonitrile using ultrafast LFP and assigned to singlet nitrene **181**.<sup>156</sup> The absorption of singlet nitrene **181** grows with time constant  $\sim 730 \text{ fs}$  and decays with time constant of  $12 \text{ ps}$  ( $k = 8.3 \times 10^{10} \text{ s}^{-1}$ ) to form naphthazirine **83**.<sup>156</sup> Assuming that the pre-exponential factor for cyclization of **181** is  $\sim 10^{13} \text{ s}^{-1}$ , the activation energy could be estimated as  $\sim 3 \text{ kcal/mol}$ . This value is in reasonable agreement with the CASPT2//CASSCF(12,12)/6-31G\* calculations (Figure 11.20),<sup>256</sup> after taking into account the typical underestimation by  $\sim 3 \text{ kcal/mol}$ <sup>106</sup> of the energy of open-shell **181** in the calculation.

Although the singlet nitrene **181** is very short-lived, its protonation leading to the formation of 1-naphthylnitrenium cation was observed in 88% formic acid using ultrafast LFP.<sup>160</sup> The rate of formation of this cation was equal to the rate of **181** decay ( $\tau = 8.4 \text{ ps}$ ). The lifetime of 1-naphthylnitrenium ion is  $860 \text{ ps}$  in 88% formic acid.

According to the RI-CC2/TZVP calculations,<sup>156</sup> the  $S_2$  excited state of 1-naphthyl azide **79** is a bound state with an equilibrium geometry similar to that of the ground  $S_0$  state (Figure 11.22). On the contrary, the  $S_1$  excited state, best characterized as  $\pi \rightarrow$  (in plane,  $\pi^*$ , azide) excitation, is dissociative toward the formation of molecular nitrogen and the singlet nitrene **181**, although a small barrier ( $\sim 2 \text{ kcal/mol}$ ) for  $\text{N}_2$  expulsion is predicted. Figure 11.22 demonstrates also an  $S_0/S_1$  crossing when the N–N coordinate is about  $1.65 \text{ \AA}$ . A similar  $S_0/S_1$  crossing may account for the low quantum yield of photolysis of parent azide **47** and its *ortho*-phenyl derivative **65a**.<sup>204</sup> However, in the case of azide **79** the quantum yield of photolysis is close to unity at ambient temperature and at  $77 \text{ K}$ .<sup>204</sup>

The calculations also predict<sup>156</sup> that for azide **79**, as well as for azide **47** and biphenyl azides, the oscillator strength of  $S_0 \rightarrow S_2$  transition is much larger than that of  $S_0 \rightarrow S_1$ . Thus UV excitation of these aryl azides is predicted to promote the ground state azide to the  $S_2$  state, which rapidly converts to the dissociative  $S_1$  state. Therefore, the time constant of arylnitrene formation does not relate to the N–N bond cleavage, but instead to the internal conversion from  $S_2$  to  $S_1$  state.

The nanosecond LFP<sup>170</sup> of 2-naphthyl azide **80** gave results similar to that of **79**, except that in this case the transient absorption of triplet nitrene **382** was not detected and the formation of 2,2'-azonaphthalene was found to be approximately 20 times slower than that of **93**. Naphthazirine **84** was detected in acetonitrile at ambient temperature using

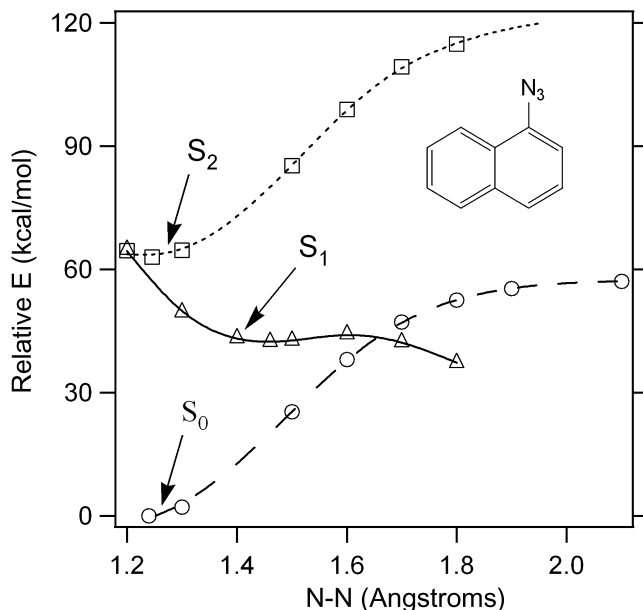


**Figure 11.22** RI-CC2/TZVP fully relaxed potential energy curves for  $N_2$  expulsion in 1-naphthyl azide **79**: ground state (open circles), first excited state (open triangles), and second excited state (open squares).<sup>156</sup> The arrows indicate the N–N bond length of the fully optimized stationary point on each respective energy surface

TRIR spectroscopy.<sup>258</sup> Its lifetime was determined to be  $150 \pm 10 \mu\text{s}$  in excellent agreement with early observation of a slow rate of growth of 2,2'-azonaphthalene.<sup>170</sup> The longer lifetime of **84** (comparing to **83**) is consistent with theoretical calculations as well (Figure 11.21), since **84** is predicted to be 4.4 kcal/mol more stable than singlet nitrene **182**, whereas the cyclization of **181** to azirine **83** is essentially thermoneutral (Figure 11.20).<sup>256</sup>

The rate constants of azirine **84** decay were determined in the presence of 25% and 50% DEA in acetonitrile at ambient temperature. The absolute bimolecular rate constant of reaction of azide **84** with DEA was estimated as  $\sim 2.5 \times 10^5 \text{ M}^{-1} \text{ s}^{-1}$ . This rate constant is slightly faster but is still similar to that of azirine **83** ( $1.4 \times 10^5 \text{ M}^{-1} \text{ s}^{-1}$ ). Thus, trapping of **84** by DEA is still the dominant process since it has a long lifetime ( $150 \mu\text{s}$ ) in the absence of the amine trap. This is consistent with the reported high yields of adducts formed upon photolysis of **80** in the presence of secondary amines.<sup>249,248,253,254</sup> A DEA adduct is inefficiently formed upon photolysis of **79** at ambient temperature because of the much shorter lifetime of naphthazirine **83** ( $\sim 3 \mu\text{s}$ ).<sup>170,258</sup>

In the ultrafast LFP study of **80**, the formation of two intermediates have been observed in acetonitrile at ambient temperature.<sup>259</sup> One of the species, the  $S_2$  excited state of **80** ( $\lambda_{\text{max}} \sim 350 \text{ nm}$ ) has a lifetime within the instrument response (300 fs) due to its rapid conversion to the dissociative  $S_1$  state. The second intermediate, singlet nitrene **182** ( $\lambda_{\text{max}} \sim 420 \text{ nm}$ ) has the shortest lifetime of any singlet aryl nitrenes observed to date – 1.8 ps ( $k = 5.6 \times 10^{11} \text{ s}^{-1}$ ).<sup>259</sup> Assuming that the pre-exponential factor for cyclization of **181** is  $\sim 10^{13} \text{ s}^{-1}$ , the activation energy to cyclization could be estimated as  $\sim 1.7 \text{ kcal/mol}$ .

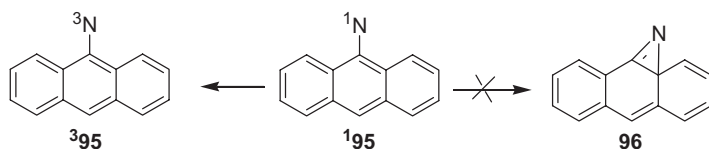
This value is in reasonable agreement with the CASPT2//CASSCF(12,12)/6-31G\* calculations (Figure 11.21),<sup>256</sup> after taking into account the expected underestimation ( $\sim 3$  kcal/mol)<sup>106</sup> of the energy of open-shell **181** in this calculation.

Unlike **79**, LFP of **80** in a glassy matrix at 77 K failed to produce a detectable transient absorption above 320 nm.<sup>258</sup> On the contrary, the triplet nitrene **382** is a primary product of 2-naphthyl azide photolysis in argon matrix at 12 K. Note, that triplet nitrene **382** absorbing at 365 nm was generated and detected by triplet sensitization.<sup>170</sup> To reconcile the observations obtained at 12 and 77 K, it was proposed, that for **182**  $k_R \gg k_{ISC}$  at 77 K, but that  $k_{ISC} \gg k_R$  at 12 K. If one assumes that  $k_{ISC} = 1.1 \times 10^7 \text{ s}^{-1}$  and  $A = 10^{13} \text{ s}^{-1}$  for the cyclization reaction, then the barrier to cyclization,  $E_a$ , can be bracketed as follows:  $0.3 < E_a < 2.1$  kcal/mol. This result is consistent with the above mentioned estimation from fs time-resolved experiments ( $E_a \sim 1.7$  kcal/mol) and theoretical predictions (Figure 11.21).<sup>256</sup>

The photochemistry of other polynuclear aromatic azide has been investigated in less detail than that of the naphthyl azides, although some azides have been studied to a certain extent. For instance, photolysis of 1-, 2-, and 9-azidoanthracenes in organic matrices at 77 K yields the corresponding triplet nitrenes, whose electronic absorption spectra<sup>171,177,204,251d,260</sup> and EPR spectra<sup>251a,d</sup> were recorded in the 1960s. The expected azo compound was formed upon irradiation of 1-azidoanthracene in ethanol.<sup>169</sup> The azo dimer was formed in the reaction of triplet 1-nitrenoanthracene with starting azide with a rate constant  $5 \times 10^8 \text{ M}^{-1} \text{ s}^{-1}$ .<sup>169</sup> The product distributions observed upon photolysis of 2-azidoanthracene in the presence of nucleophiles resemble those formed upon photolysis of 2-azidonaphthalene (**80**) and provide evidence for the intermediacy of both azirine and triplet nitrene intermediates.<sup>253</sup>

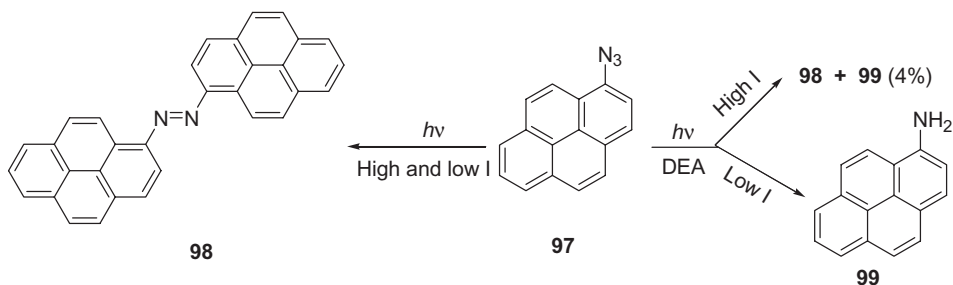
The photochemistry of 9-azidoanthracene (**94**) in solution has not been explored by chemical analysis of reaction mixtures. However, the mechanism of photolysis of **94** was investigated recently by laser flash photolysis and computational chemistry.<sup>261</sup> LFP of **94** produces singlet nitrene **195** with a lifetime of about 20 ns at both ambient temperature and 77 K. Thus the lifetime of **195** is controlled by intersystem crossing to the ground triplet state **395**. The rapid rate of ISC of **195** relative to that of singlet phenylnitrene (**152**) is in agreement with the calculated value of the singlet-triplet splitting ( $\Delta E_{ST}$ ) of this nitrene.<sup>261</sup> The  $\Delta E_{ST}$  of **95** was predicted to be 5.3 kcal/mol (CASSCF/CASPT2 procedure),<sup>261</sup> which is much smaller than that for parent **152** ( $\sim 18$  kcal/mol)<sup>106,189-194</sup> and naphthyl nitrenes **81** (13.9 kcal/mol) and **82** (16.6 kcal/mol).<sup>256</sup> The absence of cyclization of **195** to form a bridgehead **96** is also in agreement with calculations that indicate that the conversion of **195** to **96** is endothermic by 23 kcal/mol.<sup>261</sup>

More attention was devoted to the photochemistry of 1-pyrenyl azide (**97**).<sup>170,171,262-264</sup> Irradiation of **97** in deoxygenated benzene solution gives a high yield of 1,1'-azopyrene



**Scheme 11.47** Primary processes in the photochemistry of 9-azidoanthracene **94**

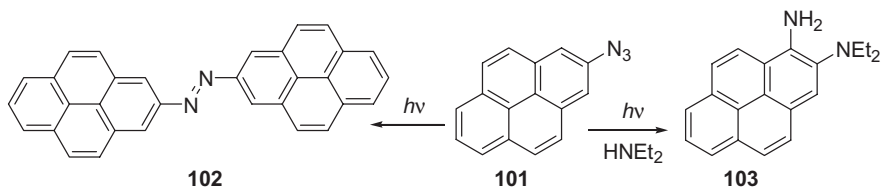
(**98**).<sup>170,171</sup> When **97** was photolyzed in DEA solution with a low-power continuous light source, a large yield (82%) of 1-aminopyrene (**99**) was obtained. High-power laser excitation of **97** gave a large yield of **98** and only a 4% yield of **99**.<sup>170</sup> Triplet sensitization of the decomposition of **97** in benzene containing 1 M DEA at low irradiation power gave **99** in 55% yield.<sup>170</sup>



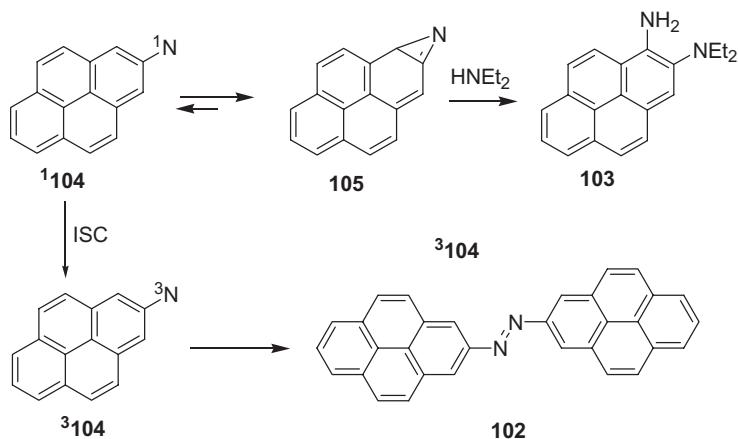
**Scheme 11.48** Products of 1-pyrenyl azide photolysis in the presence and absence of DEA and at high-power laser (High I) and low-power continuous light (Low I) sources<sup>170,171</sup>

In 1976, Sumitani, Nagakura and Yoshihara demonstrated that LFP of **97** produces a transient species with absorption maximum at 455 nm, which disappeared with a time constant of 22 ns at room temperature and with 34 ns at 77 K and decayed to a species with absorption maximum at 420 nm.<sup>264</sup> The latter species disappeared in a second-order process to give **98**. This spectrum ( $\lambda_{\text{max}} = 420 \text{ nm}$ ) was also formed on triplet sensitization and was identical to that of triplet 1-nitrenopyrene (**<sup>3</sup>100**) observed in a glassy matrix at 77 K. Therefore, the species with the 420 nm absorption maximum was assigned to triplet nitrene **<sup>3</sup>100** and its precursor with maximum at 455 nm – to singlet nitrene **<sup>1</sup>100**. This assignment is secure after taking into account all recent results on the spectroscopy and dynamics of singlet arylnitrenes,<sup>14,15,19,20</sup> although it was questioned in the 1980s.<sup>170</sup> Note, that singlet 1-pyrenylnitrene (**<sup>1</sup>100**) was the first singlet arylnitrene directly detected by spectroscopic methods.<sup>264</sup>

Thus the results of a ns time resolved LFP study of 1-pyrenyl azide are very similar to that of 1-azidoanthracene. On the contrary, the photochemistry of 2-pyrenyl azide (**101**, Scheme 11.49) is quite similar to that observed for 2-naphthyl azide **80**.<sup>170,256,258</sup> Irradiation in benzene gives primarily 2,2'-azopyrene (**102**).<sup>170</sup> In the presence of DEA (HNEt<sub>2</sub>), the product is almost exclusively 1-amino-2-diethylaminopyrene (**103**) and it reaches its maximum value at a very low concentration of DEA ( $4 \times 10^{-3} \text{ M}$ ).<sup>170</sup>



**Scheme 11.49** Photolysis products of 2-pyrenyl azide (**101**)



**Scheme 11.50** Proposed mechanism of 2-pyrenyl azide photochemistry

LFP of **101** produces a transient absorption with maximum at 420 nm.<sup>170</sup> On a longer time scale the absorption of 2,2'-azopyrene (**102**) grows by a second-order process. The 420 nm absorption band was also formed by irradiation of **101** at 77 K in glassy matrix. The EPR spectrum of triplet 2-nitrenepyrene ( $^3\mathbf{104}$ ) was detected at 77 K and at 4 K.

The same absorption band was observed in DEA as a solvent. It disappeared in a first-order process with a time constant of  $2.5 \mu\text{s}$  with formation of **103**. The authors assigned the 420 nm absorption to triplet 2-nitrenepyrene ( $^3\mathbf{104}$ ) and proposed that the conversion of singlet nitrene  $^1\mathbf{104}$  to its triplet ground state ( $^3\mathbf{104}$ ) is reversible.<sup>170</sup> However, the authors expressed some skepticism in this assignment.

Taking into account all recent results and especially the recent data on the ns time resolved LFP study of 2-naphthyl azide (**80**),<sup>258,259</sup> the following mechanism of 2-pyrenyl azide photolysis can be proposed (Scheme 11.50). In our opinion the transient absorption at 420 nm should be assigned to azirine **105**, which reacts with DEA to give **103** and serves as reservoir for triplet nitrene ( $^3\mathbf{104}$ ), which undergo dimerization or react with azide **101** to give azopyrene **102**.

Therefore, as in the case of parent phenyl azide **47** and its simple derivatives, the photochemistry of polynuclear aromatic azide, especially that of naphthyl azides **79** and **80**, is now well understood. Specifically, the dynamics of the primary photophysical processes as well as the subsequent photochemical steps have been directly investigated using a variety of modern and conventional experimental techniques and computational chemistry. It is clear now, that the difference between the photochemistry of phenyl azide (and its simple derivative) and polynuclear aromatic azide is caused mainly by the difference in the thermodynamics of the singlet nitrene rearrangement to azinine type species.

## 11.7 Conclusion

Over the last 15 years there has been dramatic progress in our understanding of the chemistry of simple acyl and aryl azides. These advancements are a direct result of the

blossoming of computational methods, nano second time resolved spectroscopy and matrix isolation techniques. As we have described in this review the photolysis of azides leads to the extrusion of molecular nitrogen and the release of singlet nitrenes which relax to form a variety of secondary and tertiary intermediates. This field has matured to the point that it is now possible to use nanosecond spectroscopy (and spectroscopic methods with faster or slower time resolution) to directly observe the seminal singlet nitrenes released upon azide photolysis and the intermediates derived from them. It is possible to measure activation barriers to the intramolecular and intermolecular processes that these species undergo. Computational methods complement the experimental techniques by predicting the potential energy surfaces and simulating the UV-Vis and IR spectra of the intermediates of interest. This work has sharpened our intuition. It is possible to use the structure-reactivity data base to qualitatively predict the behavior of the intermediates produced upon photolysis of a simple azide. Thus, this field is close to reaching scientific maturity if it has not done so already.

The new challenge is to develop the same level of understanding of the first 100 ps that follow the excitation of an azide, using femto and picosecond time resolved spectroscopy. The new goal is to understand the nature of the excited state populated by the absorption of light as a function of wavelength and to discover which excited states are dissociative and which are not. The challenge is to develop a map detailing the production of an excited state and how it relaxes to a dissociative state. The singlet nitrene so formed will surely be born with excess vibrational energy. Another goal is to learn if the 'hot' nitrene undergoes chemistry prior to relaxation to a thermalized nitrene and the role of structure, wavelength and solvent on these events. Chemists have long deduced that acyl azide excited states can undergo a concerted Curtius Rearrangement and bypass a nitrene route to isocyanates. The combination of theory and ultrafast time resolved spectroscopy should also give new insights into acyl azide excited state chemistry. A decade from now we hope to provide a review of these explorations and develop an intuition for structure-wavelength-reactivity issues on the ultrafast timescales that rivals what we have developed for the nanosecond realm.

## Acknowledgments

Support for this work by the National Science Foundation, the Russian Foundation for Basic Research and the Siberian Branch of Russian Academy of Sciences is gratefully acknowledged.

## References

- [1] *Nitrenes*; W. Lwowski, ed.; John Wiley & Sons, Inc., New York, **1970**.
- [2] *Azides and Nitrenes – Reactivity and Utility*; E.F.V. Scriven, Ed.; Academic Press, New York, **1984**.
- [3] (a) *The Chemistry of the Azido Group*, S. Patai, ed.; John Wiley & Sons, Inc., New York, **1971**. (b) *The Chemistry of Halides, Pseudo-Halides and Azides*, Supplement D, S. Patai, Z. Rappoport, eds.; John Wiley & Sons Ltd, Chichester, **1983**. (c) *The Chemistry of Halides, Pseudo-Halides and Azides, Part 1 and 2*, S. Patai, ed.; John Wiley & Sons, Ltd, Chichester, **1995**.

- [4] S. Bräse, C. Gil, K. Knepper, V. Zimmermann, *Angew. Chem. Int. Ed.* **2005**, *44*, 5188–5240.
- [5] A. Singh, E. R Thornton, F. H. Westheimer, *J. Biol. Chem.* **1962**, *237*, 3006–8.
- [6] (a) H. Bayley, J.R. Knowles, *Methods Enzymol.* **1977**, *46*, 69–114. (b) H. Bayley, *Photogenerated Reagents in Biochemistry and Molecular Biology*. Elsevier, New York, **1983**.
- [7] (a) J.F. Wang, W.D. Downs, T.R. Cech, *Science* **1993**, *260*, 504–8. (b) J.L. Chen, J.M. Nolan, M.E. Harris, N.R. Paxe, *EMBO J.* **1998**, *17*, 1515–25. (c) R. Pinard, J.E. Heckman, J.M. Burke, *J. Mol. Biol.* **1999**, *287*, 239–51. (d) K.G. Pinney, M.P. Mejia, V.M. Villalobos, *et al.*, *Bioorg. Med. Chem.* **2000**, *8*, 2417–25. (e) K.L. Buchmueller, B.T. Hill, M.S. Platz, K.M. Weeks, *J. Am. Chem. Soc.* **2003**, *125*, 10850–61.
- [8] D.S. Breslow, in *Azides and Nitrenes – Reactivity and Utility*; E.F.V. Scriven, ed.; Academic Press, New York, **1984**.
- [9] E.W. Meijer, S. Nijhuis, F.C.B.M. Von Vroonhoven, *J. Am. Chem. Soc.* **1988**, *110*, 7209–10.
- [10] (a) S.X. Cai, D.R. Glenn, J.F.W. Keana, *J. Org. Chem.* **1992**, *57*, 1299–1304. (b) H. Niino, Y. Koga, A. Yabe, *J. Photochem. Photobiol. A: Chemistry* **1997**, *106*, 9–13. (c) H. Niino, T. Sato, A. Yabe, *Appl. Phys. A* **1999**, *69*, 605–10. (d) M.D. Yan, *React. Func. Polymers* **2000**, *45*, 137–44. (e) C. Henneuse-Boxus, E. Duliere, J. Marchand-Brynaert, *Eur. Polymer J.* **2001**, *37*, 9–18. (f) S.H. Khong, S. Sivaramakrishnan, R.Q. Png, *et al.*, *Adv. Func. Mater.* **2007**, *17*, 2490–9.
- [11] E.F.V. Scriven, in *Reactive Intermediates*, R.A. Abramovitch, ed.; Plenum, New York, V. 2, **1982**.
- [12] G.B. Schuster, M.S. Platz, *Adv. Photochem.* **1992**, *17*, 69–143.
- [13] N.P. Gritsan, E.A. Pritchina, *Russ. Chem. Rev. (Uspekhi Khimii)* **1992**, *61*, 910–39.
- [14] N.P. Gritsan, M.S. Platz, W.T. Borden, in *Computational Methods in Photochemistry*; A.G. Kutateladze, ed.; Taylor & Francis, Boca Raton, **2005**.
- [15] M.S. Platz, in *Reactive Intermediate Chemistry*, R.A. Moss, M.S. Platz, M. Jons, eds.; Wiley-Interscience, Hoboken, **2004**.
- [16] F. Tiemann, *Ber. Dtsch. Chem. Ges.* **1891**, *24*, 4162–7.
- [17] W.T. Borden, N.P. Gritsan, C.M. Hadad, *et al.*, *Acc. Chem. Res.* **2000**, *33*, 765–11.
- [18] W.L. Karney, W.T. Borden, *Adv. Carbene Chem.* **2001**, *3*, 205–51.
- [19] N.P. Gritsan, M.S. Platz, *Adv. Phys. Org. Chem.* **2001**, *36*, 255–304.
- [20] N.P. Gritsan, M.S. Platz, *Chem. Rev.* **2006**, *106*, 3844–67.
- [21] H. Okabe, *J. Chem. Phys.* **1968**, *49*, 2726–33.
- [22] H. Okabe, *Photochemistry of Small Molecules*, Wiley, New York, **1978**, pp. 232–4.
- [23] J.R. McDonald, R.G. Miller, A.P. Baronovski, *Chem. Phys. Lett.* **1977**, *51*, 57–60.
- [24] A.P. Baronovski, R.G. Miller, J.R. McDonald, *Chem. Phys.* **1978**, *30*, 119–31.
- [25] F. Rohrer, F. Stuhl, *J. Chem. Phys.* **1988**, *88*, 4788–99.
- [26] (a) W.S. Drozdovski, A.P. Baronovski, J.R. McDonald, *Chem. Phys. Lett.* **1979**, *64*, 421–5. (b) K-H. Gericke, R. Theinl, F. Comes, *Chem. Phys. Lett.* **1989**, *164*, 605–11. (c) K-H. Gericke, R. Theinl, F. Comes, *J. Chem. Phys.* **1990**, *92*, 6548–55. (d) J.J. Chu, P. Marcus, P.J. Dagdigian, *J. Chem. Phys.* **1990**, *93*, 257–67. (e) K-H. Gericke, T. Haas, M. Lock, R. Theinl, F. Comes, *J. Phys. Chem.* **1991**, *95*, 6104–11.
- [27] O. Kajimoto, T. Yamamoto, T. Fueno, *J. Phys. Chem.* **1979**, *83*, 429–35.
- [28] J.C. Stephenson, M.P. Casassa, D.S. King, *J. Chem. Phys.* **1988**, *89*, 1378–87.
- [29] M.H. Alexander, H-J. Werner, P.J. Dagdigian, *J. Chem. Phys.* **1988**, *89*, 1388–1400.
- [30] (a) K-H. Gericke, T. Haas, M. Lock, F.J. Comes, *Chem. Phys. Lett.* **1991**, *186*, 427–30. (b) T. Haas, K-H. Gericke, C. Maul, F.J. Comes, *Chem. Phys. Lett.* **1993**, *202*, 108–14. (c) M. Lock, K-H. Gericke, F.J. Comes, *J. Chem. Phys.* **1996**, *213*, 385–96.
- [31] (a) J.R. McDonald, R.G. Miller, A.P. Baronovski, *Chem. Phys.* **1978**, *30*, 133–45. (b) O. Kajimoto, T. Fueno, *Chem. Phys. Lett.* **1981**, *80*, 484–7.
- [32] (a) J.A. Miller, C.T. Bowman, *Prog. Energy Combust. Sci.* **1989**, *15*, 287–38. (b) L.D. Smoot, S.C. Hill, H. Xu, *Prog. Energy Combust. Sci.* **1998**, *24*, 385–408.
- [33] (a) M. Röhrig, H.G. Wagner, *Proc. Symposium (International) on Combustion*, **1994**, *25*, 975–81.

- [34] J.C. Mackie, G.B. Bacskay, *J. Phys. Chem. A* **2005**, *109*, 11967–74.
- [35] (a) M. Rohrig, H.J. Romming, H.G. Wagner, *Ber. Bunsenges Phys. Chem. Chem. Phys.* **1994**, *98*, 1332–4. (b) E. Henon, F. Bohr, *J. Mol. Struct. THEOCHEM* **2000**, *531*, 283–99.
- [36] M. Rohrig, H.G. Wagner, *Ber. Bunsenges Phys. Chem. Chem. Phys.* **1994**, *98*, 858–63.
- [37] W. Hack, in *N-Centered Radicals*, Z.B. Alfassi, ed.; John Wiley & Sons, Inc., New York, **1998**.
- [38] M. Rohrig, H.G. Wagner, *Ber. Bunsenges Phys. Chem. Chem. Phys.* **1994**, *98*, 864–8.
- [39] C. Zetzsch, I. Hansen, *Ber. Bunsenges Phys. Chem. Chem. Phys.* **1978**, *82*, 830–3.
- [40] W. Hack, H. Kurzke, H.G. Wagner, *J. Chem. Soc., Faraday Trans. 2*, **1985**, *81*, 949–61.
- [41] T. Fueno, K. Yokoyama, S. Takane, *Theor. Chim. Acta* **1992**, *82*, 299–308.
- [42] E.D. Becker, J. Pimentel, M. Van Thiel, *J. Chem. Phys.* **1957**, *26*, 145–50.
- [43] M. McCarty, G.W. Robinson, *J. Am. Chem. Soc.* **1959**, *81*, 4472–6.
- [44] V.E. Bondybey, L.E. Brus, *J. Chem. Phys.* **1975**, *63*, 794–804.
- [45] H. Esser, J. Langen, U. Schurath, *Ber. Bunsenges Phys. Chem. Chem. Phys.* **1983**, *87*, 636–43.
- [46] A. Ramsthaler-Sommer, K.E. Eberhardt, U. Schurath, *J. Chem. Phys.* **1986**, *85*, 3760–9.
- [47] C. Blindauer, N. van Riesenbeck, K. Seranski, *et al.*, *Chem. Phys.* **1991**, *150*, 93–108.
- [48] S.L. Laursen, J.E. Grace, R.L. Dekock, S.A. Spronk, *J. Am. Chem. Soc.* **1998**, *120*, 12583–94.
- [49] H.J. Himmel, M. Junker, H. Schnöckel, *J. Chem. Phys.* **2002**, *117*, 3321–6.
- [50] P.H.H. Fischer, S.W. Charles, C.A. McDowell, *Can. J. Chem. Phys.* **1967**, *46*, 2162–5.
- [51] F.D. Wayne, H.E. Radford, *Mol. Phys.* **1976**, *32*, 1407–22.
- [52] H. Okabe, M. Lenzi, *J. Chem. Phys.* **1967**, *47*, 5241–6.
- [53] J. Masanet, A. Gilles, C. Vermeil, *J. Photochem.* **1974**/75, *3*, 417–29.
- [54] P.W. Fairchild, G.P. Smith, D.R. Crosly, J.B. Jeffries, *Chem. Phys. Lett.* **1984**, *107*, 181–6.
- [55] P.C. Engelking, W.C. Lineberger, *J. Chem. Phys.* **1976**, *65*, 4323–4.
- [56] E.P. Kyba, in *Azides and Nitrenes – Reactivity and Utility*; E.F.V. Scriven, ed.; Academic Press, New York, **1984**.
- [57] F.D. Lewis, W.H. Saunders, in *Nitrenes*; W. Lwowski, ed.; John Wiley & Sons, Inc., New York, **1970**.
- [58] R.M. Moriarty, R.C. Reardon, *Tetrahedron*, **1970**, *26*, 1379–92.
- [59] F.C. Montgomery, W.H. Saunders, *J. Org. Chem.* **1976**, *41*, 2368–72.
- [60] E.P. Kyba, R.A. Abramovitch, *J. Am. Chem. Soc.* **1980**, *102*, 735–40.
- [61] R.E. Banks, D. Berry, M.J. McGlinchey, M.J. Moore, *J. Chem. Soc. C*, **1970**, 1017–23.
- [62] A. Pancrazi, Q. Khuong-Huu, *Tetrahedron*, **1975**, *31*, 2049–56.
- [63] D.E. Milligan, *J. Chem. Phys.* **1961**, *35*, 1491–7.
- [64] M.E. Jaxcox, D.E. Milligan, *J. Mol. Spectrosc.* **1975**, *56*, 333–56.
- [65] I.R. Dunkin, P.C.P. Thomson, *Tetrahedron Lett.* **1980**, *21*, 3813–16.
- [66] J. Michl, J.G. Radziszewski, J.W. Downing, *et al.*, *Pure. Appl. Chem.* **1983**, *55*, 315–21.
- [67] I.R. Dunkin, C.J. Shields, H. Quasi, B. Seiferling, *Tetrahedron Lett.* **1983**, *24*, 3887–90.
- [68] R.S. Sheridan, G.A. Ganzer, *J. Am. Chem. Soc.*, **1983**, *105*, 6158–60.
- [69] J.G. Radziszewski, J.W. Downing, M. Jawdosiuk, P. Kovacic, J. Michl, *J. Am. Chem. Soc.* **1985**, *107*, 594–603.
- [70] J.G. Radziszewski, J.W. Downing, C. Wentrup, *et al.*, *J. Am. Chem. Soc.*, **1985**, *107*, 2799–2801.
- [71] E. Wasserman, G. Smolinsky, W.A. Jager, *J. Am. Chem. Soc.* **1964**, *86*, 3166–7.
- [72] (a) L. Barash, E. Wasserman, W.A. Jager, *J. Chem. Phys.* **1967**, *89*, 3931–5. (b) E. Wasserman, *Prog. Phys. Org. Chem.* **1971**, *8*, 319–36.
- [73] P.J. Wagner, B.J. Scheve, *J. Am. Chem. Soc.* **1979**, *101*, 378–83.
- [74] (a) S.M. Mandel, J.A.K. Bauer, A.D. Gudmundsdottir, *Org. Lett.* **2001**, *3*, 523–6. (b) S. Muthukrishnan, S.M. Mandel, J.C. Hackett, *et al.*, *J. Org. Chem.* **2007**, *72*, 2757–68.
- [75] (a) P.N.D. Singh, S.M. Mandel, R.M. Robinson, *et al.*, *J. Org. Chem.* **2003**, *68*, 7951–60. (b) P.N.D. Singh, S.M. Mandel, S. Muthukrishnan, *et al.*, *J. Am. Chem. Soc.* **2007**, *129*, 16263–72.
- [76] (a) F.D. Lewis, W.H. Saunders, *J. Am. Chem. Soc.* **1968**, *90*, 7031–3. (b) *ibid.* **1968**, *90*, 7033–8.

- [77] R.F. Klima, A.D. Gudmundsdottir, *J. Photochem. Photobiol. A: Chemistry* **2004**, *162*, 239–47.
- [78] H. Quast, P. Eckert, *Liebigs. Ann. Chem.*, **1974**, 1727–41.
- [79] N.P. Gritsan, I. Likhovotvorik, Z. Zhu, M.S. Platz, *J. Phys. Chem. A* **2001**, *105*, 3039–41.
- [80] R.F. Ferrante, *J. Chem. Phys.* **1987**, *86*, 25–32.
- [81] T. Franken, D. Perner, M.W. Bosnali, *Z. Naturforsch A* **1970**, *25*, 151–3.
- [82] R.F. Ferrante, *J. Chem. Phys.* **1991**, *94*, 4678–9.
- [83] H. Shang, C. Yu, L. Ying, X. Zhao, *J. Chem. Phys.* **1995**, *103*, 4418–26.
- [84] L. Ying, Y. Xia, H. Shang, Y. Tang, *J. Chem. Phys.* **1996**, *105*, 5798–5805.
- [85] P.G. Carrick, P.C. Engelking, *J. Chem. Phys.* **1984**, *81*, 1661–5.
- [86] P.G. Carrick, C.R. Brazier, P.F. Bernath, P.C. Engelking, *J. Am. Chem. Soc.* **1987**, *109*, 5100–2.
- [87] E.L. Chappell, P.C. Engelking, *J. Chem. Phys.* **1988**, *89*, 6007–16.
- [88] C.R. Brazier, P.G. Carrick, P.F. Bernath, *J. Chem. Phys.* **1992**, *96*, 919–26.
- [89] H. Shang, R. Gao, X. Zhao, Y. Tang, *Chem. Phys. Lett.* **1997**, *267*, 345–50.
- [90] J.H. Glowina, J. Misewich, P.P. Sorokin, in *Supercontinuum Laser Sources*, R.R. Alfano, ed.; Springer Verlag, New York, **1989**.
- [91] M.J. Travers, D.C. Cowles, E.P. Clifford, G.B. Ellison, P.C. Engelking, *J. Phys. Chem.* **1999**, *111*, 5349–60.
- [92] (a) D.R. Yakony, H.F. Schaefer, S. Rothenberg, *J. Am. Chem. Soc.* **1974**, *96*, 5974–7. (b) J. Demuyancq, D.J. Fox, Y. Yamaguchi, H.F. Schaefer III, *J. Am. Chem. Soc.* **1980**, *102*, 6204–7. (c) J.A. Pople, K. Raghavachari, M.J. Frisch, J.S. Binckley, P. v R. Schleyer, *J. Am. Chem. Soc.* **1983**, *105*, 6389–98. (d) M.T. Nguyen, *Chem. Phys. Lett.* **1985**, *117*, 290–4. (e) Y. Xie, G.E. Scuseria, B.F. Yates, Y. Yamaguchi, H.F. Schaefer III, *J. Am. Chem. Soc.* **1989**, *111*, 5181–5.
- [93] (a) C. Richards Jr., C. Meredith, S.-J. Kim, G.E. Quelch, H.F. Schaefer III, *J. Chem. Phys.* **1994**, *100*, 481–9. (b) M.T. Nguyen, D. Sengupta, T.-K. Ha, *J. Phys. Chem.* **1996**, *100*, 6499–6503. (c) J.F. Arenas, J.C. Otero, A. Sánchez-Gálvez, J. Soto, P. Viruela, *J. Phys. Chem.* **1998**, *102*, 1146–51.
- [94] J.F. Arenas, J.I. Marcos, J.C. Otero, A. Sánchez-Gálvez, J. Soto, *J. Chem. Phys.* **1999**, *111*, 551–61.
- [95] C.R. Kemnitz, G.B. Ellison, W.L. Karney, W.T. Borden, *J. Am. Chem. Soc.* **2000**, *122*, 1098–1101.
- [96] A. Hassner, in *Azides and Nitrenes – Reactivity and Utility*; E.F.V. Scriven, ed.; Academic Press, New York, **1984**.
- [97] (a) O. Meth-Cohn, N.J.R. Williams, A. MacKinnon, J.A.K. Howard, *Tetrahedron* **1998**, *54*, 9837–48. (b) J.R. Fotsing, K. Banert, *Synthesis* **2006**, 261–72.
- [98] G. Smolinsky, *J. Org. Chem.* **1962**, *27*, 3557–9. (b) G. Smolinsky, C.A. Pryde, *J. Org. Chem.* **1968**, *33*, 2411–16.
- [99] (a) A. Hassner, F.W. Fowler, *Tetrahedron Lett.* **1967**, *8*, 1545–8. (b) A. Hassner, F.W. Fowler, *J. Am. Chem. Soc.* **1968**, *90*, 2869–75.
- [100] (a) K. Isomura, M. Okada, H. Taniguchi, *Tetrahedron Lett.* **1969**, *10*, 4073–7. (b) W. Bauer, K. Hafner, *Angew. Chem. Int. Ed. Engl.* **1969**, *8*, 772–3.
- [101] (a) J.H. Boier, W.E. Krueger, G.J. Mikol, *J. Am. Chem. Soc.* **1967**, *87*, 5504–5. (b) J.H. Boier, W.E. Krueger, R. Modler, *J. Org. Chem.* **1969**, *34*, 1987–9.
- [102] O.L. Chapman, J.-P. Le Roux, *J. Am. Chem. Soc.*, **1978**, *100*, 282–5.
- [103] F.W. Fowler, A. Hassner, L.A. Levy, *J. Am. Chem. Soc.* **1967**, *89*, 2077–82.
- [104] (a) H. Bock, R. Damm, S. Aygen, *J. Am. Chem. Soc.* **1983**, *105*, 7681–5. (b) L.L. Lohr Jr, M. Hanamura, K. Morokuma, *J. Am. Chem. Soc.* **1983**, *105*, 5541–7. (c) T. Yamabe, M. Kaminoyama, T. Minato, *et al.*, *Tetrahedron* **1984**, *40*, 2095–9.
- [105] V. Parasuk, C.J. Cramer, *Chem. Phys. Lett.* **1996**, *260*, 7–14.
- [106] W.L. Karney, W.T. Borden, *J. Am. Chem. Soc.* **1997**, *119*, 1378–87.
- [107] (a) T. Curtius, *Ber.* **1890**, *23*, 3023–5. (b) T. Curtius, *Z. Angew. Chem.* **1914**, *27*, 111–14.
- [108] W. Lwowski, in *Azides and Nitrenes – Reactivity and Utility*; E.F.V. Scriven, ed.; Academic Press, New York, **1984**.

- [109] W. Lwowski, G.T. Tissue, *J. Am. Chem. Soc.* **1965**, *87*, 4022–3.
- [110] G.T. Tissue, S. Linke, W. Lwowski, *J. Am. Chem. Soc.* **1967**, *89*, 6303–7.
- [111] S. Linke, G.T. Tissue, W. Lwowski, *J. Am. Chem. Soc.* **1967**, *89*, 6308–10.
- [112] J. Muller, *Kinetic und Mechanismus der Curtius Umlagerung*, PhD thesis, University München, **1962**.
- [113] R.P. Tiger, *Polym. Sci., Ser. B (Engl. Transl.)* **2004**, *46*, 142–53.
- [114] (a) M.V. Zabalov, R.P. Tiger, *Russ. Chem. Bull.* **2005**, *54*, 2270–80. (b) M.V. Zabalov, R.P. Tiger, *Russ. Chem. Bull.* **2007**, *56*, 7–13.
- [115] J. Liu, S. Mandel, C.M. Hadad, M.S. Platz, *J. Org. Chem.* **2004**, *69*, 8583–93.
- [116] R. Puttner, K. Hafner, *Tetrahedron Lett.* **1964**, *5*, 3119–25.
- [117] E. Eibler, J. Sauer, *Tetrahedron Lett.* **1974**, *15*, 2569–72.
- [118] V.P. Semenov, A.N. Studenikov, A.D. Bepalov, K.A. Ogloblin, *Zh. Organ. Khim. (Russ)* **1977**, *13*, 2202–7.
- [119] Y. Hayashi, D. Swern, *J. Am. Chem. Soc.* **1973**, *95*, 5205–10.
- [120] M. Inagaki, T. Shingaki, T. Nagai, *Chem. Lett.* **1981**, 1419–22.
- [121] M. Inagaki, T. Shingaki, T. Nagai, *Chem. Lett.* **1982**, 9–12.
- [122] T. Autrey, G.B. Schuster, *J. Am. Chem. Soc.* **1987**, *109*, 5814–20.
- [123] M.E. Sigman, T. Autrey, G.B. Schuster, *J. Am. Chem. Soc.* **1988**, *110*, 4297–4305.
- [124] I. Woelfle, B. Sauerwein, T. Autrey, G.B. Schuster, *Photochem. Photobiol.* **1988**, *47*, 497–501.
- [125] T. Melvin, G.B. Schuster, *Photochem. Photobiol.* **1990**, *51*, 155–60.
- [126] K.-U. Clauss, K. Buck, W. Abraham, *Tetrahedron*, **1995**, *51*, 7181–92.
- [127] V. Desikan, Y. Liu, J.P. Toscano, W.S. Jenks, *J. Org. Chem.* **2007**, *72*, 6848–59.
- [128] P.A.S. Smith, in *Organic Reactions*; R. Adams, ed.; John Wiley & Sons, Inc., New York, **1946**, *3*, 337–449.
- [129] C.R. Hauser, S.W. Kantor, *J. Am. Chem. Soc.* **1950**, *72*, 4284–5.
- [130] J. Hine, *Physical Organic Chemistry*; McGraw-Hill Book Co Inc., New York, **1962**.
- [131] E.S. Gould, *Mechanism and Structure in Organic Chemistry*; Henry Holt & Co., New York, **1959**.
- [132] J.D. Roberts, M.C. Caserio, *Basic Principles of Organic Chemistry*; W.A. Benjamin Inc., New York, **1964**.
- [133] L.F. Fieser, M. Fieser, *Advanced Organic Chemistry*; Reinhold Publishing Corp., New York, **1961**.
- [134] R. C. Woodworth, P. S. Skell, *J. Am. Chem. Soc.* **1959**, *81*, 3383–3386.
- [135] N.P. Gritsan, E.A. Pritchina, *Mendeleev Commun.* **2001**, *11*, 94–6.
- [136] E.A. Pritchina, N.P. Gritsan, A. Maltsev, *et al.*, *Phys. Chem. Chem. Phys.* **2003**, *5*, 1010–18.
- [137] E.A. Pritchina, N.P. Gritsan, T. Bally, *Russ. Chem. Bull., Int. Ed. (Engl. Transl)* **2005**, *54*, 525–32.
- [138] (a) A.I. Kitaigorodski, P.M. Zorki, V.K. Belski, *Structure of the Organic Compounds. Data of Structure Study. 1929–1970*; Science, Moscow, **1980**, p. 628. (b) *ibid.*, p. 511.
- [139] C. Wentrup, H. Bornemann, *Eur. J. Org. Chem.* **2005**, 4521–4.
- [140] V. Desican, Y. Liu, J.P. Toscano, W. S. Jenks, *J. Org. Chem.* **2007**, *72*, 6848–59.
- [141] S.M. Mandel, M.S. Platz, *Org. Lett.* **2005**, *7*, 5385–7.
- [142] W. Lwowski, R. DeMauriac, *Tetrahedron Lett.* **1964**, *5*, 3285–8.
- [143] W. Lwowski, F.P. Woerner, *J. Am. Chem. Soc.* **1965**, *87*, 5490–1.
- [144] D.S. Breslow, T.J. Prosser, A.F. Marcantonio, C.A. Genge, *J. Am. Chem. Soc.* **1967**, *89*, 2384–90.
- [145] J.S. McConaghy, W. Lwowski, *J. Am. Chem. Soc.* **1967**, *89*, 2357–64.
- [146] J.S. McConaghy, W. Lwowski, *J. Am. Chem. Soc.* **1967**, *89*, 4450–6.
- [147] (a) M. Jones, K.R. Rettig, *J. Am. Chem. Soc.* **1965**, *87*, 4013–15. (b) M. Jones, K.R. Rettig, *J. Am. Chem. Soc.* **1965**, *87*, 4015–16.
- [148] C. Buron, M.S. Platz, *Organic Lett.*, **1003**, *5*, 3383–5.
- [149] R.E. Wilde, T.K.K. Srinivasan, W. Lwowski, *J. Am. Chem. Soc.* **1971**, *93*, 860–3.
- [150] J.H. Teles, G. Maier, *Chem. Ber.* **1989**, *122*, 745–8.

- [151] C. Wentrup, *Reactive Molecules*; Wiley-Interscience, New York, **1984**.
- [152] M.S. Platz, V.M. Maloney, In *Kinetics and Spectroscopy of Carbenes and Biradicals*; ed. M.S. Platz, Plenum, New York, **1990**.
- [153] M.F. Budyka, M.M. Kantor, M.V. Alfimov, *Russ. Chem. Rev. (Uspekhi Khimi)* **1992**, *61*, 48–74.
- [154] M.P. Gritsan, D. Polshakov, M.-L. Tsao, M.S. Platz, *Photochem. Photobiol. Sci.* **2005**, *4*, 23–32.
- [155] G. Burdzinski, T.L. Gustafson, J.C. Hackett, C.M. Hadad, M.S. Platz, *J. Am. Chem. Soc.* **2005**, *127*, 13764–5.
- [156] G. Burdzinski, J.C. Hackett, J. Wang, *et al.*, *J. Am. Chem. Soc.* **2006**, *128*, 13402–11.
- [157] R.D. McCulla, G. Burdzinski, M.S. Platz, *Org. Lett.* **2006**, *8*, 1637–40.
- [158] G. Burdzinski, C.T. Middleton, T.L. Gustafson, M.S. Platz, *J. Am. Chem. Soc.* **2006**, *128*, 14804–5.
- [159] J. Wang, J. Kubicki, M.S. Platz, *Org. Lett.* **2007**, *9*, 3973–6.
- [160] J. Wang, G. Burdzinski, Z. Zhu, *et al.*, *J. Am. Chem. Soc.* **2007**, *129*, 8380–8.
- [161] J. Wang, G. Burdzinski, M.S. Platz, *Org. Lett.* **2007**, *9*, 5211–14.
- [162] P.A.S. Smith, in *Azides and Nitrenes – Reactivity and Utility*; E.F.V. Scriven, ed.; Academic Press, New York, **1984**.
- [163] (a) R. Huisgen, D. Vossius, M. Appl, *Chem. Ber.* **1958**, *91*, 1–12. (b) R. Huisgen, M. Appl, *Chem. Ber.* **1958**, *91*, 12–31.
- [164] W.E. Doering, R.A. Odum, *Tetrahedron*, **1966**, *22*, 81–93.
- [165] S.E. Carroll, B. Nay, E.F.V. Scriven, H. Suschitzky, R.R. Thomas, *Tetrahedron Lett.* **1977**, *18*, 3175–8.
- [166] A.K. Schrock, G.B. Schuster, *J. Am. Chem. Soc.* **1984**, *106*, 5228–34.
- [167] T.-Y. Liang, G.B. Schuster, *J. Am. Chem. Soc.* **1986**, *108*, 546–8.
- [168] E. Leyva, M.S. Platz, G. Persy, J. Wirz, *J. Am. Chem. Soc.* **1986**, *108*, 3783–90.
- [169] A. Reiser, F.W. Willets, G.C. Terry, V. Williams, R. Marley, *Trans Faraday Soc.* **1968**, *64*, 3265–75.
- [170] A.K. Schrock, G.B. Schuster, *J. Am. Chem. Soc.* **1984**, *106*, 5234–40.
- [171] T. Yamaoka, H. Kashiwagi, S. Nagakura, *Bull. Chem. Soc. Japan* **1972**, *45*, 361–5.
- [172] E.A. Pritchina, N.P. Gritsan, *J. Photochem. Photobiol. A: Chemistry*, **1988**, *43*, 165–82.
- [173] N.P. Gritsan, E.A. Pritchina, *J. Inf. Rec. Mat.* **1989**, *17*, 391–404.
- [174] J.C. Brinen, B. Singh, *J. Am. Chem. Soc.*, **1971**, *93*, 6623–9.
- [175] E.A. Pritchina, N.P. Gritsan, T. Bally, *Phys. Chem. Chem. Phys.* **2006**, *8*, 719–27.
- [176] G. Smolinsky, E. Wasserman, Y.A. Yager, *J. Am. Chem. Soc.* **1962**, *84*, 3220–1.
- [177] A. Reiser, G. Bowes, R. Horne, R. Trans. *Faraday Soc.* **1966**, *62*, 3162–9.
- [178] T. Donnelly, I.R. Dunkin, D.S.D. Norwood, *et al.*, *J. Chem. Soc. Perkin. Trans. 2* **1985**, 307–10.
- [179] J.C. Hayes, R.S. Sheridan, *J. Am. Chem. Soc.* **1990**, *112*, 5879–81.
- [180] I.R. Dunkin, M.A. Lynch, F. McAlpine, D. Sweeney, *J. Photochem. Photobiol. A: Chemistry* **1997**, *102*, 207–12.
- [181] E.A. Pritchina, N.P. Gritsan, T. Bally, unpublished results, **2003**.
- [182] C.J. Shields, D.R. Chrisope, G.B. Schuster, *et al.*, *J. Am. Chem. Soc.* **1987**, *109*, 4723–6.
- [183] Y.Z. Li, J.P. Kirby, M.W. George, M. Poliakoff, G.B. Schuster, *J. Am. Chem. Soc.* **1988**, *110*, 8092–8.
- [184] (a) R.J. Sundberg, M. Brenner, S.R. Suter, B.P. Das, *Tetrahedron Lett.* **1970**, *11*, 2715–18; R.J. Sundberg, S.R. Suter, M. Brenner, *J. Am. Chem. Soc.* **1972**, *94*, 513–20. (b) B.A. DeGraff, D.W. Gillespie, R.J. Sundberg, *J. Am. Chem. Soc.* **1974**, *96*, 7491–6.
- [185] (a) R. Warmuth, S. Makowiec, *J. Am. Chem. Soc.* **2005**, *127*, 1084–5. (b) R. Warmuth, S. Makowiec, *J. Am. Chem. Soc.* **2007**, *129*, 1233–41.
- [186] (a) G. Porter, B. Ward, *Proc. Roy. Soc., London, A.* **1968**, *303*, 139–56. (b) K. Ozawa, T. Ishida, K. Fuke, K. Kaya, *Chem. Phys. Lett.* **1988**, *150*, 249–53.
- [187] (a) D.W. Cullin, N. Soundarajan, M.S. Platz, T.A. Miller, *J. Phys. Chem.* **1990**, *94*, 3387–91. (b) D.W. Cullin, N. Soundarajan, M.S. Platz, T.A. Miller, *J. Phys. Chem.* **1990**, *94*, 8890–6.

- [188] (a) W.D. Crow, C. Wenstrup, *Tetrahedron Lett.* **1968**, 9, 6149–52. (b) C. Wenstrup, *J. Chem. Soc.D: Chem. Commun.* **1969**, 1386–7. (c) M. Kuzaj, H. Lüerssen, C. Wenstrup, *Angew. Chem. Int. Ed. Engl.* **1986**, 25, 480–2. (d) C. Wenstrup, *Topics Current Chem.* **1976**, 62, 173–87.
- [189] S.J.I. Kim, T.P. Hamilton, H.F. Schaefer III, *J. Am. Chem. Soc.* **1992**, 114, 5349–55.
- [190] D. Hrovat, E.E. Waali, W.T. Borden, *J. Am. Chem. Soc.* **1992**, 114, 8698–9.
- [191] O. Castell, V.M. Carefa, C. Bo, R. Caballol, *J. Comput. Chem.* **1986**, 17, 42–8.
- [192] B.A. Smith, C.R. Cramer, *J. Am. Chem. Soc.* **1996**, 118, 5490–3.
- [193] M.J. Travers, D.C. Cowles, E.P. Clifford, G.B. Ellison, *J. Am. Chem. Soc.* **1992**, 114, 8699–8701.
- [194] R.N. McDonald, S.J. Davidson, *J. Am. Chem. Soc.* **1993**, 115, 10857–62.
- [195] N.P. Gritsan, T. Yuzawa, M.S. Platz, *J. Am. Chem. Soc.* **1997**, 119, 5059–60.
- [196] R. Born, C. Burda, P. Senn, J. Wirz, *J. Am. Chem. Soc.* **1997**, 119, 5061–2.
- [197] N.P. Gritsan, Z. Zhu, C.M. Hadad, M.S. Platz, *J. Am. Chem. Soc.* **1999**, 121, 1202–7.
- [198] M.-L. Tsao, M.S. Platz, *J. Am. Chem. Soc.* **2003**, 125, 12014–25.
- [199] K. Anderson, *Theor. Chim. Acta* **1995**, 91, 31–46.
- [200] R.A. McClelland, M.J. Kahley, P.A. Davidse, G. Hadzialic, *J. Am. Chem. Soc.* **1996**, 118, 4794–4803.
- [201] J.C. Fishbein, R.A. McClelland, *Can. J. Chem.* **1996**, 74, 1321–8.
- [202] J. Wang, J. Kubicki, M.S. Platz, *Org. Lett.* **2007**, 9, 3973–6.
- [203] C.J. Cramer, F.J. Dulles, D.E. Falvey, *J. Am. Chem. Soc.* **1994**, 116, 9787–8.
- [204] A. Reiser, R. Marley, *Trans. Faraday Soc.* **1968**, 64, 1806–15.
- [205] M.W. Geiger, M.E. Elliot, V.D. Karacostas, *et al.*, *Photochem. Photobiol.* **1984**, 40, 545–8.
- [206] M.F. Budyka, M.M. Kantor, M.V. Alfimov, *Russ. Chem. Bull.* **1992**, 41, 590–1.
- [207] N.P. Gritsan, H.B. Zhai, T. Yuzawa, D. Karweik, J. Brooke, M.S. Platz, *J. Phys. Chem. A* **1997**, 101, 2833–40.
- [208] N.P. Gritsan, D. Tigelaar, M.S. Platz, *J. Phys. Chem. A* **1999**, 103, 4465–9.
- [209] N.P. Gritsan, A.D. Gudmundsdóttir, D. Tigelaar, M.S. Platz, *M.S. J. Phys. Chem. A* **1999**, 103, 3458–61.
- [210] M. Cerro-Lopez, N.P. Gritsan, Z. Zhu, M.S. Platz, *J. Phys. Chem. A* **2000**, 104, 9681–6.
- [211] D.A. Polshakov, Y.P. Tsentalovich, N.P. Gritsan, *Russ. Chem. Bull.* **2000**, 49, 50–5.
- [212] N.P. Gritsan, I. Likhovotvorik, M.-L. Tsao, *et al.*, *J. Am. Chem. Soc.* **2001**, 123, 1425–33.
- [213] N.P. Gritsan, A.D. Gudmundsdóttir, D. Tigelaar, *et al.*, *J. Am. Chem. Soc.* **2001**, 123, 1951–62.
- [214] M.-L. Tsao, N.P. Gritsan, T.R. James, *et al.*, *J. Am. Chem. Soc.* **2003**, 125, 9343–58.
- [215] W.T.G. Johnson, M.B. Sullivan, C.J. Cramer, *Int. J. Quant. Chem.* **2001**, 85, 492–508.
- [216] T. Kobayashi, K. Suzuki, T. Yamaoka, *J. Phys. Chem.* **1985**, 89, 776–9.
- [217] T.-Y. Liang, G.B. Schuster, *J. Am. Chem. Soc.* **1987**, 109, 7803–10.
- [218] T. Donnelly, I.R. Dunkin, D. S.D. Norwood, *et al.*, *J. Chem. Soc. Perkin. Trans. 2*, **1985**, 307–10.
- [219] (a) R.A. Odum, A.M. Aaronson, *J. Am. Chem. Soc.* **1969**, 91, 5680–1. (b) R.A. Odum, G. Wolf, *J. Chem. Soc. Chem. Commun.* **1973**, 360–1.
- [220] R.J. Sundberg, S.R. Suter, M. Brenner, *J. Am. Chem. Soc.* **1972**, 94, 513–20.
- [221] S. Murata, S. Abe, H. Tomioka, *J. Org. Chem.* **1997**, 62, 3055–61.
- [222] E. Leyva, R. Sagredo, R. *Tetrahedron* **1988**, 54, 7367–74.
- [223] K. Lamara, A.D. Redhouse, R.K. Smalley, J.R. Thompson, *Tetrahedron* **1994**, 50, 5515–25.
- [224] M.A. Berwick, *J. Am. Chem. Soc.* **1971**, 93, 5780–6.
- [225] W.L. Karney, W.T. Borden, *J. Am. Chem. Soc.* **1997**, 119, 3347–50.
- [226] I.R. Dunkin, T. Donnelly, T.S. Lockhart, *Tetrahedron Lett.*, **1985**, 26, 359–62.
- [227] (a) R.A. Abramovitch, S.R. Challand, E.F.V. Scriven, *J. Am. Chem. Soc.* **1972**, 94, 1374–76. (b) R.A. Abramovitch, S.R. Challand, E.F.V. Scriven, *J. Org. Chem.* **1975**, 40, 1541–7.
- [228] (a) R.E. Banks, G.R. Sparkes, *J. Chem. Soc. Perkin Trans. I* **1972**, 1, 2964–70. (b) R.E. Banks, A. Prakash, *Tetrahedron Lett.*, **1973**, 14, 99–102. (c) R.E. Banks, A. Prakash, *J.*

- Chem. Soc. Perkin Trans. I* **1974**, 3, 1365–71. (d) R.E. Banks, N.D. Venayak, *J. Chem. Soc. Chem. Commun.* **1980**, 9, 900–1.
- [229] R. Poe, J. Grayzar, M.J.T. Young, *et al.*, *J. Am. Chem. Soc.* **1991**, 113, 3209–11.
- [230] (a) P.J. Crocker, N. Imai, K. Rajagopalan, *et al.*, *Bioconjugate Chem.* **1990**, 1, 419–24. (b) R.R. Drake, J.T. Slama, K.A. Wall, *et al.*, *Bioconjugate Chem.* **1992**, 3, 69–73. (c) P.R. Kym, K.E. Carlson, J.A. Katzenellenbogen, *J. Med. Chem.* **1993**, 36, 1111–19; (d) M.W. Reed, D. Fraga, D.E. Schwartz, J. Scholler, R.D. Hinrichsen, *Bioconjugate Chem.* **1995**, 6, 101–8. (e) I. Kapfer, J.E. Hawkinson, J.E. Casida, M.P. Goeldner, *J. Med. Chem.* **1994**, 37, 133–40. (f) I. Kapfer, P. Jacques, H. Toubal, M.P. Goeldner, *Bioconjugate Chem.* **1995**, 6, 109–14.
- [231] (a) R. Poe, K. Schnapp, M.J.T. Young, J. Grayzar, M.S. Platz, *J. Am. Chem. Soc.* **1992**, 114, 5054–67. (b) K.A. Schnapp, R. Poe, E. Leyva, N. Soundararajan, M.S. Platz, *Bioconjugate Chem.* **1993**, 4, 172–7. (c) K.A. Schnapp, M.S. Platz, *Bioconjugate Chem.* **1993**, 4, 178–83. (d) A. Marcinek, M.S. Platz, *J. Phys. Chem.* **1993**, 97, 12674–7. (e) A. Marcinek, M.S. Platz, S.Y. Chan, *et al.*, *J. Phys. Chem.* **1994**, 98, 412–19.
- [232] I.R. Dunkin, P.C.P. Thomson, *J. Chem. Soc. Chem. Commun.* **1982**, 1192–3.
- [233] J. Morawietz, W. Sander, *J. Org. Chem.* **1996**, 61, 4351–4.
- [234] C. Carra, R. Nussbaum, T. Bally, *Chem. Phys. Chem.* **2006**, 7, 1268–75.
- [235] (a) R.A. McClelland, P.A. Davidse, G. Hadzialic, *J. Am. Chem. Soc.* **1995**, 117, 4173–4. (b) R.A. McClelland, *Tetrahedron*, 52, 6823–58. (c) P. Suchai, R.A. McClelland, *J. Chem. Soc. Perkin Trans. 2* **1996**, 1529–30.
- [236] (a) R.A. McClelland, M.J. Kahkey, P.A. Davidse, *J. Phys. Org. Chem.* **1966**, 9, 355–60. (b) D. Ren, R.A. McClelland, *Can. J. Chem.* **1998**, 76, 78–84. (c) R.A. McClelland, A. Postigo, *Biophys. Chem.* **2006**, 119, 213–18. (d) B. Cheng, R.A. McClelland, *Can. J. Chem.* **2001**, 79, 1881–6.
- [237] D.E. Falvey, in *Reactive Intermediate Chemistry*, R.A. Moss, M.S. Platz, M. Jons, eds.; Wiley-Interscience, Hoboken, **2004**.
- [238] (a) J.A. Miller, *Cancer Res.* **1970**, 30, 559–76. (b) E.C. Miller, J.A. Miller, *Cancer*, **1981**, 47, 2327–45.
- [239] M.S. Rizk, X. Shi, M.S. Platz, *Biochemistry* **2006**, 45, 543–51.
- [240] N.P. Gritsan, *Russ. Chem. Rev. (Uspkhi Khimii)* **2007**, 76, 1139–60.
- [241] R.L. Safiullin, S.L. Khursan, E.M. Chainikova, *Kinetics and Catalysis* **2004**, 45, 640–8.
- [242] (a) P.A.S. Smith, B.B. Brown, *J. Am. Chem. Soc.* **1951**, 73, 2435–8. (b) P.A.S. Smith, B.B. Brown, *J. Am. Chem. Soc.* **1951**, 73, 2438–41. (c) P.A.S. Smith, J.H. Hall, *J. Am. Chem. Soc.* **1962**, 84, 1632–5.
- [243] J. Swenton, T. Ikeler, B. Williams, *J. Am. Chem. Soc.* **1970**, 92, 3103–9.
- [244] (a) R.J. Sundberg, R.W. Heintzelman, *J. Org. Chem.* **1974**, 39, 2546–52. (b) R.J. Sundberg, D.W. Gillespie, B.A. DeGraff, *J. Am. Chem. Soc.* **1975**, 97, 6193–6.
- [245] P.A. Lehman, R.S. Berry, *J. Am. Chem. Soc.* **1973**, 95, 8614–20.
- [246] (a) L.K. Dyllal, J.E. Kemp, *J. Chem. Soc. B* **1968**, 9, 976–9. (b) L.K. Dyllal, *Aust. J. Chem.* **1975**, 28, 2147–59. (c) S.P. Efimov, V.A. Smirnov, A.V. Pochinok, *High Ener. Chem.* **1983**, 17, 347–9. (d) R. Purvis, R.K. Smalley, H. Suschitzky, M. Alkhader, *J. Chem. Soc., Perkin Trans. I* **1984**, 249–54.
- [247] G. Rauhut, F. Eckert, *J. Phys. Chem. A* **1999**, 103, 9086–92.
- [248] S.E. Hilton, E.F.V. Scriven, H. Suschitzky, *J. Chem. Soc. Chem. Commun.* **1974**, 853–4.
- [249] S.E. Carroll, B. Nay, E.F.V. Scriven, H. Suschitzky, *Tetrahedron Lett.* **1977**, 18, 943–6.
- [250] E. Leyva, M.S. Platz, *Tetrahedron Lett.* **1987**, 28, 11–14.
- [251] (a) E. Wasserman, *Prog. Phys. Org. Chem.* **1971**, 8, 319–36. (b) J.A.R. Coope, J.B. Farmer, C.L. Gardner, C.A. McDowell, *J. Chem. Phys.* **1965**, 42, 54–9. (c) M. Kazaj, H. Luerssen, C. Wentrup, *C. Angew. Chem. Int. Ed. Eng.* **1986**, 25, 480–2. (d) R. Alvarado, J.-Ph. Grivet, C. Igier, J. Barcelo, J. Rigaudy, *J. Chem. Soc. Faraday Trans. 2*, **1977**, 73, 844–57.
- [252] (a) W. Lwowski, in *Reactive Intermediates*; eds. Jone, M; Moss R.A., John Wiley & Sons, Inc.: New York, **1981**; Vol. 1 and 2. (b) C. Wentrup, *Adv. Heterocycl. Chem.* **1981**, 28, 231–361.
- [253] (a) J. Rigaudy, C. Igier, J. Barcelo, *Tetrahedron Lett.*, **1975**, 16, 3845–8. (b) J. Rigaudy, C. Igier, J. Barcelo, *Tetrahedron Lett.*, **1979**, 20, 1837–40.

- [254] (a) S.E. Carroll, B. Nay, E.F.V. Scriven, H. Suschitzky, *Synthesis* **1975**, 710–11. (b) S.E. Carroll, B. Nay, E.F.V. Scriven, H. Suschitzky, D.R. Thomas, *Tetrahedron Lett.*, **1977**, 18, 3175–8.
- [255] I.R. Dunkin, P.C.P. Thomson, *J. Chem. Soc. Chem. Commun.* **1980**, 499–500.
- [256] A. Maltsev, T. Bally, M.-L. Tsao, *et al.*, *J. Am. Chem. Soc.* **2004**, 126, 237–49.
- [257] A. Kuhn, M. Vosswinkel, C. Wentrup, *J. Org. Chem.* **2002**, 67, 9023–30.
- [258] M.-L. Tsao, M.S. Platz, *J. Phys. Chem. A* **2004**, 108, 1169–76.
- [259] J. Wang, J. Kubicki, G. Burdzinski, *et al.*, *J. Org. Chem.* **2007**, 72, 7581–6.
- [260] A. Reiser, G.C. Terry, F.W. Willets, *Nature (London)* **1966**, 211, 410.
- [261] M.-L. Tsao, M. S. Platz, *J. Phys. Chem. A* **2003**, 107, 8879–84.
- [262] T. Tsunoda, T. Yamoka, M. Takayama, *Nippon Kagaku Kaishi* **1975**, 12, 2074–9.
- [263] T. Tsunoda, T. Yamoka, Y. Osabe, Y. Hata, *Photogr. Sci. Eng.* **1976**, 20, 188–94.
- [264] M. Sumitani, S. Nagakura, K. Yoshihara, *Bull. Chem. Soc. Jpn.* **1976**, 49, 2995–90.

# 12

## Organoazides and Transition Metals

Werner R. Thiel

*Fachbereich Chemie, Technische Universität Kaiserslautern, Erwin-Schrödinger-Str. Geb. 54,  
D-67663 Kaiserslautern, Germany*

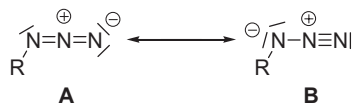
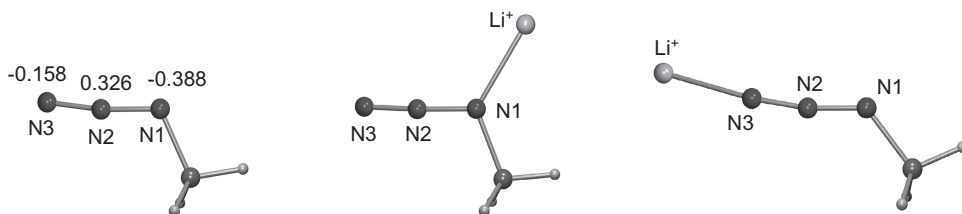
### 12.1 Introduction

In coordination chemistry, azido complexes wherein azide ions are coordinated to metal sites are known for long.<sup>1</sup> The azide ion was found in terminal as well as in bridging (1,1- $\mu$ , 1,1,1- $\mu$ , 1,3- $\mu$ ) coordination geometries. It is well established in the literature that the stability of such compounds decreases with an increase of the covalence of the M-N<sub>3</sub> bond and with an increasing M/N<sub>3</sub> ratio. Binary systems of the type M(N<sub>3</sub>)<sub>x</sub> usually decompose under formation of dinitrogen and elemental M.

As outlined by the corresponding mesomeric formulae shown in Scheme 12.1 organoazides are able to provide free electron pairs for the formation of metal complexes too.

For a deeper understanding of the donor properties of organoazides, quantum chemistry can help. Calculation of methyl azide and its adducts to a lithium cation by MP2/6-311G\* results the structural parameters and charge distributions presented in Figure 12.1 and Table 12.1.

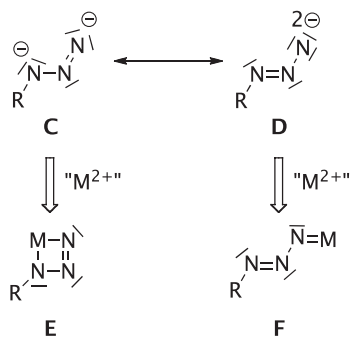
The energy difference (MP2 energies) between the two regio isomeric lithium complexes is small in the gas phase: coordination of Li<sup>+</sup> to the terminal nitrogen atom N3 – the isomer shown in Figure 12.1, right – is energetically favoured by just 1.13 kcal/mol. Taking solely the charge distribution between the nitrogen atoms of methyl azide into account, one could assume a preferred coordination to the carbon bound nitrogen atom N1 to take place. However, the terminal nitrogen atom N3, for which a pronounced participation of sp hybridization can be postulated, will provide a more directed electron pair for the coordination of the Lewis acid.

**Scheme 12.1****Figure 12.1** Calculated structures and Mulliken charges of methyl azide (left) and calculated structures of the  $\text{Li}^+$  adducts to methyl azide; characteristic bond lengths [ $\text{\AA}$ ] and bond angles [deg]**Table 12.1** Calculated characteristic bond lengths [ $\text{\AA}$ ] and bond angles [deg] of methyl azide and of its  $\text{Li}^+$  adducts

	Methyl azide	$\text{Li}^+$ adduct at N1	$\text{Li}^+$ adduct at N3
N1-N2	1.237	1.260	1.197
N2-N3	1.156	1.145	1.165
Li-N	–	1.959	1.903
N1-N2-N3	172.7	177.1	170.6
$\text{Li}^+$ -N-N	–	122.4	174.2
$\text{Li}^+$ -N1-C	–	125.9	–
C-N1-N2	–	111.8	128.4

Coordination of  $\text{Li}^+$  to the carbon bound nitrogen atom N1 (isomer shown in Figure 12.1, middle) stabilizes the negative charge at this position and therefore the mesomeric structure **B** shown in Scheme 12.1, which consequently results in a shortening of the terminal  $\text{N2}\equiv\text{N3}$  bond and an elongation (weakening) of the bond between N1 and N2. Due to this, the loss of dinitrogen ( $\text{N}_2$ ) is facilitated. The resulting nitrene species bound to a metal cation, will obviously be a highly reactive and highly oxidizing intermediate. On the other hand,  $\sigma$  donation from N3 as depicted in the structure on the right side of Figure 12.1 leads to a pronounced shortening of the  $\text{N1}=\text{N2}$  bond, due to a stabilization of the negative charge at N3.

However, transition metal sites not only possess Lewis acidic properties, they are often redox active too. Metal compounds in low and middle oxidation states can deliver electrons to substrates like organoazides. By a formal two electron reduction,  $[\text{RN}_3]^{2-}$  dianions are generated, which again can be described by at least two mesomeric forms (Scheme 12.2) and which should be stabilized due to the presence of electronegative nitrogen atoms.



Scheme 12.2

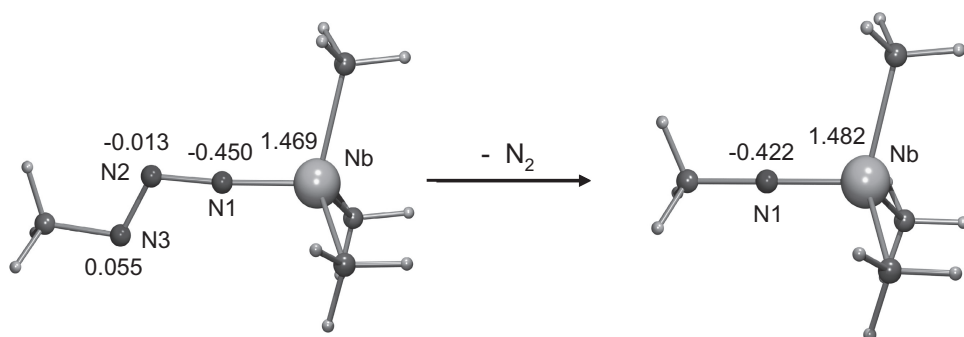


**Figure 12.2** Calculated structures and Mulliken charges of the methyl azide adduct to  $\text{NbMe}_3$  (left) and the corresponding imino complex  $\text{MeN}=\text{NbMe}_3$  (right)

Obviously such species can act either as bidentate chelating ligands including the nitrogen atoms N1 and N3 as two electron donor sites (structures **C** and **E**) in a triazametalla cyclobutene type structure or as a monodentate ligand (structures **D** and **F**) wherein the terminal nitrogen atom N3 acts as a four electron donating site similar to the carbon atom of an alkylidene type ligand. The latter coordination mode thus should preferentially be realized with high valent transition metal centres. The triazametalla cyclobutene type structure **E** will have a destabilizing effect on the N1-N2 bond and can also be considered as a transition state in the description of the metal mediated decomposition of organo azides by dinitrogen elimination. In the case of high valent (transition) metal sites, this would lead to the formation of a stable imido complex, for metal sites in lower oxidation states, a more nitrene-like character of the resulting R-N fragment can be postulated. Quantum chemical calculations (B3LYP/LANL2DZ) on the model reaction  $\text{MeN}_3=\text{NbMe}_3 \rightarrow \text{MeN}=\text{NbMe}_3 + \text{N}_2$  support these ideas (Figure 12.2, Table 12.2).

This reaction is strongly exothermic ( $\Delta H_{\text{calcd}}$ :  $-47.7$  kcal/mol) due to the formation of highly stable dinitrogen. Therefore, if the  $\eta^2$ -coordination of the organoazide (Scheme 12.2, structure **E**) is of relevance on the reaction pathway of the azide decomposition, the best way to prevent this is to avoid a free coordination site at the metal centre.

**Table 12.2** Calculated characteristic bond lengths [Å] and bond angles [deg] of  $\text{MeN}_3=\text{NbMe}_3$  and  $\text{MeN}=\text{NbMe}_3$ 

	$\text{MeN}_3=\text{NbMe}_3$	$\text{MeN}=\text{NbMe}_3$
Nb-N1	1.796	1.771
N1-N2	1.355	
N2-N3	1.291	
Nb-N1-N2	175.4	
N1-N2-N3	115.5	
N2-N3-C	111.9	
Nb-N1-C		180.0

## 12.2 Metal Complexes Co-crystallized with an Organoazide

If the metal site of a coordination compound is in a sterically and/or electronically saturated situation, coordination of an organo azide will be hindered and thus metal centred reactivity of the  $\text{N}_3$ -fragment will not occur. If additionally the other ligands coordinated to the metal site are inert against an attack by the organoazide too, no reactivity will be observed at all. There must be a multitude of such intrinsically nonreactive combinations of organoazides and (transition) metal complexes which have not found their way into literature.

In 1965 Bailey *et al.* reported the structural elucidation of a co-crystallite between bis(8-hydroxyquinolino)copper(II) and picryl azide.<sup>2</sup> A similar system is known from free 8-hydroxyquinoline and picryl azide.<sup>3</sup> The driving force for the formation of these compounds is a charge transfer by  $\pi$ -interaction between the electron rich 8-hydroxyquinoline or the 8-hydroxyquinolino ligand of the transition metal complex and the electron accepting picryl site resulting in deeply coloured products. Therefore, two equivalents of picryl azide per copper(II) complex were found in the solid state structure (Figure 12.3).

The authors did not report the thermal stability of the copper(II) complex. However, they mention, that it is 'noteworthy that picryl azide reacts with a variety of olefins, norbornene, pinene, cyclopentene, cyclooctene, and others, with exceptional ease'. The fact, that the copper(II) does not decompose this organoazide can clearly be attributed to the efficient shielding of the copper(II) centre by the two 8-hydroxyquinolino ligands.

## 12.3 Cationic Metal Complexes with Organoazide Containing Anions

Another direct way to synthesize an inert system will be salt formation between a well-shielded metal cation and an organoazide containing anion. In a recent publication Cao *et al.* reported the synthesis of cationic cobalt(III) and nickel(II) ethylenediamine complexes with 4,4'-diazido-2,2'-stilbenedisulfonate ( $\text{dasb}^{2-}$ ) as the counter ion.<sup>4</sup> The authors chose this special anion for the formation of hydrogen bound supramolecular structures, which are well established for organodisulfonates of the type  $^- \text{O}_3\text{S-linker-SO}_3^-$ . The  $\text{NH}_2$  protons of the ethylenediamine ligands were acting as proton donors. Additionally the  $\text{dasb}^{2-}$  ligand provides a rigid organic backbone and two azido substituents, which

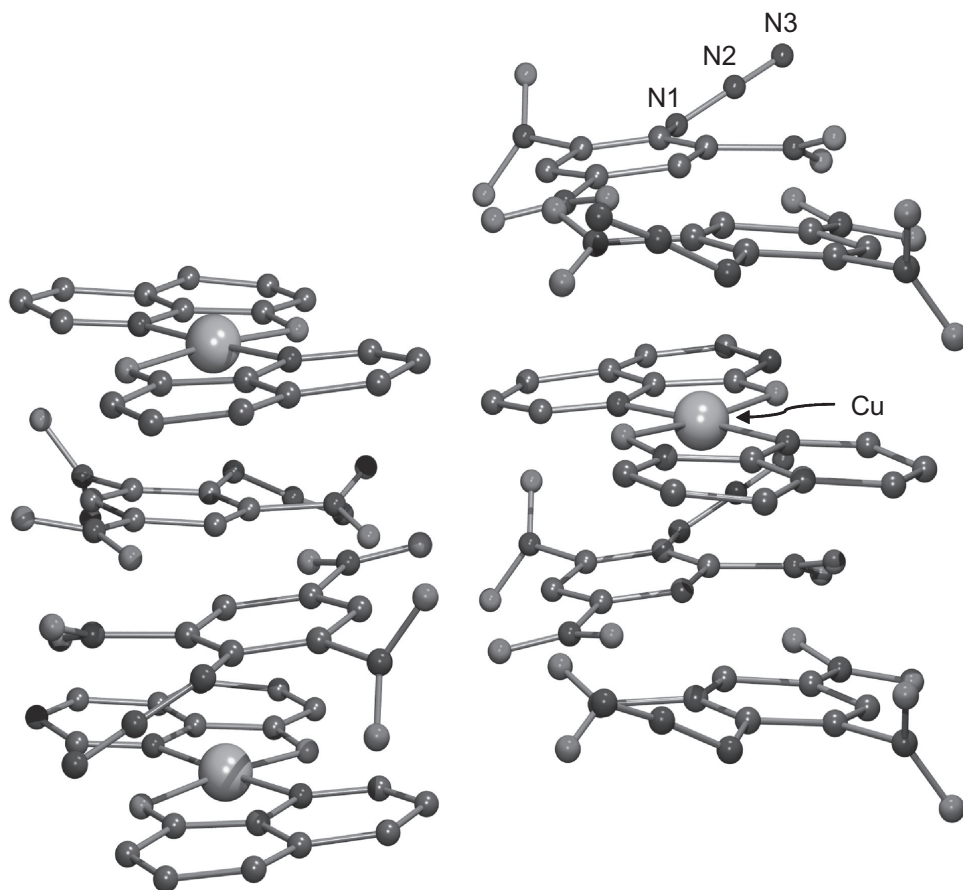


**Figure 12.3** Solid state structure of bis(8-hydroxyquinolino)copper(II)-(picrylazide)

can act as weak hydrogen bond acceptors too. For the nickel(II) compound, a sheet type of structure is built up by hydrogen bonds between the cation and the sulfonate groups of the anion and the sheets are packed to a 3D framework by weak hydrogen bonds involving the azido substituents. The high stability of these compounds was illustrated by TGA experiments: the cobalt(III) and nickel(II) frameworks are losing only co-crystallized water molecules and ethylenediamine ligands up to temperatures of 177 °C and 212 °C, respectively.

#### 12.4 Metal Complexes with Ligands Bearing a Non-coordinating Organoazide Unit

The next step to bring the organoazide ‘closer’ to the metal site would be to connect both fragments *via* a ligand backbone. The probably simplest examples for such type of